Charles University

Faculty of Science

Study programme: Biology

Branch of study: Immunology

Bc. Tereza Hnízdilová

Antitumor activity of IL-2 and IL-7 immunocomplexes in combination with αCTLA-4 and αPD-1 mAbs

Protinádorová aktivita IL-2 a IL-7 imunokomplexů v kombinaci αCTLA-4 a αPD-1 monoklonálními protilátkami

Diploma thesis

Supervisor: RNDr. Marek Kovář, Ph.D.

Prague, 2019

Prohlášení:

Prohlašuji, že jsem závěrečnou práci zpracovala samostatně a že jsem uvedla všechny použité informační zdroje a literaturu. Tato práce ani její podstatná část nebyla předložena k získání jiného nebo stejného akademického titulu.

V Praze dne ……..

……

Tereza Hnízdilová

Acknowledgements

I would like to express my gratitude to my supervisor RNDr. Marek Kovář, Ph.D., for giving me the opportunity to work in his laboratory and for his excellent guidance. I would also like to thank to all my colleagues from the Laboratory of Tumor Immunology for practical help and valuable advice.

My family, friends and boyfriend also deserve my huge thanks for their support and patience.

Abstract

Biological activity of IL-2 and IL-7 *in vivo* is significantly increased when complexed with some of the respective anti-cytokine mAb. Different immune cell subsets can be preferentially stimulated depending on the anti-IL-2 mAb used to complex IL-2. IL-2/anti-IL-2 mAb S4B6 immunocomplexes (IL-2/S4B6) induce preferential expansion of $CD122^{high}$ cells whereas IL-2/anti-IL-2 mAb JES6-1 immunocomplexes (IL-2/JES6-1) highly selectively stimulate $CD25^{high}$ cells in mice. Similarly, IL-7/anti-IL-7 mAb M25 immunocomplexes (IL-7/M25) possess higher stimulatory activity for both naïve and memory $CD8^+$ T cells *in vivo* in comparison to free IL-7. CTLA-4 and PD-1 molecules are inhibitory receptors which negatively regulate proliferation, survival and effector functions of T cells. Blocking antibodies against these molecules represent promising immunotherapeutic tool for treatment of malignant diseases.

We examined possible synergism of IL-2/S4B6 and αCTLA-4 plus αPD-1 mAbs in tumor-bearing mice. We found that the expansion of recently activated $CD8^+$ T cells driven by IL-2/S4B6 was further augmented by αCTLA-4 plus αPD-1 mAbs. However, these two immunotherapeutic approaches did not show synergistic antitumor activity in any mouse tumor model tested.

Next, we showed that IL-7/M25 possessed higher biological activity in terms of stimulation of proliferation of $CD4^+$ and $CD8^+$ T and B cells *in vivo* in comparison to free IL-7. Moreover, IL-7/M25 had no stimulatory activity for Tregs. We thus tested possible antitumor activity of IL-7/M25 in combination with αCTLA-4 plus αPD-1 mAbs. Unexpectedly, IL-7/M25 but not free IL-7 dampened the antitumor activity of αCTLA-4 plus αPD-1 mAbs in all tested mouse tumor models. This paradoxical effect of IL-7/M25 is not mediated via TGF-β or IL-10 production.

Key words

IL-2, IL-7, IL-2/S4B6 immunocomplex, IL-2/JES6-1 immunocomplex, IL-7/M25 immunocomplex, αCTLA-4 and αPD-1 blocking mAbs, tumor immunotherapy

Abstrakt

In vivo biologická aktivita IL-2 a IL-7 je výrazně zvýšena, pokud je cytokin vázán v komplexu s anti-cytokin monoklonální protilátkou. V závislosti na konkrétním klonu protilátky je pak v případě IL-2 možné selektivně stimulovat různé populace imunokompetentních buněk. Imunokomplex složený z IL-2 a anti-IL-2 mAb S4B6 (IL-2/S4B6) expanduje hlavně $CD122^{high}$ buňky, zatímco imunokomplex složený z IL-2 a anti-IL-2 mAb JES6-1 (IL-2/JES6-1) vysoce selektivně stimuluje pouze $CD25^{high}$ buňky. Imunokomplex složený z IL-7 a anti-IL-7 mAb M25 má v porovnání s volným IL-7 výrazně vyšší stimulační aktivitu pro naivní i paměťové $CD8^+$ T lymfocyty. CTLA-4 a PD-1 jsou inhibiční receptory, které regulují T buněčnou odpověď. Blokační protilátky proti takovým molekulám jsou jedním ze slibných imunoterapeutických přístup v léčbě nádorů.

Studovali jsme možný synergický protinádorový efekt IL-2/S4B6 a blokačních protilátek proti CTLA-4 a PD-1. Prokázali jsme, že expanze aktivovaných $CD8^+$ T lymfocytů mediovaná IL-2/S4B6 je dále potencována blokací CTLA-4 a PD-1 molekul. Poněkud překvapivě však tyto imunoterapeutické přístupy nevykazovaly synergické protinádorové působení v žádném z testovaných myších nádorových modelů.

Dále jsme prokázali, že IL-7/M25 navozuje v porovnání s volným IL-7 intenzivní proliferaci $CD4^+$ a $CD8^+$ T a B lymfocytů *in vivo*. IL-7/M25 navíc nestimuluje Treg buňky. Proto jsme se rozhodli otestovat, zda bude IL-7/M25 potencovat protinádorovou aktivitu blokačních protilátek proti CTLA-4 a PD-1. Kombinovaná léčba IL-7/M25 s αCTLA-4 a αPD-1 protilátkami však překvapivě vykazovala výrazně horší terapeutický efekt než samotná CTLA-4 a PD-1 blokace ve všech testovaných myších nádorových modelech. Tento paradoxní efekt IL-7/M25 není mediován produkcí TGF-β nebo IL-10.

Klíčová slova

IL-2, IL-7, IL-2/S4B6 imunokomplex, IL-2/JES6-1 imunokomplex, IL-7/M25 imunokomplex, αCTLA-4 and αPD-1 blokační protilátky, nádorová imunoterapie

List of abbreviations

AICD	Activation-induced cell death
AP-1	Activator protein-1
Bcl-2	B-cell lymphoma-2
Blimp-1	B lymphocyte maturation protein-1
BSA	Bovine serum albumin
CFSE	Carboxyfluorescein succinimidyl ester
cpm	Counts per minute
CTLA-4	Cytotoxic T lymphocyte antigen-4
DN	Double negative
DP	Double positive
EAE	Experimental autoimmune encephalomyelitis
eq.	Equivalent
Ezh2	Enhancer of zeste homolog 2
FACS	Fluorescence activated cell sorting
FasL	Fas ligand
FcRn	Neonatal Fc receptors
FcRγ	Fc receptors for IgG
FCS	Fetal calf serum
FCS	Forward scatter
FDA	Food and Drug Administration
FLIP	Fas-associated death domain-like IL-1B-converting enzyme-like inhibitory protein
FOXO1	Forkhead box protein O1
FoxP3	Forkhead box $P3^{+}$
FVD	Fixable Viability Dye
GABPα	Guanine adenosine-binding protein alpha
Gfi-1	Grow factor independence-1
GVHD	Graft-versus-host disease
h	Human
HIV	Human immunodeficiency virus
i.p.	Intraperitoneal
i.v.	Intravenous

ic	Immunocomplexes
ICOS	Inducible T cell costimulator
IFN-γ	Interferon gamma
IL	Interleukin
IL-2ic	IL-2/anti-IL-2 mAb immunocomplexes
IL-7ic	IL-7/anti-IL-7 mAb immunocomplexes
ILC2	Type 2 innate lymphoid cells
JAK	Janus kinase
K_d	Dissociation constant
LAK	Lymphokine-activated killer
m	Murine
mAb	Monoclonal antibody
MAPK	Mitogen-activated protein kinase
MDSCs	Myeloid-derived suppressor cells
MHC	Major histocompatibility complex
MP	Memory phenotype
N.D.	Not determined
NF-κB	Nuclear factor κ-light-chain-enhancer of activated B cells
NFAT	Nuclear factor of activated T cells
NKT cell	Natural killer T cell
OVA	Ovalbumin
PBS	Phosphate buffer saline
PD-1	Programmed death-1
PD-L1	Programmed death-ligand 1
PD-L2	Programmed death-ligand 2
PEG	Polyethylene glycol
PI3K	Phosphoinositide 3-kinase
PIP3	Phosphatidylinositol (3,4,5)-triphosphate
PKB	Protein kinase B
PMA	Phorbol myristate acetate
pSTAT5	Phosphorylated signal transducer and activator of transcription 5
r	Recombinant
R	Receptor
RT-PCR	Reverse transcription polymerase chain reaction

s	Soluble
s.c.	Subcutaneous
SCID	Severe combined immunodeficiency syndrome
SHC	Src homology and collagen
SIIN.	SIINFEKL
SLE	Systemic lupus erythematosus
SP	Single positive
STAT	Signal transducer and activator of transcription
TCR	T cell receptor
TF	Transcription factor
TGF-β	Transforming growth factor beta
Treg	T regulatory cell
TSLP	Thymic stromal lymphopoetin
VLS	Vascular leak syndrome

Table of contents

1. INTRODUCTION

Interleukin (IL)-2 is a cytokine produced mainly by activated T cells. IL-2 supports proliferation, survival and effector functions of activated T lymphocytes and NK cells. Immunocomplexes (ic) composed of recombinant (r) IL-2 and anti-IL-2 monoclonal antibody (mAb) (IL-2ic) were shown to possess dramatically increased biological activity *in vivo* in comparison to free IL-2. The main mechanism of this interesting phenomenon is extremely increased half-life of the cytokine in circulation after its preassociation with anti-IL-2 mAb. Two functionally different IL-2ic, selectively stimulating distinct populations of immunocompetent cells were described. IL-2ic composed of IL-2 and anti-IL-2 mAb S4B6 (IL-2/S4B6) expand predominantly $CD122^{high}$ cell populations, while IL-2ic composed of IL-2 and anti-IL-2 mAb JES6-1 (IL-2/JES6-1) highly selectively stimulate $CD25^{high}$ cells. IL-2/S4B6 show potent antitumor activity in several experimental mouse tumor models. However, the therapeutic effect of IL-2/S4B6 is significant only in case that they are administrated shortly after the inoculation of tumor cells.

Cytotoxic T lymphocyte antigen-4 (CTLA-4) and programmed death-1 (PD-1) molecules are negative regulators of immune responses. αCTLA-4 and αPD-1 blocking mAbs are typical representatives of so-called immune checkpoint inhibitors. These mAbs showed antitumor activity in a vast number of both mouse experimental tumor models and human malignant diseases. Combination of cancer immunotherapies seems to be a promising strategy in the field of cancer immunotherapy. We hypothesize that IL-2/S4B6 may synergize with other T cell-stimulating approaches such as αCTLA-4 and αPD-1 mAbs. We believe that robust expansion of memory and recently activated $CD8^+$ T and NK cells driven by IL-2/S4B6 combined with blockage of inhibitory signaling in T cells could result in durable antitumor responses.

Increased *in vivo* biological activity of cytokine/anti-cytokine mAb ic was described not only for IL-2, but also for IL-7. IL-7/anti-IL-7 mAb complexes (IL-7ic) composed of rIL-7 and anti-IL-7 mAb M25 (IL-7/M25) were reported to be far more potent than free IL-7 in terms of expansion of peripheral T cells in mice. We thus aim to characterize the effects of IL-7/M25 on T cell populations in detail and investigate their potential antitumor activity in combination with αCTLA-4 and αPD-1 mAbs. Thus, we assume that pre-expansion of T cell population with IL-7/M25 could significantly improve antitumor efficacy of immune checkpoint blockage.

2. AIMS OF THE THESIS

The general aim of the study was to investigate the potential of IL-2/S4B6 and IL-7/M25 to boost the anticancer activity of immune checkpoint inhibitors αCTLA-4 and αPD-1 mAbs. The main aims of the thesis are:

- to characterize the potential of IL-2/S4B6 and IL-2/JES6-1 to drive expansion of recently activated $CD4^+$ and $CD8^+$ T cells and compare it to free IL-2

- to determine whether the expansion of recently activated $CD8^+$ T cells mediated by IL-2/S4B6 and IL-2/JES6-1 is further potentiated by administration of αCTLA-4 plus αPD-1 mAbs

- to test possible synergism of antitumor activity of IL-2/S4B6 and αCTLA-4 plus αPD-1 mAbs in experimental syngeneic mouse tumor models of colorectal carcinoma (CT26 and MC38) and T cell lymphoma (EL4)

- to characterize the biological activity of IL-7/M25 *in vitro* and *in vivo* in various populations of immunocompetent cells and compare it to free IL-7

- to test whether IL-7/M25 is capable to boost antitumor activity of αCTLA-4 plus αPD-1 mAbs in experimental syngeneic mouse tumor models of colorectal carcinoma (CT26 and MC38) and melanoma (B16F10)

3. LITERATURE REVIEW

3.1. The Biology of IL-2

3.1.1. IL-2 structure and genetics

Human (h) IL-2 is 15.5-16 kDa secreted glycoprotein which belongs to type I cytokine family [1]. The sequencing of the human and murine (m) *il2* gene was completed in 1983 [2] and 1985 [3], respectively. *Il2* gene is located on chromosome 4 in humans and codes for a protein consisting of 153 amino acids [2]. The gene expression is positively regulated by 3 major transcription factors (TF); activator protein-1 (AP-1), nuclear factor κ-light-chain-enhancer of activated B cells (NF-κB) and nuclear factor of activated T cells (NFAT). Upon TCR activation, these TFs bind to enhancer region located approximately 300 base pairs (bp) upstream of the *il2* gene and enable its transcription [4]. IL-2 secretion is negatively regulated by an autoregulatory feedback loop controlled mainly via induction of B lymphocyte maturation protein-1 (Blimp-1) which serves as a transcriptional repressor [5].

3.1.2. Sources of IL-2

Upon activation, several immune cell subsets are reported to secrete IL-2. The main producers of the cytokine are activated $CD4^+$ T cells, followed by activated $CD8^+$ T cells and, to a lesser extent, dendritic cells (DC), B cells, natural killer (NK) cells and natural killer T NKT cells [6-8]. Optimal and sustainable IL-2 secretion by T cells is triggered only in case of receiving both signal 1 (delivered by the interaction of CD3/T cell receptor (TCR) complex with specific peptide bound to major histocompatibility complex (MHC)) and signal 2 (ensured by CD28-CD80/86 interaction). CD28 signaling leads to activation of NFAT, NF-κB and AP-1 which induces IL-2 production by activated T cells. Moreover, CD28 signaling stabilizes *il2* mRNA [9]. Produced IL-2 works in an autocrine and paracrine manner [1]. Interestingly enough, $CD3^+CD4^+CD25^+$ forkhead box $P3^+$ (FoxP3) T regulatory (Treg) cells don't produce IL-2 even when activated [10].

3.1.3. IL-2 receptor

IL-2 binds to IL-2 receptor (R) complex consisting of three subunits; IL-2Rα (CD25), IL-2Rβ (CD122) and IL-2Rγ (common γ-chain, γ_c, CD132) (Fig. 1). CD122 and CD132 are

shared subunits for IL-2/IL-15R, whereas CD25 is unique for IL-2. CD132 is a part of IL-2, IL-4, IL-7, IL-9, IL-15 and IL-21 receptor complexes [1].

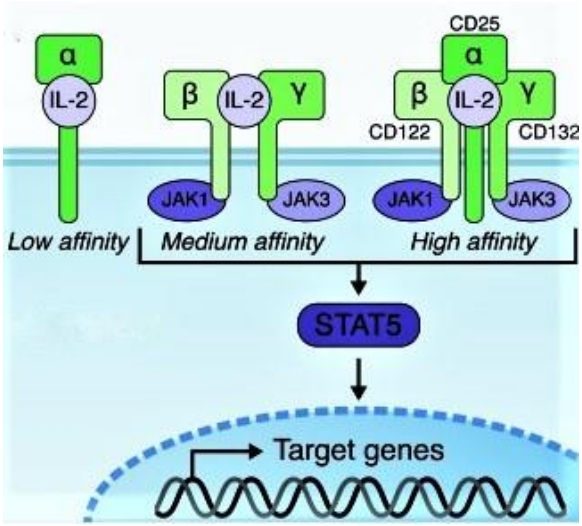

Figure 1. Composition of IL-2R. IL-2Rα (CD25) binds IL-2 with low affinity and isn't capable of signal transduction. CD122 and CD132 together form a medium affinity IL-2R. High-affinity IL-2R is formed when CD25, CD122 and CD132 are present. Intracellular domains of CD122 and CD132 are associated with JAK1 and JAK3. IL-2 signaling triggers activation of STAT5. Adopted from Niu *et al.* with minor changes made [11].

All three subunits are required for the formation of heterotrimeric high-affinity IL-2R (dissociation constant (K_d) ~ 10^{-11} M). However, only CD122 and CD132 are indispensable for signal transduction and can together form heterodimeric intermediate-affinity IL-2R (K_d ~ 10^{-9} M) which is fully competent to signal. CD25 per se binds IL-2 with low affinity (K_d ~ 10^{-8} M) [12]. CD25 alone is not capable to generate intracellular signal due to the absence of cytoplasmatic signaling domain [13]. Association of CD25 with dimeric IL-2R enhances the affinity for IL-2 by about 100-fold [1].

Binding of IL-2 to IL-2Rαβγ leads to the formation of quaternary complex, which is internalized together, although its members have a different fate inside the cell. While IL-2, CD122 and CD132 are targeted for lysosomal degradation, CD25 is recycled to the plasma membrane via endosomes. Accordingly, CD25 is much more stable surface protein than CD122 and CD132, whose half-life on the cell surface is less than 1 hour [14].

CD132 subunit is expressed on most hematopoietic cells [12]. Expression of the intermediate-affinity IL-2R is low but detectable on naïve $CD8^+$ T cells and memory $CD4^+$ T cells but virtually absent on naïve $CD4^+$ T cells. NK cells and memory $CD8^+$ T cells express high levels of dimeric IL-2R [15]. However, these cells cannot utilize homeostatic levels of IL-2 that are present in organism in steady-state conditions. Low physiological levels of IL-2 are utilized only by cells expressing trimeric IL-2R such as Tregs which constitutively express high levels of CD25 together with intermediate levels of CD122 and CD132 [16]. Of note,

several other cell types, including type 2 innate lymphoid cells (ILC2), pulmonary endothelial cells, early developing pre-T and pre-B cells express low levels of CD25 [17-19].

Upon TCR stimulation, activated T cells rapidly initiate the expression of CD25 which increases their responsiveness to IL-2 and enables selective expansion of antigen-activated T cells [20]. CD25 can be transiently expressed also by activated NK cells and B cells [21, 22].

3.1.4. Signaling pathways

Signaling via either dimeric or trimeric IL-2R engages Janus kinase (JAK)/signal transducer and activator of transcription (STAT), mitogen-activated protein kinase (MAPK) and phosphoinositide 3-kinase (PI3K)/protein kinase B (PKB, Akt) signaling pathways [1].

Binding of IL-2 to IL-2R leads to heterodimerization of the cytoplasmic tails of CD122 and CD132 and subsequent activation of associated JAK1 and JAK3. These kinases phosphorylate key tyrosine residues on CD122 [23]. Consequently, STAT proteins are recruited to the site. Phosphorylated STAT proteins dimerize and translocate to cell nucleus where they regulate transcription of genes affecting cell activation, differentiation and survival [1]. Phosphorylated tyrosine residues on CD122 can also recruit Src homology and collagen (SHC) adaptor protein. Activated SHC provides a platform for activation of MAPK pathway kinases. Lastly, IL-2 signaling induces activation of PI3K/Akt pathway [1].

The kinetics of activation of the respective pathway dictates the specificity of IL-2 signaling. IL-2-regulated phosphoproteome in cytotoxic T lymphocytes has recently been mapped using high-resolution mass spectrometry techniques. Approximately 90% of IL-2R signaling was reported to be JAK1/3 dependent in this study [24]. In contrast to effector T cells, Tregs were described to express increased amount of phosphatase and tensin homolog (PTEN) and so preventing activation of PI3K [25]. Regarding the fact that absence of PTEN leads to the loss of expression of CD25 and FoxP3 by Tregs, this phosphatase seems to be important for controlling distinct functions in Tregs versus effector T cells [26].

3.1.5. Biological activities

IL-2 exerts its pleiotropic effects on several populations of immunocompetent cells (Fig. 2). It was initially described to be a T cell grow factor [27]. IL-2 is required for proliferation, expansion and survival of activated $CD4^+$ and $CD8^+$ T cells. [28]. IL-2 provides activated T cells with anti-apoptotic signals via upregulation of B-cell lymphoma-2 (bcl-2) [29]. IL-2 is essential for determining the magnitude of memory immune responses and, together with other

γ_c cytokines, controls homeostasis of memory $CD8^+$ T cells [30]. IL-2 promotes differentiation of naïve $CD4^+$ T cells into effector T_h1 and T_h2 cells, while it inhibits generation of T_h17 cells [31].

However, the most crucial role of IL-2 is to prevent autoimmunity. Under steady-state *in vivo* conditions, low homeostatic levels of IL-2 provide generation and survival of Tregs [32, 33]. Suppressive activities of Tregs, such as expression of cytotoxic T-lymphocyte–associated antigen 4 (CTLA-4) and CD73, depend critically on IL-2 [34]. Among other activities resulting in downregulation of immune responses, IL-2 enhances activation-induced cell death (AICD). It mediates Fas-dependent apoptosis in T cells by enhancing Fas ligand (FasL) transcription and surface expression. Moreover, IL-2 inhibits transcription of Fas-associated death domain-like IL-1B-converting enzyme-like inhibitory protein (FLIP) which is a negative regulator of Fas-mediated apoptosis [35].

IL-2 was reported to enhance cytotoxic activity of NK cells and to support the production of NK cell-derived cytokines [36]. Due to the fact that ILC2 express low but significant levels of trimeric IL-2R (Fig. 2), they can be stimulated by this cytokine to produce IL-5 [37].

Tregs dependence on IL-2 is best illustrated by mouse knockout models. Deficiency in IL-2 or in CD25 leads to multi-organ inflammation and fatal systemic autoimmune disorder due to the lack of Tregs in both mice and humans [15]. A similar failure of immune peripheral tolerance is observed in $CD122^{-/-}$ mice. Additionally, these mice lack NK cells due to an absence of IL-15 responsiveness [38]. T, B and NK cells in CD132 deficient mice or humans fail to develop which results in severe combined immunodeficiency syndrome (SCID) [39].

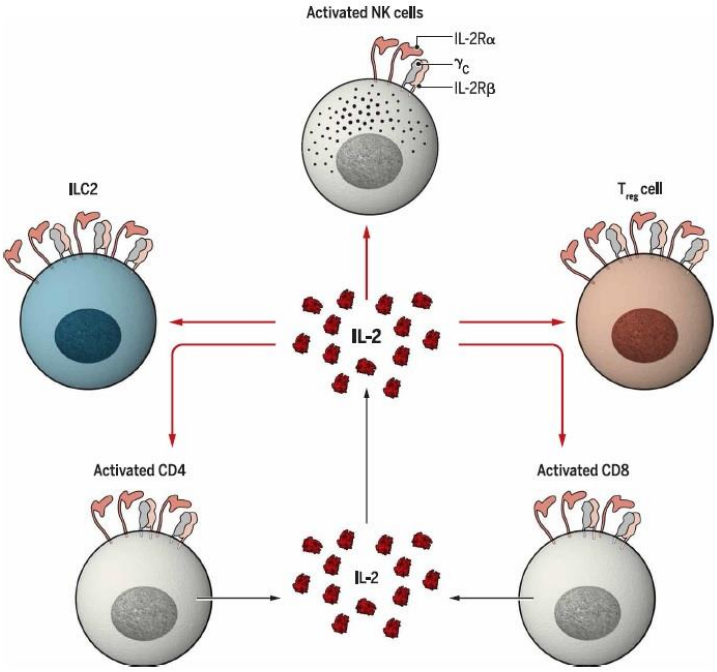

Figure 2. Immune cell populations expressing high-affinity IL-2R. IL-2 is produced by activated $CD4^+$ T cells and, to a lesser extent, by activated $CD8^+$ T cells. It is required for their proliferation, expansion and survival. IL-2 is also indispensable for maintenance of homeostasis and suppressive capacity of Tregs. Activated NK cells and ILC2 were reported to express high-affinity IL-2R and thus can utilize IL-2 signal. Adopted from Abbas *et al.* [40].

3.1.6. Clinical applications

IL-2 was discovered in 1976 as a grow-promoting factor for T cells *in vitro* [27]. Its potential anti-cancer effects began to be tested soon afterwards. Studies carried out in mice showed that combination of IL-2 treatment with adoptive transfer of autologous lymphokine-activated killer (LAK) cells led to more robust antitumor response than either approach alone [41]. 25 cancer patients in whom the standard therapy had failed were treated with autologous LAK cells and high dose of IL-2 in an initial clinical study in 1985. The study confirmed anticancer properties of IL-2 as 4 of 7 patients with metastatic melanoma and 3 of 3 patients with metastatic renal cancer showed significant tumor regression [42].

Studies using IL-2 as a single therapeutic modality followed soon after. In a study held by Rosenberg and others, 283 patients with metastatic renal cell carcinoma and metastatic melanoma were treated with high dose of IL-2. IL-2 administration led to 7% complete and 13% partial responses in renal carcinoma patients and 7% complete and 10% partial response in metastatic melanoma patients [43]. IL-2 therapy was associated with increased frequencies of lymphocytes in the tumor site and the antitumor responses were remarkably durable in comparison with other cancer therapies accessible at the time. Hence, Food and Drug

Administration (FDA) approved high dose of IL-2 for treatment of metastatic melanoma and renal carcinoma in 1998 and 1992, respectively [44].

IL-2 has also been used to boost immune responses in human immunodeficiency virus (HIV)-infected patients. The therapy did not show any beneficial effect for the patients, even though a significant increase in $CD4^+$ cell count was observed [45].

Despite its promising potential, IL-2 immunotherapy is limited by severe disadvantages. IL-2 has a serum half-life of only several minutes due to its rapid elimination from blood circulation. Thus, to achieve a satisfactory anti-tumor effect, the cytokine needs to be administrated repeatedly and in high doses. However, high dose of IL-2 can result in serious toxicities. The adverse effects of high dose of IL-2 include fever, tachycardia, hypotension, nausea, vomiting, diarrhea, pulmonary edema or renal failure [44]. Many of these toxicities can be explained by the development of the vascular leak syndrome (VLS). The VLS is caused by direct binding of IL-2 to $CD31^+$ lung endothelial cells, which express low levels of high-affinity IL-2R. IL-2 activates these cells which leads to increased vascular permeability and acute vasodilatation. This is followed by extravasation of fluid into organs, predominantly lungs, causing a life-threatening pulmonary edema [19]. Finally, IL-2 administration for cancer therapy may lead to unwanted Treg stimulation. Indeed, high dose IL-2 treatment resulted in about 6-fold increase in the frequency of Treg cells in peripheral blood of cancer patients which may dampen the antitumor effect of the cytokine [46].

Regardless of the adverse effects, high doses of IL-2 used in cancer immunotherapy were shown to boost effector functions of cytotoxic T cells and NK cells whereas low doses of the cytokine preferentially expand Tregs. Tregs constitutively express high levels of trimeric IL-2R which enables them to use low concentrations of IL-2 which is insufficient to cause global immune activation [47]. Low-dose IL-2 therapy showed efficacy in patients with various autoimmune diseases, such as hepatitis virus-associated vasculitis, chronic graft-versus-host disease (GVHD), ulcerative colitis and systemic lupus erythematosus (SLE) in a single clinical trial [48].

3.1.7. Strategies to improve efficacy of IL-2 based therapy

Several approaches such as generation of IL-2/anti-IL-2 mAb ic and IL-2 muteins are being developed in order to fine-tune pleiotropic and somewhat opposing effects of IL-2 [49, 50].

3.1.7.1. IL-2/anti-IL-2 mAb ic

In vivo biological activity of IL-2 can be significantly increased by complexing with anti-IL-2 mAb before administration [49]. This intriguing phenomenon was firstly described by Boyman *et al.* although hints already existed that it would work for other cytokines such as IL-3, IL-4 and IL-7 [51]. IL-2ic are composed of IL-2 and an anti-IL-2 mAb at molar ratio 2:1. Interestingly, S4B6 mAb can potentiate both exogenous and endogenous mIL-2 [49].

An important property of IL-2ic is that target cell specificity can be modulated in contrast to free IL-2. Depending on the clone of the mAb used to complex IL-2, IL-2ic can selectively stimulate either $CD25^{high}$ cells or $CD122^{high}$ cells in mouse system [49]. Thus, two functionally distinct IL-2ic were reported. Complexes composed of IL-2 and anti-IL-2 mAb S4B6 (IL-2/S4B6) stimulate predominantly cells expressing high levels of CD122 such as memory $CD8^+$ T cells and NK cells. Conversely, IL-2ic consisting of IL-2 and anti-IL-2 mAb JES6-1 (IL-2/JES6-1) selectively expand $CD25^{high}$ cells, most notably Treg cells and activated T cells [49, 52].

3.1.7.1.1. IL-2/S4B6

Daily injections of IL-2/S4B6 resulted in a vigorous expansion of memory phenotype (MP) $CD8^+$ T cells in spleen and lymph nodes within seven days in mice. When compared to mice treated with the same amount of free IL-2, the increase in absolute numbers was more than 100-times [49]. Huge large increase in numbers of NK cells was observed in mice receiving IL-2/S4B6 whereas $CD4^+$ T cells and B cells were only minimally affected. Moderate increase in Treg counts was also noted [49].

Comparable results were obtained using IL-2ic made of another anti-IL-2 mAb JES6-5H4 or anti-human IL-2 mAb MAB602. IL-2/S4B6 potently expanded MP $CD8^+$ T cells in both wild-type and $CD25^{-/-}$ mice demonstrating that IL-2/S4B6 acts independently of CD25. Administration of S4B6 alone recapitulated the effect of IL-2/S4B6, although to much lower extent, implying that S4B6 bound to endogenous IL-2 and promoted its increase of biological activity. This effect was completely abolished in $IL\text{-}2^{-/-}$ mice [49].

IL-2/S4B6 drove a dramatic *in vivo* expansion of antigen-activated $CD8^+$ T cells in comparison to the same amount of free IL-2. These cells established a robust population of memory cells which were able to develop effector functions upon encounter with appropriate MHC-I bound peptide [52]. IL-2/S4B6 administration also induced expression of costimulatory

molecule CD137 on both adoptively transferred activated $CD8^+$ T cells and endogenous memory $CD8^+$ T cells in mice [53].

Another study showed that IL-2/S4B6 treatment avoided the development of VLS as IL-2/S4B6 poorly stimulated $CD122^{low}$ endothelial lung cells. Moreover, the dose of complexed IL-2 needed for the same effect was reduced in comparison to free IL-2 [19]. IL-2/S4B6 displayed an increased serum half-life in mice by about 20-fold compared to the cytokine alone [52, 54].

Taken together, IL-2/S4B6 could be used therapeutically in cancer treatment. In support of this notion, several works reported favorable antitumor properties of IL-2/S4B6 in various syngeneic mouse tumor models [19, 50, 52, 55]. IL-2/S4B6 treatment of B16F10 melanoma-bearing mice resulted in a complete cure of 4 out of 6 mice whereas administration of free IL-2 in the same dosage had a negligible effect [52]. Krieg *et al.* showed that five daily injections of IL-2/S4B6, but not IL-2 alone, prevented establishment of lung tumor metastasis in the melanoma tumor model [19]. IL-2/S4B6 showed efficacy also in MC38 colon carcinoma, BCL1 B cell leukemia and LLC Lewis lung carcinoma [50, 52]. However, the treatment was beneficial only in case that the IL-2/S4B6 administration began shortly after the inoculation of tumor cells. Repetitive doses of IL-2/S4B6 provided no significant RENCA renal cell carcinoma growth inhibition in mice, although an increased immune cell infiltration into the tumor site was observed [56].

The ability of IL-2/JES6-5H4 to affect tolerant tumor-specific $CD8^+$ T cells, which represent one of the barriers in immunotherapeutic cancer treatment, has recently been explored [57]. Using a Alb:Gag mouse model where an immunodominant leukemia antigen Gag is expressed both by healthy liver and murine FBL leukemia cells, the authors showed that IL-2/JES6-5H4 treatment rescued tumor-reactive Gag-specific $CD8^+$ T cells from a state of established tolerance. Gag specific $CD8^+$ T cells were adoptively transferred into Alb:Gag mice bearing FBL leukemia and they became tolerant shortly after the adoptive transfer. They didn't affect survival of mice in comparison to untreated mice. However, 80% of mice treated with IL-2/JES6-5H4 after the adoptive transfer were long-term survivors [57].

IL-2/S4B6 or its functional analogues were also successfully combined with other anti-tumor agents, such as irradiation or inhibitor of enhancer of zeste homolog 2 (Ezh2) [58, 59].

IL-2/S4B6 administration was proven to provide protection against bacterial and viral pathogens [60, 61]. Naïve mice pretreated with IL-2/S4B6 showed reduced bacterial burden in spleen and liver after infection with *Listeria monocytogenes*. All IL-2/S4B6 pretreated mice

survived the infective dose, whereas five of nine control mice died. The protective effect of IL-2/S4B6 was dependent on both $CD8^+$ T cells and NK cells. Surprisingly, increasing the number of IL-2/S4B6 injections from three to five led to a complete loss of the protective effect showing that overstimulation can occur. Mice treated with five injections exhibited decreased production of interferon gamma (IFNγ) and increased programmed death (PD-1) expression on $CD8^+$ T cells in spleen compared to mice treated with three injections [60]. Another study demonstrated IL-2/S4B6 efficacy in herpes simplex virus-1 (HSV-1) infection model. Mice treated with IL-2/S4B6 after infection showed reduced virus levels and lesion severity compared to untreated mice [61].

3.1.7.1.2. IL-2/JES6-1

IL-2/JES6-1 act selectively on $CD25^{high}$ cells. Three daily injections of IL-2/JES6-1 increased Treg cell numbers in spleen by about 15-fold, whereas $CD8^+$ T cells and NK cells weren't significantly affected [49, 62]. Similar effect was seen when IL-2ic composed of rhIL-2/anti-human IL-2 mAb 5344 were used [54]. Treg cell expansion after three injections was rapid and observed in spleen, lymph nodes, bone marrow, liver and gut. However, it declined to baseline level 2 weeks after the last dose [62]. Tregs expanded *in vivo* via IL-2/JES6-1 administration were fully functional and expressed considerable higher levels of CD25, CTLA-4 and inducible T cell costimulator (ICOS) in comparison to Tregs expanded by an equivalent dose of free IL-2 [62, 63]. Based on a study performed with thymectomized mice, IL-2/JES6-1 acted by expanding peripheral Tregs rather than inducing thymic Treg generation [63]. Similarly to IL-2/S4B6, IL-2/JES6-1 were shown to be highly stimulatory for activated $CD8^+$ T cells as these cells express high levels of CD25. IL-2/JES6-1 were more potent than IL-2/S4B6 In terms of expansion of recently activated $CD8^+$ T cells [52].

Potential therapeutic applications of IL-2/JES6-1 have been evaluated in several preclinical models. IL-2/JES6-1 administration had beneficial effects in experimental models of myasthenia gravis [63], chronic proteinuric renal disease [64] and dextran sodium sulfate-induced colitis [65]. Webster *et al*. showed IL-2/JES6-1 efficacy in prevention of allogeneic pancreatic islet rejection and experimental autoimmune encephalomyelitis (EAE) [62]. Three doses of IL-2/JES6-1 prior to EAE induction protected mice from developing a severe disease. However, when IL-2/JES6-1 was administered after EAE induction, no amelioration of the disease was observed. This happened probably because IL-2/JES6-1 stimulated not only Tregs, but also CD25 expressing activated effector T cells. In support of

this notion, administration of IL-2/JES6-1 together with rapamycin after the disease induction led to a marked reduction of the disease severity [62]. IL-2/JES6-1 pretreatment allowed a long-term survival of allogeneic pancreatic islets in 82% of hosts in the absence of immunosuppressive drugs while no allograft was accepted in free IL-2 pretreated group of mice (Fig. 3) [62].

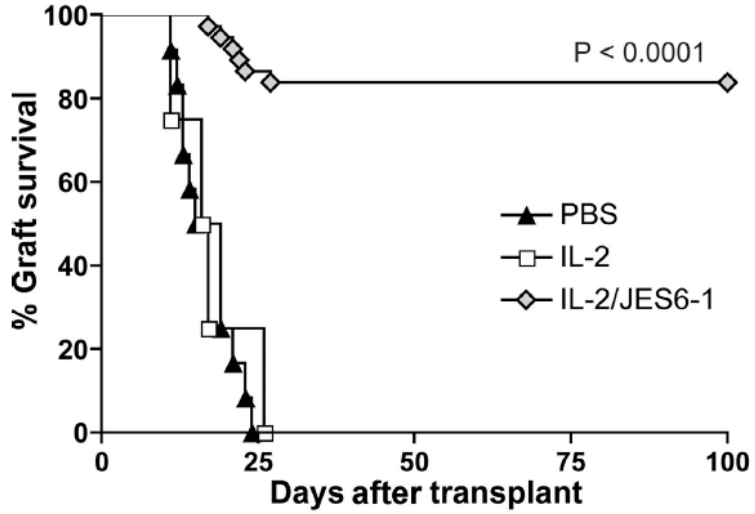

Figure 3. IL-2/JES6-1 treatment prevents pancreatic island allograft rejection. Diabetic C57BL/6 mice were treated with PBS, IL-2 or IL-2/JES6-1 on days -3, -2 and -1. On day 0, the mice were transplanted with MHC mismatched pancreatic islets. Graft survival was monitored. Adopted from Webster *et al*. [62].

Another group tested IL-2/JES6-1 capacity to replace the adoptive cell therapy with polyclonal recipient Tregs using MHC incompatible bone marrow transplantation model [66]. IL-2/JES6-1 administration prior to the bone marrow transplantation didn't support the allograft acceptance in mice implying that the effect of IL-2/JES6-1 may vary with the transplanted tissue. IL-2/JES6-1 induced not only significant expansion of Tregs but also, to a lesser extent, increased the number of $Ki67^+$ conventional $CD4^+$, $CD8^+$ T and NK cells. IL-2/JES6-1 administration also mobilized $CD25^+$ B cells to migrate from bone marrow to secondary lymphoid organs [66].

Only prophylactic, but not therapeutic treatment with IL-2/JES6-1 was found effective in reducing the joint inflammation induced by chikungunya virus. Moreover, IL-2/JES6-1 administration after virus infection worsened the course of the disease supposedly due to the enhancement of expansion of the proinflammatory virus-specific $CD25^+FoxP3^-$ effector $CD4^+$ T cells [67].

3.1.8.1.3. Mechanism of enhanced biological activity and selectivity of IL-2ic *in vivo*

Several mechanisms for the agonistic *in vivo* activity of IL-2ic have been proposed. Compared to free IL-2, both IL-2/S4B6 and IL-2/JES6-1 display a prolonged biological half-life in circulation. The association of IL-2 with a large molecule such as mAb increases the apparent molecular weight of the cytokine and thus increases its lifespan [54, 68].

It has been suggested that IL-2ic might bind to Fc receptors for IgG (FcRγ) and be presented *in trans* to T cells. However, FcRγs were shown not to play any role in the enhancing effect of IL-2ic [68]. Interestingly, the increased half-life of IL-2/JES6-1 is crucially dependent on neonatal Fc receptors (FcRn). IL-2/S4B6 rather benefit from avoiding interaction of IL-2 with CD25 as the omnipresent expression of CD25 on Tregs may lead to decreased IL-2 availability to IL-2Rβγ expressing cells [54].

As far as the selectivity of IL-2ic is concerned, it has been proposed that different functional properties of IL-2/S4B6 and IL-2/JES6-1 arose from different IL-2 epitopes recognized by these 2 mAbs [49]. Data based on the crystal structure of IL-2/JES6-1 showed that JES6-1 binding to IL-2 sterically blocks binding of CD122 and CD132. Moreover, it also induces an allosteric change in CD25-interacting epitope of IL-2 leading to a reduced binding affinity for CD25. That implies that only cells expressing high levels of CD25, such as Tregs and activated T cells, can utilize IL-2/JES6-1. IL-2/JES6-1 requires dissociation of the complex permitting IL-2 signaling to occur (Fig. 4). $CD25^{low}$ expressing cells are unresponsive to IL-2/JES6-1 as they don't express enough CD25 to displace the JES6-1 mAb which is necessary to allow signaling. $CD25^{high}$ cells in the presence of IL-2/JES6-1 upregulate CD25 rendering them even more susceptible to IL-2/JES6-1 and thus creating a positive transcriptional feedback loop [65].

Conversely, S4B6 binding to IL-2 covers the CD25-binding site on the cytokine and thus blocks IL-2/CD25 interaction. It also causes a slight conformational change of IL-2 resulting in increased affinity to CD122 in comparison with unbound IL-2. Cells expressing high levels of IL-2Rβγ, such as MP $CD8^+$ T cells and NK cells, are therefore favored to bind IL-2/S4B6 regardless of their CD25 expression. IL-2/S4B6 bind to the dimeric IL-2 without previous dissociation (Fig. 4) [65].

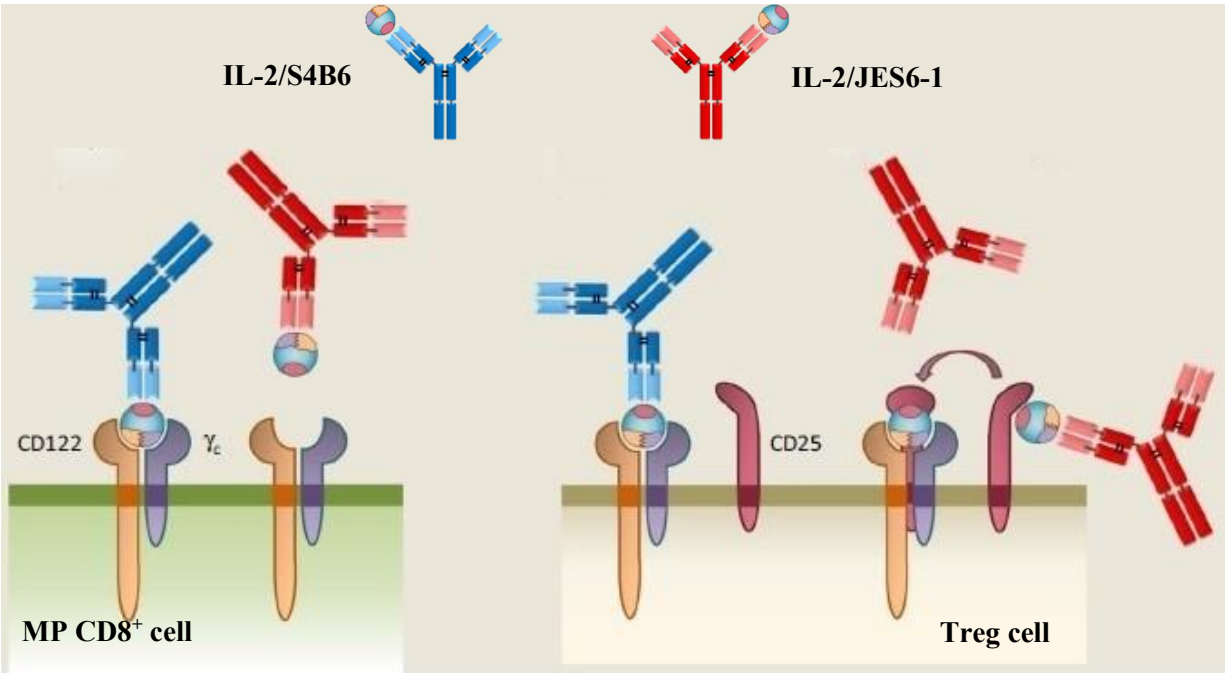

Figure 4. IL-2ic selectivity. IL-2/S4B6 (blue) stimulate cells with high expression of CD122/CD132 regardless of their CD25 expression. IL-2/S4B6 thus expand both memory $CD8^+$ T cells and Treg cells. IL-2/S4B6 binds to dimeric IL-2R without previous dissociation. IL-2/JES6-1 (red) depend on the presence of CD25 which must be highly expressed by the cell enabling the signaling to occur. It is thus capable to stimulate Treg cells but not MP $CD8^+$ T cells. IL-2 must dissociate from the IL-2/JES6-1 prior to the signal transduction. Adopted from Arenas-Ramirez *et al*. with minor changes made [69].

3.1.7.2. IL-2 muteins

The design of mutated IL-2 molecules represents another approach to improve efficacy and reduce toxicity of IL-2 based therapy. IL-2 mutein with reduced affinity to IL-2Rβγ called BAY 50-4798 was designed in order to disrupt IL-2 signaling in NK cells as these cells were thought to be the major drivers of IL-2-mediated toxicity. BAY 50-4798 was tested in clinical trials as a single anti-cancer agent but a reduced toxicity in comparison to unmanipulated IL-2 wasn't observed [70].

Another IL-2 mutant named IL-2 superkine H9 exerts reduced binding to CD25 and enhanced binding to CD122/CD132 and possesses considerable anti-tumor activity in several mouse tumor models [50]. Taken together, engineering of IL-2 mutated variants provides an interesting tool to modulate IL-2 responses and increases efficacy of IL-2 immunotherapy.

3.2. The Biology of IL-7

3.2.1. IL-7 structure and genetics

IL-7 is secreted glycoprotein which belongs to type I cytokine family. The gene for hIL-7 is located on chromosome 8q12-13 and consists of six exons and five introns [71]. Based on its sequence, the molecular weight of hIL-7 should be 17.4 kDa but glycosylation leads to an active cytokine of 25 kDa. A high degree of homology (81%) exists between the hIL-7 and the mIL-7 [72].

3.2.2. Sources of IL-7

IL-7 is a tissue-derived cytokine produced by non-hematopoietic cells, mainly stromal and epithelial cells in the thymus and bone marrow [72, 73]. Northern blot analysis of reverse transcription polymerase chain reaction (RT-PCR) detected presence of IL-7 mRNA in various other cell types such as intestinal epithelium [74], skin keratinocytes [75] and platelets [76]. Immune cells were reported not to produce IL-7, although some exceptions exist, namely follicular [77] and mature dendritic cells [78]. Epstein-Barr virus-transformed B cells derived from patients with Burkitt's lymphoma were also shown to produce IL-7 [79].

3.2.3. IL-7 receptor

IL-7R is a heterodimer consisting of the α chain (CD127) and CD132. As mentioned above, CD132 is a shared with five other cytokine receptors. CD127 is a shared subunit of IL-7 and thymic stromal lymphopoietin (TSLP).

IL-7R is expressed on lymphoid cells, most notably on developing, naïve and memory T cells and pre-B cells [72]. Upon activation, effector T cells transiently decrease CD127 expression and their ability to respond to IL-7 is thus reduced [80]. CD127 is expressed by ILC group 1, 2 and 3, with a notable exception of NK cells [81]. CD127 can also be detected on some monocytes and DCs [82]. Soluble CD127 (sCD127) exists in human plasma in nanomolar concentrations [83].

Cd127 transcription is negatively regulated by IL-7R signaling so that the maximal possible number of T cells could share the IL-7 signal in the presence of limiting amounts of the cytokine [84]. Transcription of *cd127* gene is positively regulated by forkhead box protein O1 (FOXO1) [85] and guanin adenosine-binding protein alpha (GABPα) [86]. Grow factor independence-1 (Gfi-1) is a negative regulator of IL-7 gene expression [84].

3.2.4. Signaling pathways

IL-7 signals through 2 major pathways; JAK/STAT and PI3K/Akt (Fig. 5). IL-7 binding to IL-7R leads to the recruitment of JAK1 and JAK3. JAK3 is associated with CD132, whereas Jak1 is associated with CD127. Jak1/3 phosphorylate tyrosine residues on the cytoplasmic tails of CD127 and CD132 creating a platform for STAT5 binding. Phosphorylated STAT 5 (pSTAT5) form dimers which are translocated to the cell nucleus where they impact genes associated with cell differentiation and survival [72].

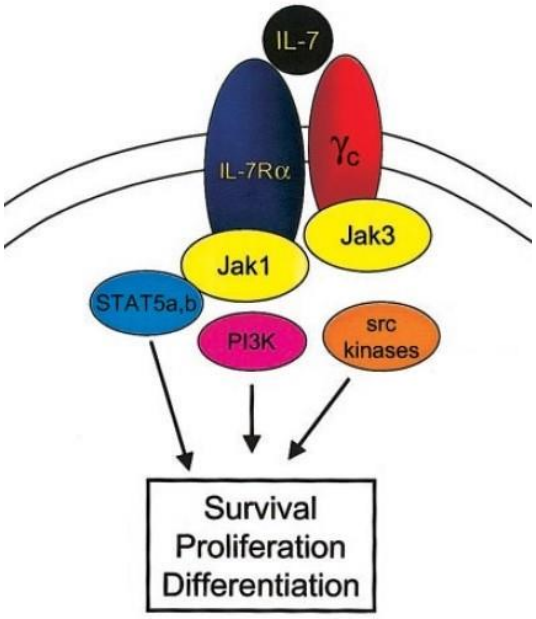

Figure 5. IL-7R signaling. IL-7 signals through a dimeric IL-7R composed of IL-7Rα (CD127) and γ_c-chain (CD132). The intracellular parts of both receptor subunits are associated with JAK 1 and JAK3. Activation of JAK1/3 leads to phosphorylation of STAT5. IL-7 binding also leads to activation of PI3K and Src kinases and results in cell survival, proliferation and differentiation. Adopted from Fry *et al*. with minor changes made [72].

IL-7 binding to CD127 leads to phosphorylation of key tyrosine residue in the cytoplasmic part of CD127 which becomes a site of PI3K binding. Activated PI3K produces phosphatidylinositol (3,4,5)-triphosphate (PIP3) which activates Akt. Akt is responsible for phosphorylating a plethora of cytoplasmic proteins which thereafter regulate cell survival, size and metabolism [87].

3.2.5. Biological activities

IL-7 plays a critical role in B and T cell development. IL-7 was found to be indispensable for development of B cells in mice, but not in humans [88, 89]. Administration of IL-7 leads to an expansion of both immature and mature B cells in mice [90].

Double negative (DN) thymocytes are at some stages of development critically dependent on IL-7 signaling [91]. Double positive (DP) thymocytes were shown not to respond to IL-7 [72]. However, single positive (SP) recent thymic emigrants regain expression of IL-7R and dependence on IL-7 [92].

IL-7 provides developing T cells with survival signals via induction of bcl-2 [93]. IL-7 upregulates the expression of anti-apoptotic mediator bcl-2 whereas it inhibits the expression of proapoptotic proteins bad and bax [94].

Once T cells leave the thymus, their homeostatic maintenance is dependent on contact with self-peptide/MHC complex and IL-7 [95]. IL-7 is a key cytokine to ensure survival and glucose metabolism of naïve T cell [96]. Naïve T cells fail to survive upon adoptive transfer to IL-7$^{-/-}$ mice [97]. The only exception seems to be Tregs which express low levels of CD127 and are dependent exclusively on IL-2 signaling. However, in case of disrupted IL-2 signaling, IL-7 may contribute to Treg homeostasis [98].

In case of increased availability of IL-7, for example when exogenous IL-7 is injected or under lymphopenic conditions, the cytokine can induce homeostatic proliferation of naïve T cells without the need of encounter their cognate antigen [99].

In vivo levels of IL-7 are tightly regulated in steady-state conditions. It has recently been shown that ILC play a major regulatory role in this process as these cells create an IL-7 sink and their IL-7 consumption limits IL-7 availability for B and T cells. It is worth mentioning that unlike T cells, ILC do not downregulate CD127 after IL-7 signaling [100].

T cells lose their dependence on IL-7 upon activation [80]. However, it was shown that IL-7 administration to mice during the effector phase can prevent T cell exhaustion [101]. IL-7, together with IL-15, contributes to the survival and proliferation of central memory T cells. CD127$^{-/-}$ CD8^{+} T cells fail to become memory T cells after viral infection [97].

IL-7 is a non-redundant cytokine for the development of γδ T cells as IL-7$^{-/-}$ mice entirely lack these cells. Contrary to that, the development of NK is almost unaffected by the absence of this cytokine [102].

Absence of IL-7 or IL-7R results in severe lymphopenia in mice and absence of T cells in humans [72, 88].

3.2.6. Clinical applications

IL-7 is an attractive cytokine for immunotherapy. Naïve T cells respond rapidly to IL-7 stimulation, making this cytokine a possible agent for reconstitution of T cell activities in

patients with impaired T cell populations [103]. Together with the fact that IL-7 doesn't expand Tregs, IL-7 was proposed to have beneficial effects in cancer treatment.

Administration of IL-7 was found effective in several mouse tumor models. IL-7 treatment was shown to increase $CD4^+$ and $CD8^+$ T cell subsets and reduce tumor growth in a mouse LLC Lewis lung carcinoma model. The authors also observed a suppression of activity of the tumor-induced Tregs after IL-7 administration [104]. Similar results were obtained in IL-7-treated mice bearing Meth A fibrosarcoma [105].

The first clinical trial for evaluation of IL-7 antitumor effect was reported in 2006. In this study, patients with metastatic melanoma or metastatic sarcoma were treated with rIL-7. Enhanced counts of $CD4^+$ and $CD8^+$ and unchanged counts of Tregs, B cells, NK cells were observed. Although no significant toxicity of the treatment was found, no objective responses were achieved [106].

In other clinical trial, effects of IL-7 in patients with refractory cancer of various types were studied. Administration of IL-7 led to significant proliferation of both peripheral naïve $CD4^+$ and $CD8^+$ T cells with intact functional capacities. The expansion of these cells resulted in the increase of TCR diversity by an increase of the naïve T cell pool size. Numbers of Tregs were not increased after the treatment. A comparison between IL-2 and IL-7 treatment was also done in this study. IL-2 significantly boosted Tregs and $CD8^+$ effector cells, while IL-7 preferentially expanded naïve $CD4^+$ and $CD8^+$ T cells and, to a lesser extent, memory $CD8^+$ T cells [103].

Low level of anti-IL-7 mAbs was found in sera of some patients in both trials. It was possible because of the lack of glycosylation of this *Escherichia coli* produced IL-7. However, these anti-IL-7 mAbs didn't appear to neutralize endogenous IL-7 [103].

Fully glycosylated IL-7 was used in a clinical trial evaluating the effect of IL-7 on the expansion of the $CD4^+$ T cell pool of HIV-infected patients. IL-7 therapy led to an increased thymic output and an increase of $CD4^+$ and $CD8^+$ cell counts which lasted a year after the last dose but failed to reduce viral load [107]. A more recent study confirmed that administration of IL-7 restored naïve and central memory T cell pool and was well tolerated among HIV patients. However, a clinical benefit of IL-7 treatment in HIV patients remains to be proven [108].

3.2.7. Strategies to improve efficacy of IL-7 based therapy

3.2.7.1. IL-7/anti-IL-7 mAb ic

The phenomenon of increased *in vivo* biological activity of cytokine/anti-cytokine mAb ic in comparison to free cytokine is not unique to IL-2. Enhanced agonistic effect of IL-7ic was reported 13 years before the description of IL-2ic [51]. Currently, there are several papers available reporting that IL-7 potency is significantly improved after it is complexed with anti-IL-7 mAb prior to administration *in vivo*.

Finkelman *et al.* showed that IL-7ic composed of rhIL-7 and neutralizing anti-human-IL-7 mAb M25 (IL-7/M25) were markedly more potent in terms of increasing pre-B cell counts in mice than either agent alone. Three injections of 5 μg of IL-7 premixed with 25 μg of M25 resulted in nine-fold increase in the absolute number of splenocytes in mice whereas the same amount of IL-7 or M25 alone had a negligible effect. The massive increase of the number of splenocytes was found to be caused predominantly by immature $B200^{+}IgM^{-}IgD^{-}$ B cells whose percentage in spleen increased from 2% to 38% after IL-7/M25 administration. A similar expansion of these cells occurred after three IL-7/M25 injections also in bone marrow which, according to the authors, appeared rather white than red. No change in counts of mature B cells was observed in either spleen or bone marrow. The authors also tested *in vivo* biological activity of another IL-7ic consisting of rhIL-7 and non-neutralizing anti-mouse-IL-7 mAb M23 (IL-7/M23). IL-7/M23 failed to have any effects on splenocytes or bone marrow cells [51].

Research of IL-7ic was reopened in 2008 [109]. Boyman *et al.* studied the effects of IL-7/M25 on T cells. They showed that IL-7/M25 had a longer serum half-life compared to free IL-7 in mice. *In vivo* administration of IL-7/M25, but not free IL-7, had a strong mitogenic effect on naïve and memory $CD4^{+}$ and $CD8^{+}$ T cells in both normal and lymphopenic mice. The increase of peripheral T cell numbers after IL-7/M25 administration was mediated by inducing homeostatic proliferation of peripheral T cells rather than by enhancing thymic export. Three doses of IL-7/M25 at 2-day intervals led to an increased cellularity of spleen, lymph nodes and thymus. Expanded cells were shown to be predominantly immature B cells in spleen, which was in accordance with the previous finding of Finkelman *et al*. Mature T cells expanded preferentially in lymph nodes whereas developing DP T cells underwent the most prominent expansion in thymus. 2 doses of IL-7/M25 were able to restore thymopoiesis in $IL\text{-}7^{-/-}$ mice while free IL-7 or M25 alone were not capable to do so. However, the effect of IL-7/M25 was rather short-lived as the $IL\text{-}7^{-/-}$ mice returned to lymphopenic state three weeks after the last dose of IL-7/M25. Carboxyfluorescein succinimidyl ester (CFSE)-labeled $CD45^{+}$ cells isolated

from lymph nodes of CD45.1 mice were adoptively transferred into B6 (CD45.2) congenic mice which were then injected with IL-7, M25 or IL-7/M25 and the fate of the donor cells was observed. Donor mature B cells proliferate minimally whereas significant proliferation of mature T cells was noted in IL-7/M25 treated mice only. $CD4^+$ T cells were less responsive than $CD8^+$ T cells. In another experiment, MP $CD44^{high}$ or naïve $CD44^{low}$ $CD8^+$ T cells were sorted from the lymph nodes of CD45.1 mice and injected into B6 mice after being labeled with CFSE. IL-7/M25 administration induced a prominent expansion of both donor naïve and MP T cells [109]. Injection of M25 alone had no effect in any of the above-mentioned experiments showing that, unlike S4B6, M25 cannot boost the activity of the endogenous cytokine. The authors also tested ability of other anti-IL-7 mAbs, this time anti-mouse, MAB207 and MAB407, to enhance the biological activity of rmIL-7. However, neither IL-7/MAB207 nor IL-7/MAB407 was able to enhance the activity of IL-7 [109].

The object of another study was to shed light on the mechanism whereby M25 increases IL-7 potency [110]. An interesting finding was that even though IL-7/M25 was administered to mice intraperitoneally (i.p.), the stimulation by IL-7/M25 was available to cells within the T cell zones of secondary lymphoid organs as preventing the T cells of IL-7/M25 treated mice from homing to the lymph nodes abolished the proliferation of T cells observed in IL-7/M25-treated mice with untouched ability to egress secondary lymphoid tissues. The authors then described the contribution of FcγR and FcRn to the enhanced *in vivo* potency of IL-7/M25. IL-7/M25-mediated T cell proliferation wasn't affected in FcγR deficient mice but was greatly impaired in FcRn deficient mice suggesting that FcRn extended *in vivo* half-life of the complex. However, IL-7-Fc fusion protein was less potent than IL-7/M25 in terms of induction of proliferation of mature T cells in mice implying there was an additional mechanism besides the involvement of FcRn. M25 ability to enhance IL-7 potency was found to be dose-dependent as increasing molar excess of M25 corelated with decreasing ability of IL-7/M25 to drive T cell proliferation in mice. M25 thus seemed to prevent IL-7/IL-7R interaction when present in excess but to enhance the cytokine biological activity when bound to IL-7. The authors proposed that the unique IL-7 neutralizing specificity of M25 contributed to the activity of IL-7/M25. M25 binding to IL-7 was proposed to prevent the rapid utilization of the cytokine *in vivo* and to increase IL-7 availability by competing with IL-7R [110].

A more recent paper addressed the problem of the decreased number and the worsened function of naïve T cells in elderly individuals. It was shown that only IL-7/M25, but not free IL-7, could restore the homeostatic proliferation of naïve T cells in aged mice [111].

3.3. Immune checkpoints

Immune checkpoints are negative regulators of immune response. CTLA-4 and PD-1 are prototypical examples of such molecules. Blocking these targets using mAbs results in increased activation of the immune system and thus represent promising immunotherapeutic tool for treating various malignant diseases. Durable regression of immunogenic tumors can be achieved in patients when CTLA-4 and PD-1 molecules are inhibited, either alone or in combination [112].

3.3.1. CTLA-4

CTLA-4 (CD152) is a membrane glycoprotein whose expression rise rapidly on T cells upon activation. It is constitutively expressed on Tregs. Its major function is to prevent excessive immune activation by inhibiting activated T cell proliferation and IL-2 production [113]. CTLA-4 exerts its negative regulatory effects via competition with CD28 for CD80/CD86 ligation. Although both CTLA-4 and CD28 can bind CD80/86, CTLA-4 does so with a higher affinity (~10-fold). CTLA-4/CD80-86 ligation not only mediates inhibitory signaling into the activated T cell, but also leads to a decreased availability of CD80/86 co-stimulatory receptors to recently activated CD28-expressing T cells (Fig. 6) [112].

The anti-CTLA-4 mAb termed ipilimumab was the first checkpoint inhibitor to be tested and approved for cancer treatment in humans [112, 114]. A clinical trial conducted on patients with BRAF wild-type metastatic melanoma showed that the response rate of patients treated with ipilimumab was 19% [115]. In 2011, ipilimumab was approved by the FDA for therapy of advanced melanoma. As the immune equilibrium is disrupted when CTLA-4 is blocked, ipilimumab treatment involves adverse effects. Adverse side effects of any grade were reported in 86.2% of ipilimumab-treated patients. The most common side effects include diarrhea, fatigue and pruritis. However, more severe adverse effects, such as induction of colitis or interstitial nephritis, can occur [115].

3.3.2. PD-1

PD-1 (CD279) receptor was initially described to induce activated T cell death [116]. It is expressed by exhausted effector T cells that have been overstimulated or have received reduced help from $CD4^+$ T cells. After interaction with its ligand, it serves as a negative immune checkpoint as PD-1 inhibits T cell proliferation and reduces T cell survival (Fig. 6). It activates an inhibitory pathway in which signaling molecules downstream of TCR are dephosphorylated.

PD-1 interacts with two ligands, programmed death-ligand 1 (PD-L1, CD274) and programmed death-ligand 2 (PD-L2, CD273) [112]. Both ligands have a broad expression on various immune and non-immune cell types, such as antigen-presenting cells and tumor cells [117].

There are currently 5 anti-PD-1 or anti-PD-L1 mAbs approved by FDA for treatment of various cancers [112]. A clinical trial showed that nivolumab treatment led to 44% response rate in metastatic melanoma patients. Combined administration of ipilimumab and nivolumab reached 58% response rate. However, nivolumab treated melanoma patients suffered from adverse effects in 82.1% of cases and combination treated patients in 95.5% of cases. Most of the adverse events provoked by nivolumab or ipilimumab plus nivolumab administration were relatively mild, such as diarrhea or fatigue, although severe complications including colitis appear occasionally [115]. Nivolumab as a monotherapy is currently approved for treatment of various malignant diseases, such as melanoma, urothelial carcinoma, non-small-cell lung cancer, Hodgkin's disease, hepatocellular carcinoma, renal cell carcinoma and head and neck cancer [118].

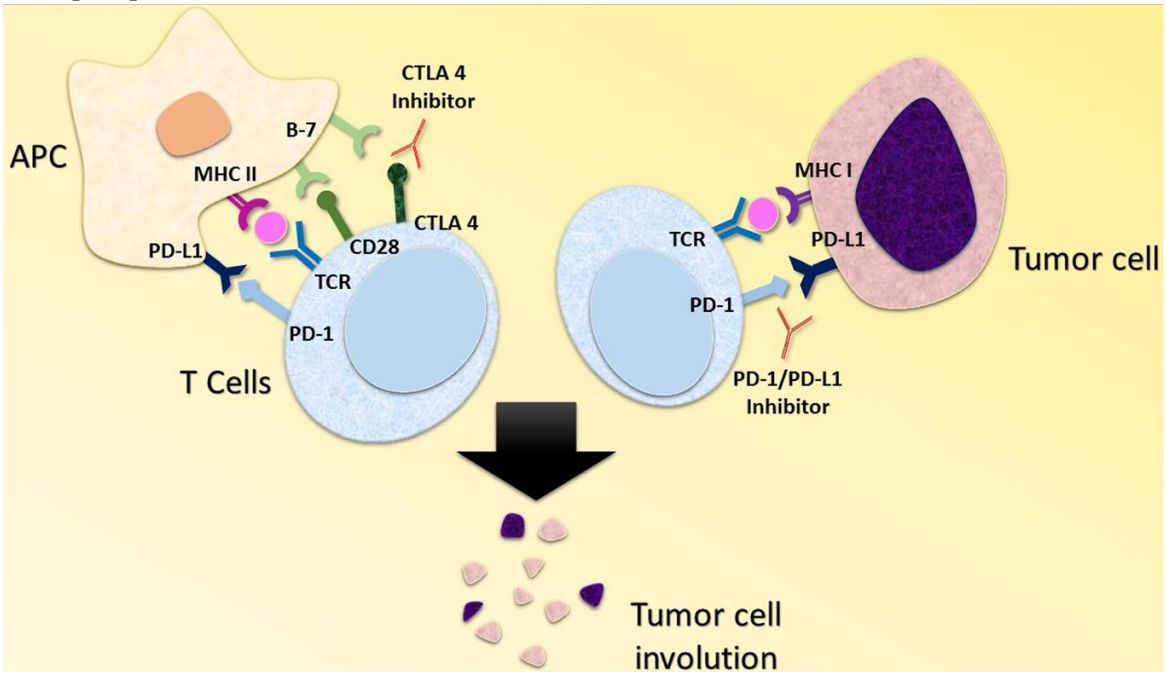

Figure 6. Mechanism of CTLA-4 and PD-1 inhibition of T cell response. CTLA-4 mAb neutralizes CTLA-4 inhibitory receptor on T cells rendering B-7 (CD80/CD86) on APC available for CD28 binding. T cells thus receive a costimulatory signal which is essential for their efficient and long-term activation. Negative regulatory receptor PD-1 is usually overexpressed on effector T cells undergoing exhaustion. Blocking the PD-1 pathway via αPD-1 or αPD-L1 mAbs enables activated T cells to perform their effector functions. CTLA-4 and/or PD-1 inhibition on tumor-specific T cells can lead to tumor cell destruction. Adopted from Chae et al. [119]

4. MATERIALS AND METHODS

4.1. Solutions

Phosphate buffer saline (PBS)

9 g NaCl

1.2 g $Na_2HPO_4 \cdot 12H_2O$

0.2 g $Na_2H_2PO_4 \cdot H_2O$

Distilled H_2O was added to total volume of 1 l. The pH was adjusted to 7.4 by 4 M NaOH.

ELISA blocking buffer

PBS supplemented with 1% bovine serum albumin (BSA, Sigma-Aldrich)

ELISA wash buffer

PBS supplemented with 0.05% TWEEN 20 (Sigma-Aldrich)

AutoMACS separation buffer

PBS supplemented with 0.5% BSA and 2 mM EDTA (Invitrogen)

CFSE staining buffer

PBS supplemented with 0.1% BSA

Flow cytometry buffer

PBS supplemented with 2% fetal calf serum (FCS, Invitrogen) and 2 mM EDTA

RPMI media for cell cultivation

RPMI 1640 (Sigma-Aldrich) supplemented with 10% FCS, 2 mM glutamine (Sigma-Aldrich), 1 mM sodium pyruvate (Sigma-Aldrich), 100 U/ml penicillin (Sigma-Aldrich), 100 µg/ml streptomycin (Sigma-Aldrich), 4.5 g/l glucose (Sigma-Aldrich), 10 mM HEPES (Sigma-Aldrich) and 50 mM 2-merkaptoethanol (Sigma-Aldrich)

4.2. Cells

4.2.1. Tumor cell lines

Murine B16F10 melanoma, CT26 colon carcinoma, EL4 T cell lymphoma and MC38 colon carcinoma tumor cell lines (ATCC) were used in the experiments. The cell lines underwent regular check for the presence of mycoplasma.

4.2.3. Cell cultivation

Cells were kept in complete RPMI 1640 media in culture flasks. Flasks were kept in CO_2 incubator (Sanyo MCo-18AIC, Japan) in atmosphere containing 5% CO_2 at 37°C. Cells were manipulated in laminar flow cabinet (Telestar Bio-II-A/G, Spain) under sterile conditions. The first passage of cells was used for all experiments.

The number of cells was determined using automatic cell counter (Life Technologies C10227, USA).

4.3. Cytokines, mAbs and ic

4.3.1. Cytokines and mAbs used *in vitro* and *in vivo*

RmIL-2 (Peprotech) and rmIL-7 (Miltenyi Biotech) were used in the experiments. Anti-mouse CTLA-4 mAb clone 9H10 (Bioxcell) and anti-mouse PD-1 mAb clone 29F1A12 (Bioxcell) were used when checkpoint inhibitor administration was indicated.

4.3.2. Preparation of ic

IL-2ic were formed by preincubating IL-2 with either anti-mouse IL-2 mAb clone S4B6 (Bioxcell) or anti-mouse IL-2 mAb clone JES6-1A12 (Biolegend) at 2:1 cytokine:mAb molar ratio. It was diluted in PBS to the required concentration after 15 min of incubation at room temperature. IL-7ic were formed by preincubating IL-7 with either anti-human/anti-mouse IL-7 mAb clone M25 (Bioxcell) or anti-mouse IL-7 mAb clone MAB407 (R&D Systems) at 2:1 cytokine:mAb molar ratio. It was diluted in PBS to the required concentration after 15 min of incubation at room temperature.

4.4. Experimental mice

C57BL/6 and BALB/c female mice were obtained from breeding facility at the Institute of Physiology of the CAS, v.v.i. OT-I/CD45.1, OT-II/CD45.1, OT-I (CD45.2) and OT-II (CD45.2) female mice were obtained from breeding facility at the Institute of Microbiology of the CAS, v.v.i. Mice were housed at the laboratory animal experimental facility at the Institute of Microbiology of the CAS, v.v.i. and used for experiments at 2-5 month of age.

4.4.1. In vivo administration of cytokines, mAbs and ic

For analysis of biological activity of IL-2ic and IL-7ic *in vivo*, naïve C57BL/6 or BALB/c were i.p. injected with IL-2 (1 µg), or IL-7 (1 µg), or IL-2/S4B6 (1 µg of IL-2 equivalent (eq.)), or IL-2/JES6-1 (1 µg of IL-2 eq.), or M25 mAb (5 µg), or IL-7/M25 (1 µg of IL-7 eq.), or IL-7/MAB407 (1 µg of IL-7 eq.) as indicated for each experiment. The reagents were administrated in 250 µl of PBS per dose. The control mice were injected with PBS. The injection site was disinfected with Jodisol prior to injection in order to prevent potential infection.

4.5. Isolation of cells from mice and preparation of single cell suspension

Mice were sacrificed by cervical dislocation and their inguinal, brachial, axillar and mesenteric lymph nodes and/or spleen were harvested and placed into C Tubes (Milteyi Biotec) with 5 ml of flow cytometry buffer, AutoMACS separation buffer or cell media depending on the experiment. Organs were kept at room temperature. Organs were homogenized using gentleMACS Tissue Dissociator (Miltenyi Biotec). The cell suspension was filtered through a 70 µm filter (BD Falcon) and centrifuged (250 g, 10 min, 24°C). The supernatant was discarded, and the cell pellet was resuspended in 3 ml of ACK lysing buffer (Sigma-Aldrich) in order to get rid of erythrocytes. The reaction was stopped by adding the respective buffer to total volume of 50 ml. The cells were then centrifuged (250 g, 10 min, 4°C), resuspended in 2-5 ml of the respective ice-cold buffer and filtered through a 30 µm filter (BD Falcon). The cells were kept on ice from this point on.

4.6. $CD4^+$ and $CD8^+$ T cell purification

Single cell suspensions of cells pooled from lymph nodes and spleens of mice were prepared as described in chapter 4.5. The number of cells in suspension was determined. The cells were centrifuged (250 g, 10 min, 4°C) and resuspended in 400 µl of AutoMACS separation buffer per 10^8 total cells. $CD4^+$ or $CD8^+$ T cells were subsequently purified by negative selection using $CD4^+$ or $CD8a^+$ T Cell Isolation Kit, mouse (Miltenyi Biotec). The labeling and purification were done automatically on AutoMACS Pro Separator (Miltenyi Biotec, Germany). The purities were 88% or higher for $CD4^+$ T cells and 93% or higher for $CD8^+$ T cells.

4.7. CFSE staining

Purified $CD4^+$ or $CD8^+$ T cells were prepared as described in chapter 4.6. The number of cells in suspension was determined. Cells were centrifuged (250 g, 10 min, 4°C) and resuspended in ice-cold CFSE staining buffer. Cells were centrifuged (250 g, 10 min, 4°C) again and resuspended in 1 ml of CFSE staining buffer warmed to 37°C per 10^7 total cells. 5 mM CFSE (Vybrant CFDA SE Cell Tracer Kit, Invitrogen) in DMSO was added to cells prior to placing them in a 37°C water bath. 40 ml of ice-cold complete RPMI 1640 media containing 10% FCS was added after 7-10 min incubation to stop the staining procedure. The cells were centrifuged (250 g, 10 min, 4°C) twice, resuspended in complete RPMI 1640 media and kept on ice.

4.8. Flow cytometry

Single cell suspensions of cells from lymph nodes and/or splenocytes of mice were prepared as described in chapter 4.5. The number of cells in suspension was determined. Cells were seeded into 96-well V-bottom plates in 200 µl of flow cytometry buffer at $1x10^6$ cells per well. Plates were centrifuged (250 g, 5 min, 4°C) and each well was resuspended in 20 µl of 10% mouse serum. Plates were kept on ice for 30 min and centrifuged (250 g, 5 min, 4°C) afterwards. Cells were then stained with 10 µl of mix of fluorochrome conjugated mAbs for surface cell antigens and kept on ice in dark for 30 min. Fixable Viability Dye (FVD) was included in the mix so that only viable cells could be used for analysis. Plates were centrifuged (250 g, 5 min, 4°C) twice. Flow cytometry analysis followed subsequently in case surface antigen expression only was of our interest.

FoxP3 Transcription Factor Staining Buffer Set (eBioscience) was used to fixate and permeabilize cells for staining of intracellular markers. It was used following the manufacturer's instructions. After the fixation and permeabilization, cells were stained for intracellular markers Ki67, FoxP3, or IL-10 and kept on ice in dark for 30 min. Plates were centrifuged (250 g, 5 min, 4°C) twice. Cells were transferred into polypropylene tubes in 100 µl of flow cytometry buffer and were analyzed by flow cytometry.

The analysis was performed on LSRII cytometer (BD Biosciences, USA). The data were analyzed using FlowJo software (Tree Star). The basic gating strategy comprised of exclusion of FVD^+ dead cells and doublets.

B220-PE, CD3-eF450, CD3-PeCy7, CD4-FITC, CD4-PerCP, CD8-A700, CD8-V500 (BD Biosciences), CD25-APC, CD25-PE, CD44-PE, CD44-eF450, CD45.1-APC, CD45.1-eF450, CD62L-FITC, CD122-APC, FoxP3-PE, FVD-eF780, Ki67-A700 and NK1.1-APC mAbs were used in flow cytometry experiments. The mAbs were purchased from eBioscience if not stated otherwise.

4.9. *In vitro* T cell proliferation assay

4.9.1. *In vitro* naïve T cell proliferation assay

$CD4^+$ and $CD8^+$ T cells from OT-II and OT-I mice, respectively, were purified under sterile conditions as described in chapter 4.6. The number of cells in suspension was determined. Cells were seeded into 96-well flat-bottom plates in 200 µl of complete RPMI 1640 media at $1x10^5$ cells per well. Cells were incubated with 50 µl of IL-7, or IL-2, or IL-7/M25, or IL-7/MAB407 in concentrations ranging from 0.01 to 100 ng/ml. Plates were then cultured in CO_2 incubator for 72 h. [^{3}H] thymidine (20 kBq, Lacomed) was added for the last 8 h of incubation. Plates were harvested onto glass fiber filters using Harvester 96 Mach 3 (Tomtec, USA) and dried at room temperature. Radioactivity of each well was measured using Microbeta 1450 scintillator (Wallac, Finland).

4.9.2. *In vitro* activated T cell proliferation assay

$CD4^+$ and $CD8^+$ T cells from OT-II and OT-I mice, respectively, were purified under sterile conditions as described in chapter 4.6. The number of cells in suspension was determined. Cells were seeded into 96-well flat-bottom plates in 200 µl of complete RPMI 1640 media supplemented with 10 µg/ml of anti-mouse CD3 mAb (eBioscience) at $1x10^5$ cells/well.

Cells were incubated with 50 µl of IL-7, or IL-2, or IL-7/M25, or IL-7/MAB407 in concentrations ranging from 0.01 to 100 ng/ml. Plates were then cultured in CO_2 incubator for 72 h. [^{3}H] thymidine (20 kBq, Lacomed) was added for the last 8 h of incubation. Plates were harvested onto glass fiber filters using Harvester 96 Mach 3 (Tomtec, USA) and dried at room temperature. Radioactivity of each well was measured using Microbeta 1450 scintillator (Wallac, Finland).

4.10. *In vitro* naïve T cell survival assay

$CD4^+$ and $CD8^+$ T cells from OT-II and OT-I mice, respectively, were purified under sterile conditions as described in chapter 4.6 and labeled with CFSE as described in chapter 4.7. The number of cells in suspension was determined. Cells were seeded into 96-well flat-bottom plates in 200 µl of complete RPMI 1640 media at $5x10^5$ cells per well. Cells were incubated with 50 µl of IL-7, or IL-2, or IL-7/M25, or IL-7/MAB407 in concentrations ranging from 0.01 to 100 ng/ml. Plates were then cultured in CO_2 incubator for 120 h. Cells were then harvested and transferred into 96-well V-bottom plates in 200 µl of flow cytometry buffer. From this point on, the procedure was identical to that described in chapter 4.8. The cell viability, size and CFSE dilution were determined by flow cytometry. Only surface cell markers were stained and analyzed.

4.11. Intracellular staining of IL-10 expression

C57BL/6 mice were i.p. injected with 4 daily doses of IL-7 (1 µg), M25 (5 µg) or IL-7/M25 (1 µg of IL-7 eq.) in 200 µl of PBS. Mice were sacrificed 24 h after the final dose and single cell suspensions from their spleen were prepared as described in chapter 4.5. The number of cells in suspension was determined. Cells were seeded into 96-well flat-bottom plates in 200 µl of complete RPMI 1640 media supplemented with phorbol myristate acetate (PMA, 100 ng/ml, Sigma-Aldrich) and ionomycin (1 µg/ml, Sigma-Aldrich) at $1x10^6$ cells per well. Plates were then cultured in CO_2 incubator for 6 h. Brefeldin A (2.5 µg/ml, Sigma-Aldrich) was added for final 2 h of incubation. Cells were then harvested and transferred into 96-well V-bottom plates in 200 µl of flow cytometry buffer. From this point on, the procedure was identical to that described in chapter 4.8. Surface cell marker expression together with intracellular expression of IL-10 were analyzed by flow cytometry.

4.12. ELISA of cytokine levels in murine serum

BALB/c mice were i.p. injected with 4 daily doses of IL-7 (1 μg), M25 (5 μg) or IL-7/M25 (1 μg of IL-7 eq.) in 200 μl of PBS. Mice were sacrificed by being bled out 48 h after the final dose. Their blood was collected and centrifuged (500 g, 10 min, 4°C). The supernatant was collected and centrifuged again (500 g, 10 min, 4°C) in order to get sera. Mouse IFN-γ, IL-4, IL-6, IL-10 or transforming growth factor beta (TGF-β) DuoSet ELISA kits (R&D Systems) were used to determine cytokine levels from sera following the manufacturer's instructions.

Briefly, 96-well plate was coated with capture antibody and incubated overnight at room temperature. The plate was washed 3-times with ELISA wash buffer using automatic ELISA washer (Bio-Rad). The plate was blocked by adding ELISA blocking buffer for 1 h. The plate was washed 3-times with ELISA wash buffer. Sera samples and standards were added afterwards and incubated for 2 h. The plate was washed 3-times with ELISA wash buffer. Detection antibody was added and incubated for 2 h. The plate was again washed 3-times with ELISA wash buffer. Streptavidin-horse radish peroxidase conjugate was added to wells. The plate was incubated in dark for 20 min. The plate was washed 3-times with ELISA wash buffer. Tetramethylbenzidine (R&D Systems) substrate was subsequently added, and the plate was incubated 15 min in dark. The color change in sample and standard wells were checked. The reaction was stopped by adding 2M H_2SO_4 in the wells. ELISA microplate reader (Bio-Rad) set to 450 nm and 650 nm was used to measure the optical density of each well. The cytokine concentration in sera was calculated from standard calibration curve determined by GraphPad Prism 8 software (GraphPad Software).

4.13. Adoptive transfer experiments

$CD4^+$ and $CD8^+$ T cells from OT-II and OT-I mice, respectively, were purified as described in chapter 4.6. The cells were counted and adoptively transferred into C57BL/6 (CD45.2) recipient mice via intravenous (i.v.) tail vein injection at $7.5x10^5$ $CD8^+$ and $1.5x10^6$ $CD4^+$ T cells/mouse. Mice were either left untreated (negative control) or treated with i.p. injected (75 μg) of Ovalbumin (75 μg) (Sigma-Aldrich) 24 h after the cell transfer. Mice were treated 8 h later with 4 daily i.p. doses of IL-2 (1-1.5 μg), IL-7 (1 μg), IL-2/S4B6 (1-1.5 μg of IL-2 eq.), IL-2/JES6-1 (1-1.5 μg of IL-2 eq.), IL-7/M25 (1 μg of IL-7 eq.) or IL-7/MAB407 (1 μg of IL-7 eq.) as indicated for each experiment. In some experiments, αCTLA-4 (100 μg) plus

αPD-1 (100 µg) mAbs were i.p. administrated at indicated time points. All reagents were administrated in 250 µl of PBS.

Recipient mice were sacrificed by cervical dislocation 24 h after the final dose and their spleens were harvested. Single cell suspensions of splenocytes were prepared as described in chapter 4.5. A subsequent flow cytometry analysis of the donor cells followed. The flow cytometry procedure was performed as described in chapter 4.8. Only surface cell markers were stained and analyzed.

4.14. Tumor therapy experiments

4.14.1. *In vivo* inoculation of tumor cells

Media containing soluble EL4 T cell lymphoma cells was aspirated from culture flask and centrifuged (250 g, 5 min, 4°C). Cell pellets were resuspended in ice-cold PBS and viable cells were counted. The right dorsal flank of C57BL/6 mice was shaved by electric clippers and 100 µl of the tumor cell suspension was subcutaneously (s.c.) injected. EL4 T lymphoma cells were injected at $1x10^5$ cells/mouse.

Media from flasks with adherent tumor cell lines (B16F10, CT26 and MC38) was removed and cells were washed with EDTA. Trypsin-EDTA mixture was added to cover the cell layer and the flasks were incubated at room temperature until cells detachment. Trypsinization then was stopped by adding 3 ml of FCS. Cells were then aspirated from the flask and centrifuged (250 g, 5 min, 4°C). Cell pellets were resuspended in ice-cold PBS and viable cells were counted. The right dorsal flank of C57BL/6 (B16F10, MC38) or BALB/c (CT26) mice was shaved by electric clippers and 100 µl of the tumor cell suspension was s.c. injected. B10F10 melanoma cells were injected at $5x10^5$ cells/mouse. CT26 colon carcinoma cells were injected at $2x10^5$ cells per mouse. MC38 colon carcinoma cells were injected at $5x10^5$ cells/mouse.

4.14.2. Tumor treatment regimen

Tumor-bearing mice were treated with IL-2/S4B6 (1-2.5 µg of IL-2 eq.), IL-7 (1 µg), IL-7/M25 (1 µg of IL-7 eq.) or IL-7/MAB407 (1 µg of IL-7 eq.) and/or αCTLA-4 (15-100 µg) plus αPD-1 (15-100 µg) mAbs at indicated time points via i.p. injection. One group of mice

was left untreated and served as a control. All reagents were administrated in 250 µl of PBS. The experimental group treated with αCTLA-4 plus αPD-1 mAbs is referred to as mAbs group.

4.14.3. Assessment of therapeutic effects of the treatment

The tumor area was assessed by measuring its length and width by caliper every 2-5 days. Tumor area presented in graphs was calculated as length x width. Survival of experimental mice was recorded. Mice surviving for more than 120 days with no signs of disease were considered to be cured.

4.15. Statistical analysis

Data are presented as means +/- SD, unless stated otherwise. Statistical significance was determined by two-tailed unpaired Student t test. Statistical significance of mice survival experiments was determined by log-rang Mantel-Cox test. P values of $*p < 0.05$, $**p < 0.01$ and $***p < 0.001$ were considered statistically significant.

5. RESULTS

5.1. T cell stimulatory activity and antitumor effect of IL-2ic

5.1.1. Effects of IL-2ic on recently activated T cells *in vivo*

The expansion of activated $CD8^+$ T cells driven by IL-2/S4B6 and IL-2/JES6-1 has already been reported [52]. However, our knowledge is rather limited regarding expansion of recently activated $CD4^+$ T cells by IL-2ic. To test whether IL-2ic are more potent than free IL-2 in terms of expansion of recently activated $CD4^+$ T cells, we conducted an adoptive transfer experiment.

Purified OT-I/CD45.1 $CD8^+$ and OT-II/CD45.1 $CD4^+$ T cells were i.v. transferred into C57BL/6 (CD45.2) congenic recipient mice (n=3) at $7.5x10^5$ and $1.5x10^6$ cells per mouse, respectively. One group of mice was left untreated and served as a negative control. Other groups received i.p. injection of ovalbumin (OVA) 24 h after the cell transfer. Mice were further treated with 4 daily doses of free IL-2 (1 μg), IL-2/S4B6 (1 μg of IL-2 eq.), IL-2/JES6-1 (1 μg of IL-2 eq.) (Fig. 7A). Spleens of the recipient mice were harvested 24 h after the final dose and the donor T cells were analyzed by flow cytometry.

As expected, both IL-2/S4B6 and IL-2/JES6-1 were significantly more potent in mediating expansion of OVA-activated donor OT-I $CD8^+$ T cells than free IL-2. IL-2/JES6-1 induced greater expansion of activated $CD8^+$ T cells than IL-2/S4B6 (Fig. 7B, 7D). Free IL-2 induced 5.5-fold expansion compared to the negative control whereas IL-2/S4B6 and IL-2/JES6-1 mediated 17.9 and 222.4-fold expansion of the adoptively transferred $CD8^+$ T cell population, respectively (Fig. 7B, 7D).

However, neither IL-2/S4B6 nor IL-2/JES6-1 were able to mediate expansion of activated $CD4^+$ OT-II T cells (Fig. 7B, 7C).

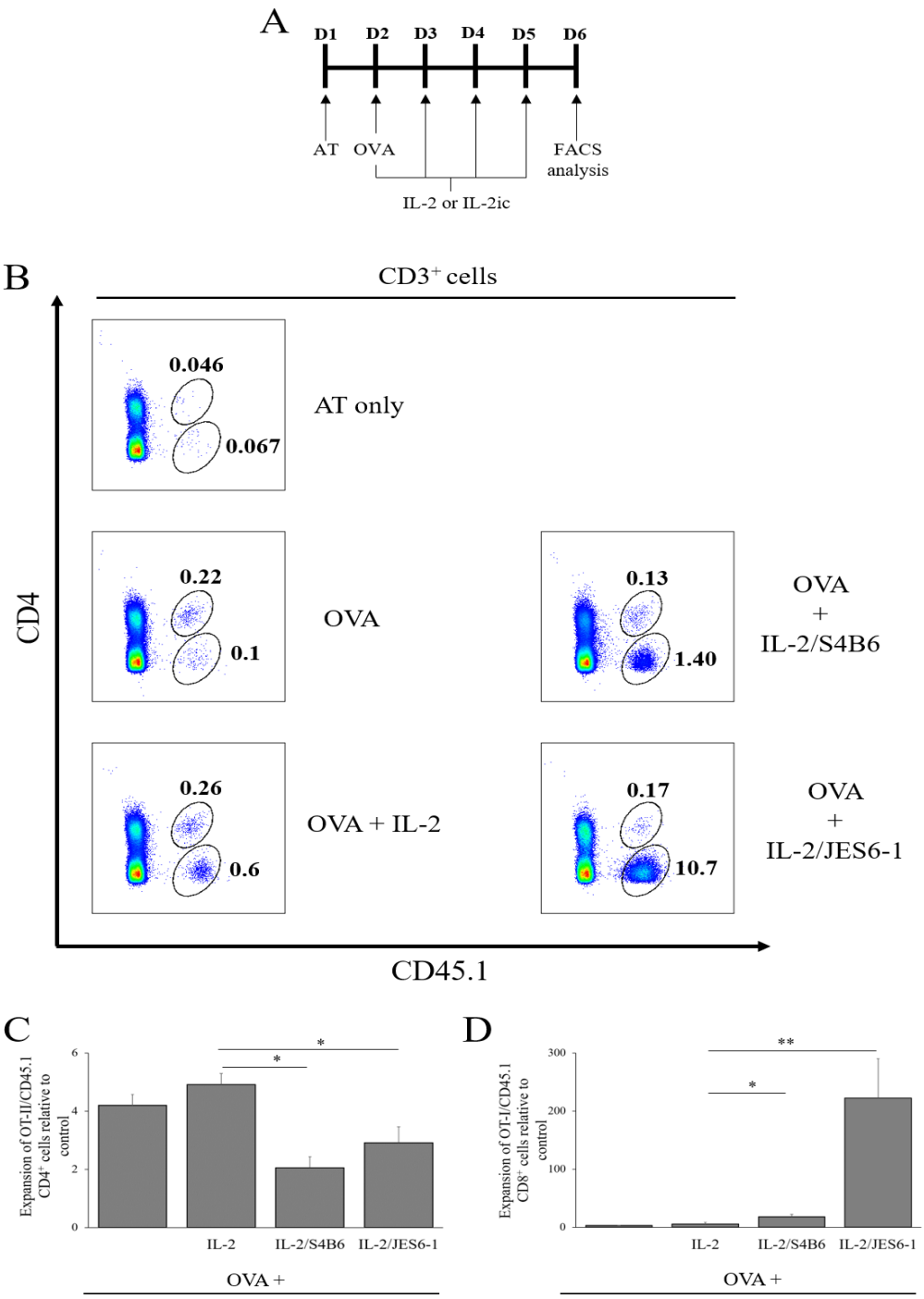

Figure 7. IL-2ic drive massive expansion of recently activated CD8$^+$ T cells but not recently activated CD4$^+$ T cells. (**A**) Schema of the adoptive transfer experiment. 7.5x10^5 OT-I/CD45.1 CD8$^+$ and 1.5x10^6 OT-II/CD45.1 CD4$^+$ T cells were adoptively transferred (AT) into C57BL/6 (CD45.2) recipient mice (n=3) and stimulated with i.p. administrated OVA (75 µg). Mice were then either left with no further treatment or injected with IL-2 (1 µg), IL-2/S4B6 (1 µg of IL-2 equivalent (eq.)) or IL-2/JES6-1 (1 µg of IL-2 eq.) for 4 consecutive days. Negative control group (AT only) was left untreated after the cell transfer. Mice were sacrificed 24 h after the final dose and single-cell suspensions of their spleens were analyzed by flow cytometry. (**B**) Relative expansion of activated donor CD3$^+$CD8$^+$ T cells (CD3$^+$CD45.1$^+$ CD4$^-$, lower gate) and CD3$^+$CD4$^+$ T cells (CD3$^+$CD45.1$^+$ CD4$^+$, upper gate). One representative mouse is shown. Quantification of relative numbers of donor OT-II/CD45.1 CD4$^+$ (**C**) and OT-I/CD45.1 CD8$^+$ T cells (**D**) relative to negative control. Data are presented as means +/- SD. Statistical significance was determined by two-tailed unpaired Student t test, *p < 0.05, **p < 0.01.

5.1.2. Expansion of recently activated $CD8^+$ T cells mediated by IL-2ic and αCTLA-4 plus αPD-1 mAbs

One of our goals was to find out whether expansion of recently activated T cells driven by IL-2ic would be further potentiated by CTLA-4 plus PD-1 blockade. As $CD8^+$ T cells are believed to be the key players in tumor cell eradication, we decided to omit $CD4^+$ T cells in following experiments.

5.1.2.1. Expansion of SIINFEKL-activated OT-I $CD8^+$ T cells mediated by IL-2ic and αCTLA-4 plus αPD-1 mAbs

To test our hypothesis, we performed an adoptive transfer experiment. Purified OT-I/CD45.1 $CD8^+$ T cells were adoptively transferred into C57BL/6 (CD45.2) recipient mice (n=3) at $7.5x10^5$ cells per mouse and activated with i.p. injection of SIINFEKL peptide (4 µg) next day. One group of mice was left untreated and served as a negative control. The other groups were injected with either 1 single dose of poly I:C (75 µg) or 4 daily doses of IL-2/S4B6 (1.5 µg of IL-2 eq.) or IL-2/JES6-1 (1.5 µg of IL-2 eq.) with or without αCTLA-4 (100 µg) plus αPD-1 (100 µg) mAbs (mAbs) (Fig. 8A). Mice were sacrificed and their spleens were harvested 24 h after the final dose and analyzed by flow cytometry.

SIINFEKL peptide alone caused 3.7-fold expansion of donor $CD8^+$ T cells in comparison to the negative control (Fig. 8B, 8C). There was about 7-fold expansion when SIINFEKL peptide was injected together with poly I:C (Fig. 8B, 8C). Activated $CD8^+$ T cells from IL-2/S4B6-treated mice showed 30-fold expansion on average. About the same expansion of activated $CD8^+$ T cells was observed in mice with simultaneous administration of IL-2/S4B6 and αCTLA-4 plus αPD-1 mAbs (Fig. 8B, 8C). IL-2/JES6-1 alone expanded the activated $CD8^+$ T cells by 83-fold. Simultaneous treatment with αCTLA-4 plus αPD-1mAbs didn't lead to any further potentiation (Fig. 8B, 8C).

Next, we analyzed CD25 expression on the donor OT-I/CD45.1 $CD8^+$ T cells in order to check the activation status of these cells. There was no significant difference between IL-2/S4B6 treatment alone and in combination with αCTLA-4 plus αPD-1 mAbs. The relative numbers of $CD25^+$ cells within all OT-I/CD45.1 $CD8^+$ T cells were on average 22.1 and 28.8%, respectively (Fig. 9). The same phenomenon was observed for IL-2/JES6-1 treatment alone and in combination with blocking mAbs. The average numbers of $CD25^+$ cells within the adoptively transferred cells were 51.9 and 52.4%, respectively (Fig. 9).

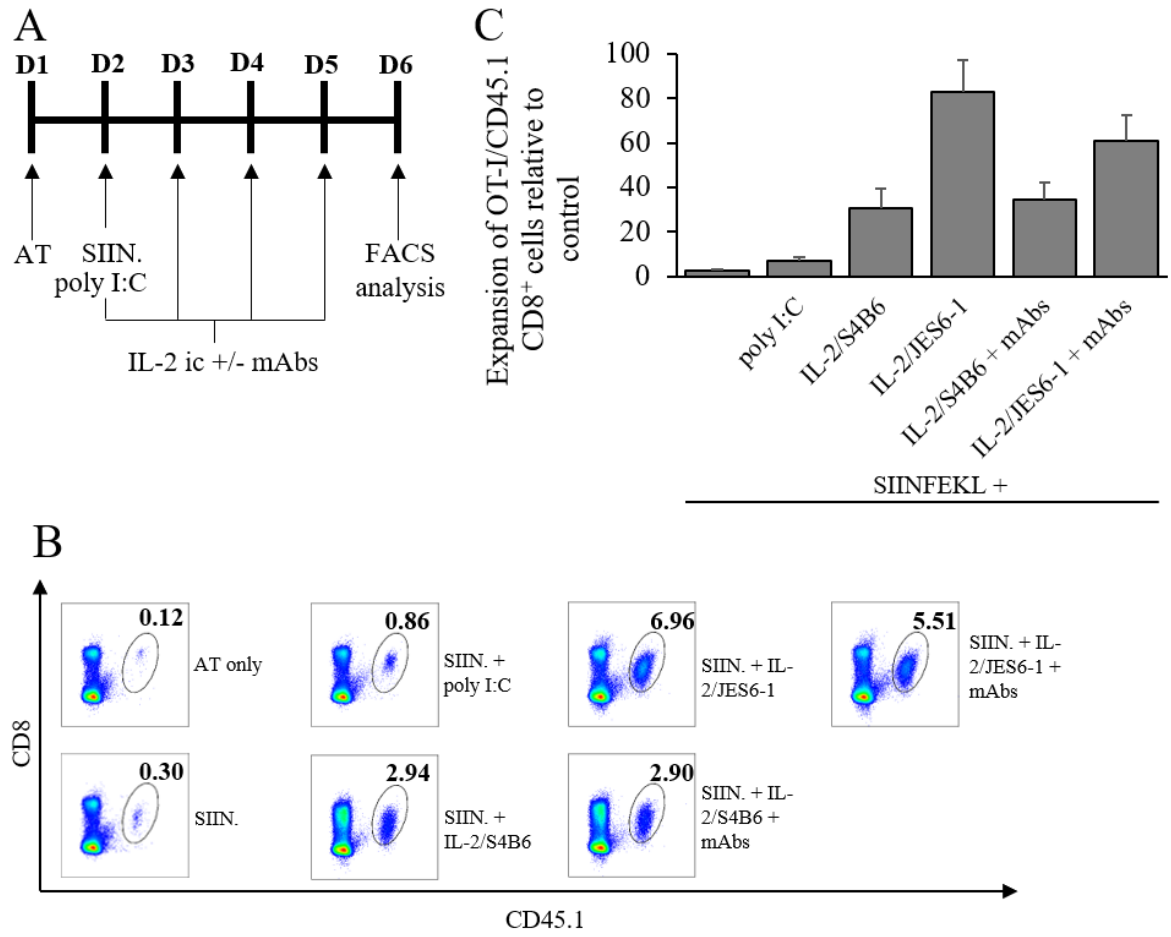

Figure 8. CTLA-4 plus PD-1 blockade doesn't potentiate expansion of SIINFEKL-activated adoptively transferred OT-I/CD45.1 CD8$^+$ cells driven by IL-2ic. (A) Schema of the adoptive transfer experiment. 7.5x10^5 OT-I/CD45.1 CD8$^+$ T cells were adoptively transferred (AT) into C57BL/6 (CD45.2) recipient mice (n=3) and stimulated with i.p. administrated SIINFEKL (SIIN., 4 µg). Mice were then either left with no further treatment or injected with either one single dose of poly I:C (75 µg) or 4 daily doses IL-2/S4B6 (1.5 µg of IL-2 equivalent), IL-2/JES6-1 (1.5 µg of IL-2 eq.) with or without simultaneous injection of αCTLA-4 mAb (100 µg) plus αPD-1 mAb (100 µg) (=mAbs). Negative control group (AT only) was left untreated after the cell transfer. Mice were sacrificed 24 h after the final dose and single-cell suspensions of their spleens were analyzed by flow cytometry. (**B**) Relative expansion of activated donor CD45.1$^+$CD8$^+$ T cells. One representative mouse is shown. (**C**) Quantification of relative numbers of donor OT-I/CD45.1 CD8$^+$ T cells relative to negative control. Data are presented as means +/- SD. Statistical significance was determined by two-tailed unpaired Student t test.

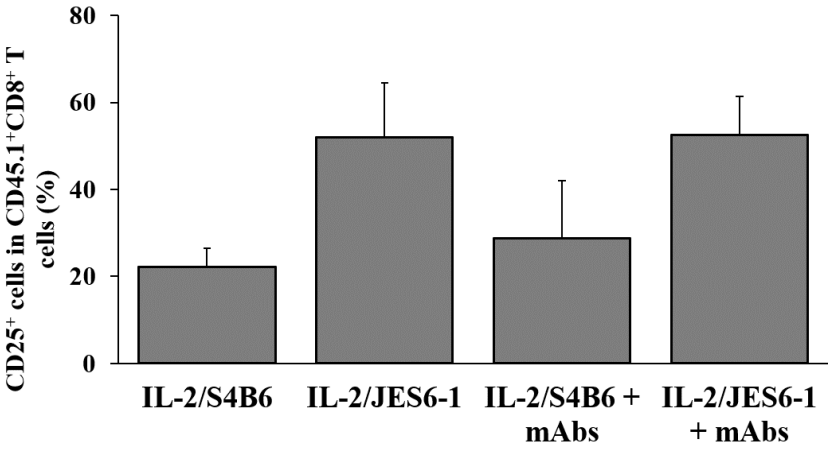

Figure 9. CTLA-4 plus PD-1 blockade doesn't increase CD25 expression on SIINFEKL-activated OT-I/CD45.1 CD8$^+$ T cells expanded by IL-2ic. The donor CD45.1$^+$CD8$^+$ T cells from the experiment described in Fig.8 were flow analyzed for CD25 expression by flow cytometry. Percentage of CD25$^+$ cells within CD45.1$^+$CD8$^+$ T cells in spleen 4 days after cell activation is shown. Data are presented as means +/- SD. Statistical significance was determined by two-tailed unpaired Student t test.

5.1.2.2. Expansion of OVA-activated OT-I CD8$^+$ T cells mediated by IL-2ic and αCTLA-4 plus αPD-1 mAbs

CTLA-4 plus PD-1 blockade didn't potentiate expansion of recently activated T cells driven by IL-2ic (Fig. 8B, 8C). However, SIINFEKL peptide was used to activate OT-I CD8$^+$ T cells in the experiment. SIINFEKL is a small peptide which might, upon i.p. injection, immediately bind to any MHC-I molecule and directly activate OT-I CD8$^+$ T cells without going through the antigen-presenting machinery in secondary lymphoid organs. The effect of CTLA-4 plus PD-1 blockade thus might not be noticeable.

In order to create a more physiologic situation, we decided to use OVA to activate T cells in the next experiment. OVA is a large molecule which needs to be fragmented and presented via APC. CTLA-4 and PD-1 blockade thus might manifest in this case.

The adoptive transfer was carried out as described previously (Fig. 10A). OVA induced donor cell activation and 3.2-fold expansion in spleen when compared to the negative control (Fig. 10B, 10C). The addition of poly I:C led to 10.8-fold expansion of OT-I/CD45.1 CD8$^+$ T cells. IL-2/S4B6 treatment caused 15.5-fold expansion of the OVA-activated CD8$^+$ T cells. The relative number of OT-I CD8$^+$ T cells increased significantly in hosts which underwent simultaneous IL-2/S4B6 and αCTLA-4 plus αPD-1 mAbs treatment. We observed 76.4-fold expansion of the adoptively transferred cell population in this case (Fig. 10B, 10C). IL-2/JES6-1 treatment alone induced 48.7-fold expansion of OVA-activated CD8$^+$ T cells. Combination of IL-2/JES6-1 administration with checkpoint blockade led to mild, but not statistically significant increase, as there was a 70-fold expansion of the activated donor cells in this group (Fig. 10B, 10C).

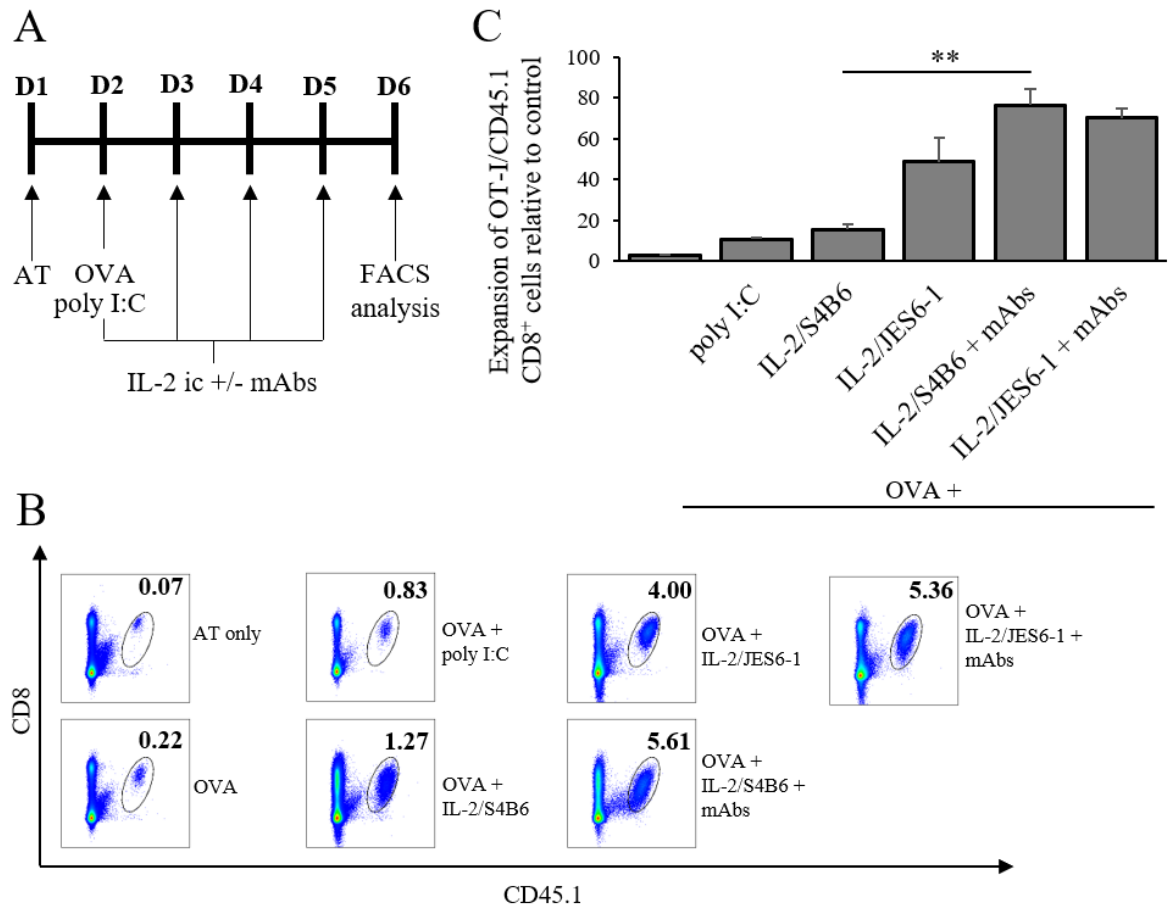

Figure 10. CTLA-4 plus PD-1 blockade potentiates expansion of OVA-activated adoptively transferred OT-I/CD45.1 CD8$^+$ cells driven by IL-2/S4B6. (**A**) Schema of the adoptive transfer experiment. 7.5x10^5 OT-I/CD45.1 CD8$^+$ T cells were adoptively transferred (AT) into C57BL/6 (CD45.2) recipient mice (n=3) and stimulated with i.p. administrated OVA (75 µg). Mice were then either left with no further treatment or injected with either one single dose of poly I:C (75 µg) or 4 daily doses IL-2/S4B6 (1.5 µg of IL-2 equivalent (eq.)) or IL-2/JES6-1 (1.5 µg of IL-2 eq.) with or without simultaneous injection of αCTLA-4 mAb (100 µg) plus αPD-1 mAb (100 µg) (mAbs). Negative control group (AT only) was left untreated after the cell transfer. Mice were sacrificed 24 h after the final dose and single-cell suspensions of their spleens were analyzed by flow cytometry. (**B**) Relative expansion of activated donor CD45.1$^+$CD8$^+$ T cells. One representative mouse is shown. (**C**) Quantification of relative numbers of donor OT-I/CD45.1 CD8$^+$ T cells relative to negative control. Data are presented as means +/- SD. Statistical significance was determined by two-tailed unpaired Student t test, **p < 0.01.

We also checked CD25 expression in donor OT-I/CD45.1 CD8$^+$ T cells in order to confirm our previous finding. Again, we observed a significant difference between IL-2/S4B6 alone and IL-2/S4B6 combined with checkpoint blockade-treated mice. The relative numbers of CD25$^+$ cells within CD45.1$^+$CD8$^+$ T cells were 14.4 and 32%, respectively (Fig. 11). There was no significant difference between IL-2/JES6-1 treatment alone and in combination with αCTLA-4 plus αPD-1 mAbs. The relative numbers of CD25$^+$ cells within all OT-I/CD45.1 CD8$^+$ T cells were on average 50.4 and 59.6%, respectively (Fig. 11).

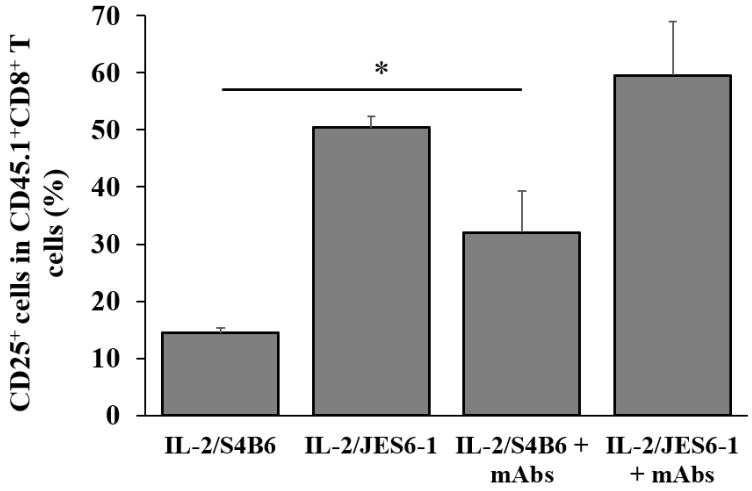

Figure 11. CTLA-4 plus PD-1 blockade increases CD25 expression on OVA-activated OT-I/CD45.1 CD8$^+$ T cells expanded by IL-2/S4B6. The donor CD45.1$^+$CD8$^+$ T cells from the experiment described in Fig. 10 were analyzed by flow cytometry for CD25 expression. Percentage of CD25$^+$ cells within CD45.1$^+$CD8$^+$ T cells in spleen 4 days after cell activation is shown. Data are presented as means +/- SD. Statistical significance was determined by two-tailed unpaired Student t test, *$p < 0.05$.

5.1.3. Antitumor activity of IL-2/S4B6 in combination with αCTLA-4 plus αPD-1 mAbs

IL-2/S4B6 has been shown to induce a massive expansion of MP CD8$^+$ T cells and NK cells *in vivo*, while Tregs were only moderately affected [49]. Antitumor activity of IL-2/S4B6 treatment has already be proven in several mouse tumor models [50, 52]. Potent anticancer properties of checkpoint inhibitors have been documented many times in both mice and humans [112].

According to our previous finding, CTLA-4 and PD-1 inhibition further augmented expansion of recently activated CD8$^+$ T cells driven by IL-2/S4B6 (Fig. 10). We thus presumed that there might be a synergistic effect between these immunotherapeutic approaches. To test our hypothesis, we performed a set of experiments in several mouse tumor models and compared the antitumor properties of either agent alone or in combination.

5.1.3.1. IL-2/S4B6 and αCTLA-4 plus αPD-1 mAbs combination therapy in CT26 tumor model

We tested possible synergism of antitumor effects of IL-2/S4B6 and αCTLA-4 plus αPD-1 mAbs in syngeneic orthotopic CT26 colorectal carcinoma model. BALB/c mice (n=6) were s.c. inoculated with $2x10^5$ CT26 tumor cells on day 0. Mice received i.p. injection of PBS or IL-2/S4B6 (2.5 μg of IL-2 eq.) on days 4, 5, 6 and/or αCTLA-4 (100 μg) plus αPD-1 (100 μg) mAbs on days 7, 10 and 13 (Fig. 12A). Tumor size was measured, and survival of mice was recorded.

IL-2/S4B6 monotherapy failed to have any effect on either tumor growth (Fig. 12B) or survival of the experimental animals (Fig. 12C). On the contrary, CTLA-4 plus PD-1 blockade was efficient in reducing the tumor burden with 3 out of 6 mice being long-term survivors (Fig. 12B, 12C). No beneficial effect over the checkpoint inhibition therapy alone was observed when mice were treated with both IL-2/S4B6 and αCTLA-4 plus αPD-1 mAbs (Fig. 12B, 12C).

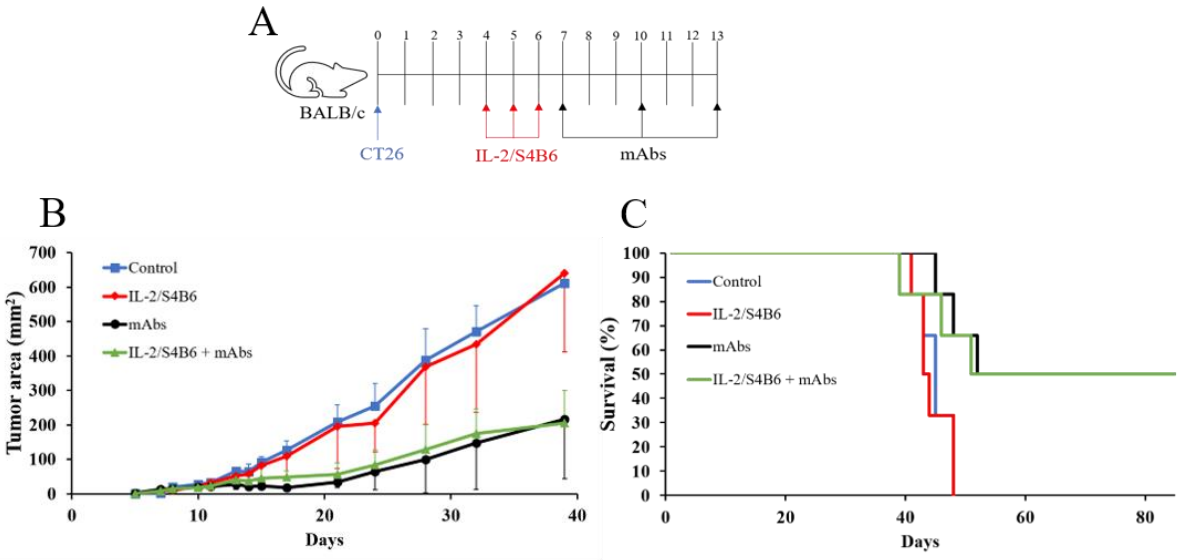

Figure 12. IL-2/S4B6 don't improve the antitumor effect of αCTLA-4 plus αPD-1 mAbs in mouse CT26 colon carcinoma tumor model. (A) Schema of the tumor therapy experiment. BALB/c mice (n=6) were s.c. inoculated with $2x10^5$ CT26 cells in 100 µl PBS on day 0. Mice were i.p. injected with PBS (control) or IL-2/S4B6 (2.5 µg of IL-2 eq.) on days 4, 5, 6 and/or αCTLA-4 (100 µg) plus αPD-1 (100 µg) mAbs (mAbs) on days 7, 10 and 13. (**B**) Growth of CT26 tumors (mean +/- SD). (**C**) Experimental mice survival. Statistical significance was determined by two-tailed unpaired Student t test for tumor growth assessment and log-rang Mantel-Cox test for survival analysis.

5.1.3.2. IL-2/S4B6 and αCTLA-4 plus αPD-1 mAbs combination therapy in MC38 tumor model

We observed no additive effect in anticancer activity of IL-2/S4B6 and αCTLA-4 plus αPD-1 mAbs combination therapy in CT26 tumor model (Fig 12B, 12C). However, IL-2/S4B6 alone showed no efficacy in this model. We decided to test whether CTLA-4 plus PD-1 blockade could benefit from the addition of IL-2/S4B6 in syngeneic orthotopic MC38 colon carcinoma as antitumor effect of IL-2/S4B6 has already been described for this model [50].

C57BL/6 mice (n=8) were s.c. inoculated with $5x10^5$ MC38 tumor cells on day 0. Mice received i.p. injection of PBS or IL-2/S4B6 (2.5 µg of IL-2 eq.) on days 5, 6, 7 and/or αCTLA-4 (15 µg) plus αPD-1 (15 µg) mAbs on days 7, 10 and 13 (Fig. 13A). We decided to lower the dosage of αCTLA-4 plus αPD-1 mAbs from 100 µg to 15 µg in comparison to the previous experiment (Fig. 12) in order to enable the manifestation of possible additive effect of IL-2/S4B6.

IL-2/S4B6 treatment alone didn't show any effect in either tumor growth inhibition (Fig. 13B) or mice survival (Fig. 13C). The growth of MC38 tumors in αCTLA-4 plus αPD-1 mAbs-treated mice wasn't significantly inhibited in comparison to the control group (Fig. 13B). However, the checkpoint inhibition alone led to a complete cure of 2 out of 8 experimental mice (Fig. 13C). No additional value of IL-2/S4B6 was observed as none of the mice treated with the dual therapy survived the experiment (Fig. 13C).

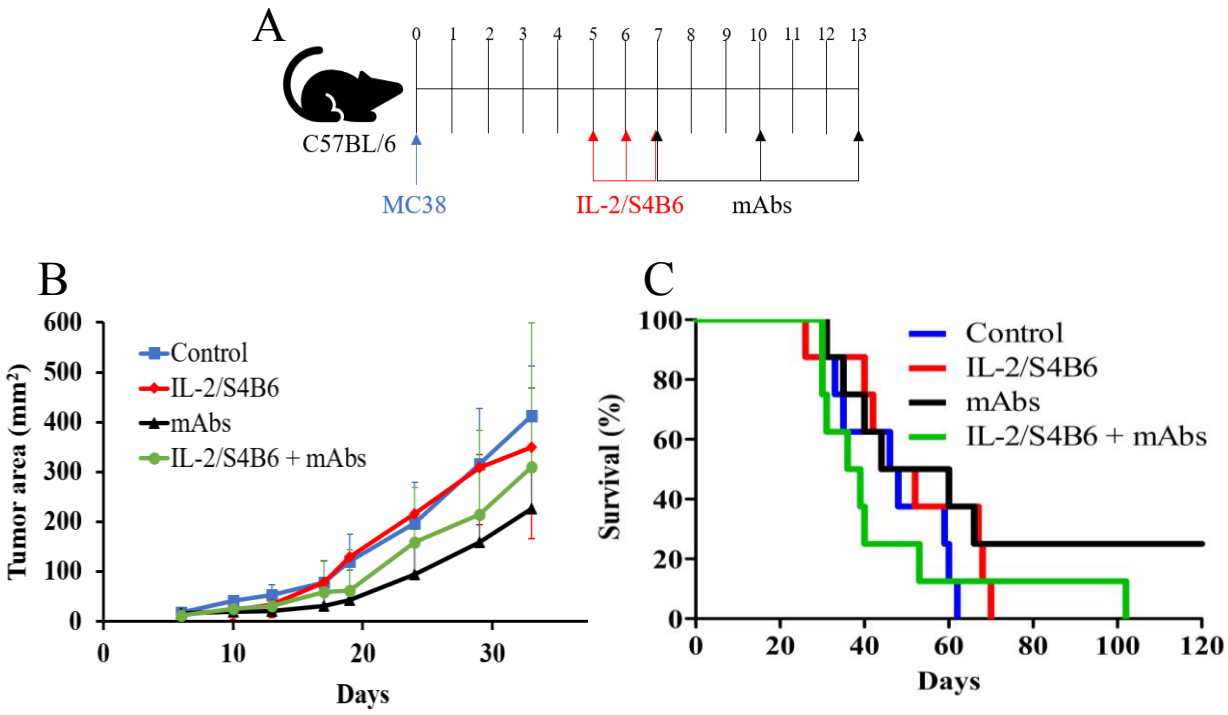

Figure 13. IL-2/S4B6 don't improve the antitumor effect of αCTLA-4 plus αPD-1 mAbs in mouse MC38 colon carcinoma tumor model. (A) Schema of the tumor therapy experiment. C57BL/6 mice (n=8) were s.c. inoculated with $5x10^5$ MC38 cells in 100 µl PBS on day 0. Mice were i.p. injected with PBS (control) or IL-2/S4B6 (2.5 µg of IL-2 eq.) on days 5, 6, 7 and/or αCTLA-4 (15 µg) plus αPD-1 (15 µg) mAbs (mAbs) on days 7, 10 and 13. (**B**) Growth of MC38 tumors (mean +/- SD). (**C**) Experimental mice survival. Statistical significance was determined by two-tailed unpaired Student t test for tumor growth assessment and log-rang Mantel-Cox test for survival analysis.

5.1.3.3. IL-2/S4B6 and αCTLA-4 plus αPD-1 mAbs combination therapy in MC38 tumor model using higher dosage

IL-2/S4B6 treatment has shown very little antitumor effect so far (Fig. 12, 13). In our next experiment, we thus decided to adopt the exact dosing regimen of IL-2/S4B6 that had previously been proven efficient [50].

C57BL/6 mice (n=7) were s.c. inoculated with $5x10^5$ MC38 tumor cells on day 0. Mice received i.p. injection of PBS or IL-2/S4B6 (1.5 µg) on days 4, 5, 6, 7 and 8 and/or αCTLA-4 (40 µg) plus αPD-1 (40 µg) mAbs on days 7, 10 and 13 (Fig. 14A).

IL-2/S4B6 alone slightly, but not significantly, slowed down the MC38 tumor progression (Fig. 14B). It also slightly prolonged survival of mice with 1 out of 7 mice being completely cured (Fig. 14C). Treatment with αCTLA-4 plus αPD-1 mAbs as a monotherapy led to significant antitumor response. Significant reduction of the tumor burden compared to the control group was observed (Fig. 14B) as well as complete cure of 4 out of 7 mice (Fig. 14C). The combination treatment, however, didn't bring any extra value (Fig. 14B). Significant prolongation of lifespan was observed in the group receiving combination therapy in comparison to the control. However, only 2 out of 7 mice were long-term survivors (Fig. 14C) so the combination therapy tended to worsen the outcome in comparison to the checkpoint inhibition therapy alone.

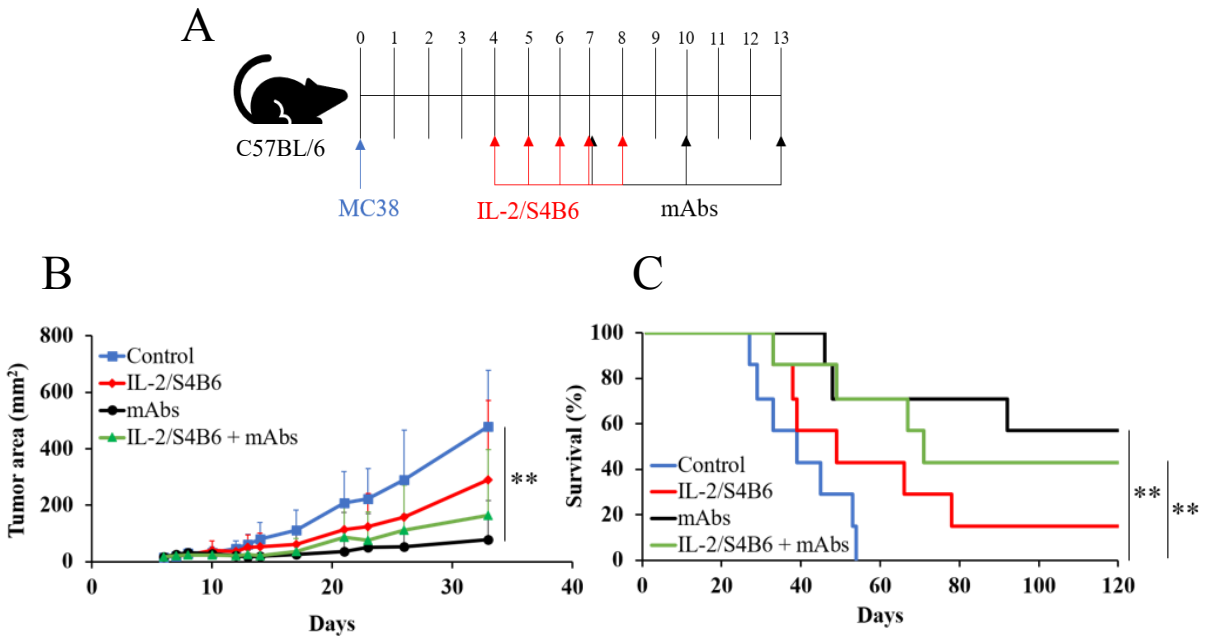

Figure 14. IL-2/S4B6 don't improve the antitumor effect of αCTLA-4 plus αPD-1 mAbs in mouse MC38 colon carcinoma tumor model. (A) Schema of the tumor therapy experiment. C57BL/6 mice (n=7) were s.c. inoculated with $5x10^5$ MC38 cells in 100 µl PBS on day 0. Mice were i.p. injected with PBS (control) or IL-2/S4B6 (1.5 µg of IL-2 eq.) on days 4, 5, 6, 7 and 8 and/or αCTLA-4 (40 µg) plus αPD-1 (40 µg) mAbs (mAbs) on days 7, 10 and 13. (**B**) Growth of MC38 tumors (mean +/- SD). (**C**) Experimental mice survival. Statistical significance was determined by two-tailed unpaired Student t test for tumor growth assessment and log-rang Mantel-Cox test for survival analysis, **p < 0.01.

5.1.3.4. IL-2/S4B6 and αCTLA-4 plus αPD-1 mAbs combination therapy in EL4 lymphoma tumor model

Despite to previous unfavorable results, we decided to test whether IL-2/S4B6 would mediate improved responses of checkpoint inhibitor therapy in one more experimental tumor model, EL4 T cell lymphoma.

C57BL/6 mice (n=8) were s.c. inoculated with $1x10^5$ EL4 tumor cells on day 0. Mice received i.p. injection of PBS or IL-2/S4B6 (2.5 µg of IL-2 eq.) on days 5, 6 and 7 and/or αCTLA-4 (100 µg) plus αPD-1 (100 µg) mAbs on days 7, 10 and 13 (Fig. 15A).

Surprisingly, only mice treated with αCTLA-4 plus αPD-1 mAbs showed convincing antitumor responses (Fig. 15B, 15C). The CTLA-4 plus PD-1 blockade markedly suppressed EL4 tumor growth while IL-2/S4B6 and mAbs combination was unable to do so (Fig. 15B). There was a significant attenuation of αCTLA-4 plus αPD-1 mAbs-mediated antitumor effect when administered together with IL-2/S4B6 (Fig. 15B, 15C). The prolongation of lifespan wasn't significant in any group compared to control, although a slight effect was observed in the mAbs group with 1 out of 8 mice being long-term survivor (Fig. 15C).

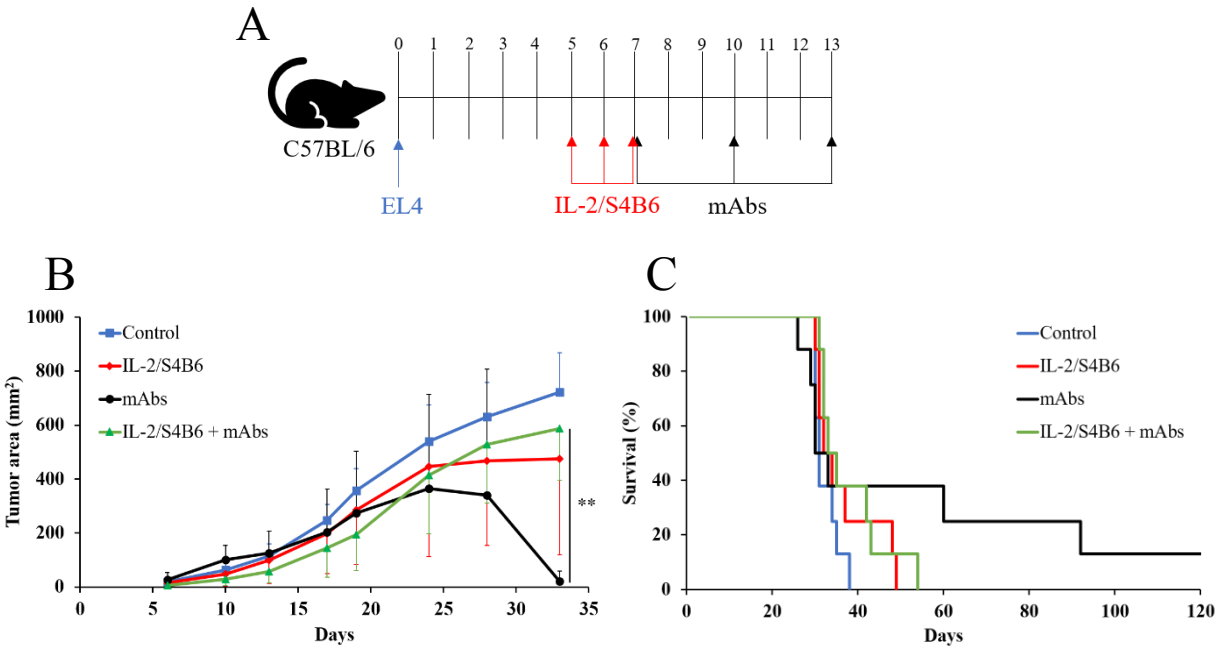

Figure 15. IL-2/S4B6 tend to dampen the antitumor effect of αCTLA-4 plus αPD-1 mAbs in mouse EL4 lymphoma tumor model. (A) Schema of the tumor therapy experiment. C57BL/6 mice (n=8) were s.c. inoculated with $1x10^5$ EL4 cells in 100 µl PBS on day 0. Mice were i.p. injected with PBS (control) or IL-2/S4B6 (2.5 µg of IL-2 eq.) on days 5, 6 and 7 and/or αCTLA-4 (100 µg) plus αPD-1 (100 µg) mAbs (mAbs) on days 7, 10 and 13. (**B**) Growth of EL4 tumors (mean +/-SD). (**C**) Experimental mice survival. Statistical significance was determined by two-tailed unpaired Student t test for tumor growth assessment and log-rang Mantel-Cox test for survival analysis, $^{**}p < 0.01$.

5.2. The stimulatory activity and antitumor effect of IL-7ic

5.2.1. Biological activity of IL-7ic *in vitro*

To elucidate the biological activity of IL-7ic, we focused on their effect on T cells *in vitro*. We used 2 different anti-IL-7 mAbs which were described to form complexes with rmIL-7; anti-human-IL-7 mAb M25 and anti-mouse-IL-7 mAb MAB407.

5.2.1.1. Proliferation of naïve $CD4^+$ and $CD8^+$ T cells in vitro

We tested the activity of IL-7/M25 and IL-7/MAB407 in induction of proliferation of naïve $CD4^+$ and $CD8^+$ T cells *in vitro*. We sought to not only compare the effects of IL-7ic with free IL-7, but also to compare biological activity between IL-2 and IL-7.

We decided to use T cells from OT-I and OT-II transgenic mice to examine the effect of IL-2, IL-7 and IL-7ic on naïve T cells only as OT-I and OT-II mice lack memory cells. $CD8^+$ and $CD4^+$ T cells from lymph nodes and spleen of OT-I or OT-II mice, respectively, were purified and cultured in media containing titrated concentrations of IL-2, IL-7, IL-7/M25, or IL-7/MAB407. Cells were harvested 72 h later. [^{3}H] thymidine was added for the last 8 h of incubation and its incorporation was measured in order to determine the ability of naïve $CD4^+$ and $CD8^+$ T cells to proliferate.

IL-2 was much more potent than IL-7 in inducing proliferation of naïve OT-II $CD4^+$ T cells *in vitro* (Fig. 16A). Even concentrations as high as 100 ng/ml of IL-7 didn't provoke remarkable expansion of naïve $CD4^+$ T cells in comparison to IL-2 (Fig. 16A). The same was found for naïve OT-I $CD8^+$ T cells (Fig. 16C). Naïve $CD8^+$ T cells were in general more prone to proliferate in higher concentrations of IL-2 than naïve $CD4^+$ T cells (Fig. 16A and 16C). Both IL-7/M25 and IL-7/MAB407 induced only mild proliferation of naïve $CD4^+$ (Fig. 16B) and $CD8^+$ T cells (Fig. 16D). Their capacity to induce proliferation of naïve T cells *in vitro* was comparable to IL-7. IL-7/M25 and IL-7/MAB407 though didn't show agonistic activity *in vitro* (Fig. 16B, 16D). Again, naïve $CD8^+$ T cells responded to cytokine signals better than naïve $CD4^+$ T cells which showed only decent proliferation in the presence of free IL-7 and IL-7ic (Fig.16B and 16D).

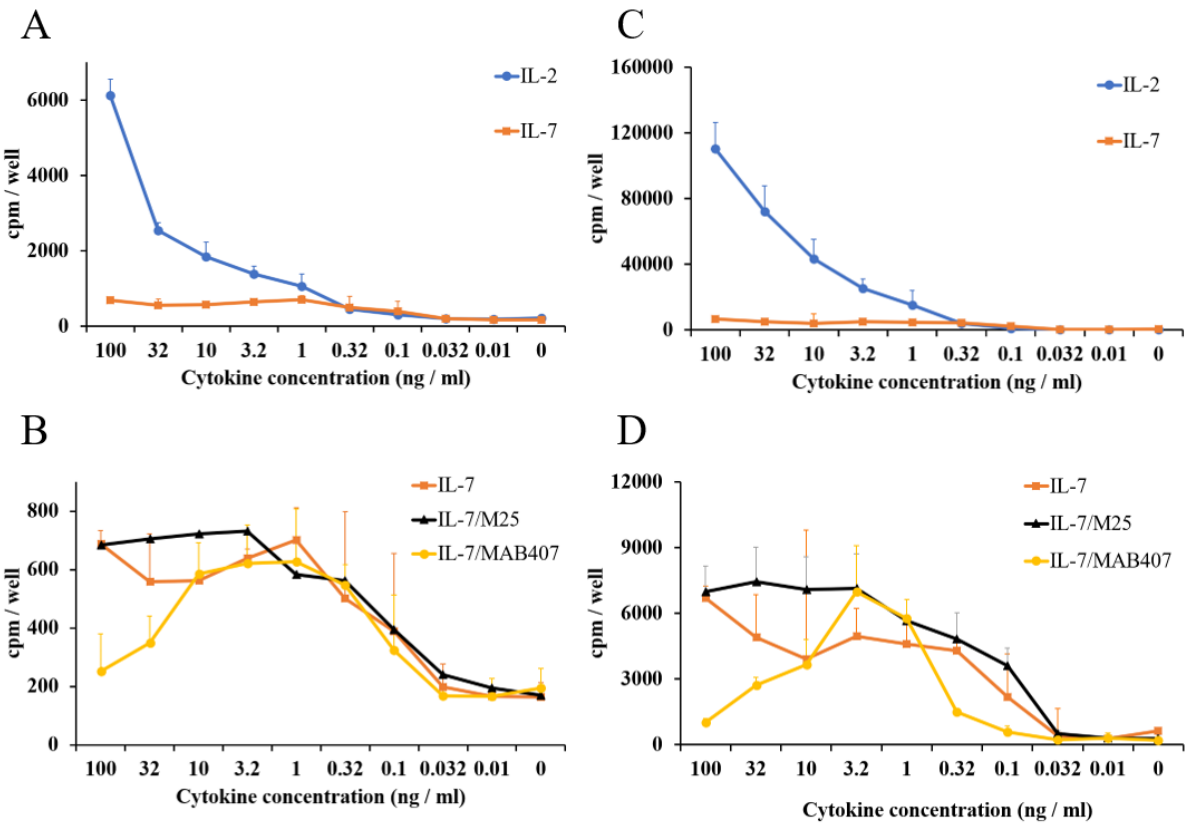

Figure 16. IL-2 but not IL-7 induces naïve OT-II CD4$^+$ and OT-I CD8$^+$ T cell proliferation *in vitro*. CD8$^+$ and CD4$^+$ T cells were sorted by negative selection from spleen and lymph nodes of naïve OT-I and OT-II mice, respectively. Cells were seeded into 96-well flat-bottom plates at 1x10^5/well in 200 µl media. IL-2, IL-7, IL-7/M25 or IL-7/MAB407 were added at concentrations ranging from 0.01 to 100 ng/ml. Plates were cultivated in 5% CO_2 at 37°C. Cells were harvested 72 h later. [^{3}H] thymidine was added for the last 8 h and its incorporation to the cell DNA was measured. Proliferation of naïve OT-II CD4$^+$ T cells incubated with ranging concentrations of IL-2 and IL-7 (**A**) or IL-7, IL-7/M25 and IL-7/MAB407 (**B**). Proliferation of naïve OT-I CD8$^+$ T cells incubated with IL-2 and IL-7 (**C**) or IL-7, IL-7/M25 and IL-7/MAB407. Data are presented as means of 4 measurements +/- SD.

5.2.1.2. Proliferation of activated CD4$^+$ and CD8$^+$ T cells in vitro

We examined the capacity of IL-2, IL-7, IL-7/M25 and IL-7/MAB407 to drive proliferation of activated CD4$^+$ and CD8$^+$ T cells *in vitro*. CD8$^+$ and CD4$^+$ T cells from lymph nodes and spleen of C57BL/6 mice were purified and cultured in media supplemented with αCD3 mAb (10 µg/ml) in order to activate T cells. Titrated concentrations of IL-2, IL-7, IL-7/M25, or IL-7/MAB407 were added. The cells were harvested 72 h later. [^{3}H] thymidine was added for the last 8 h of incubation and its incorporation was measured in order to determine the proliferation of activated CD4$^+$ and CD8$^+$ T cells in presence of cytokines or IL-7ic.

IL-2 potently enhanced proliferation of activated CD4$^+$ T cells while IL-7 induced only decent proliferation of these cells even at high concentrations (Fig. 17A). However, IL-7 served as a mitogenic factor for activated CD8$^+$ T cells although IL-2 was again far more potent in this regard (Fig. 17C). The proliferation rate of activated CD4$^+$ T cells in the presence of IL-7/M25 or IL-7/MAB407 was minimal and comparable to IL-7 alone (Fig. 17B). No superior activity

to IL-7 was observed for proliferation of activated CD8$^+$ T cells induced by IL-7/M25 or IL-7/MAB407 (Fig. 17D).

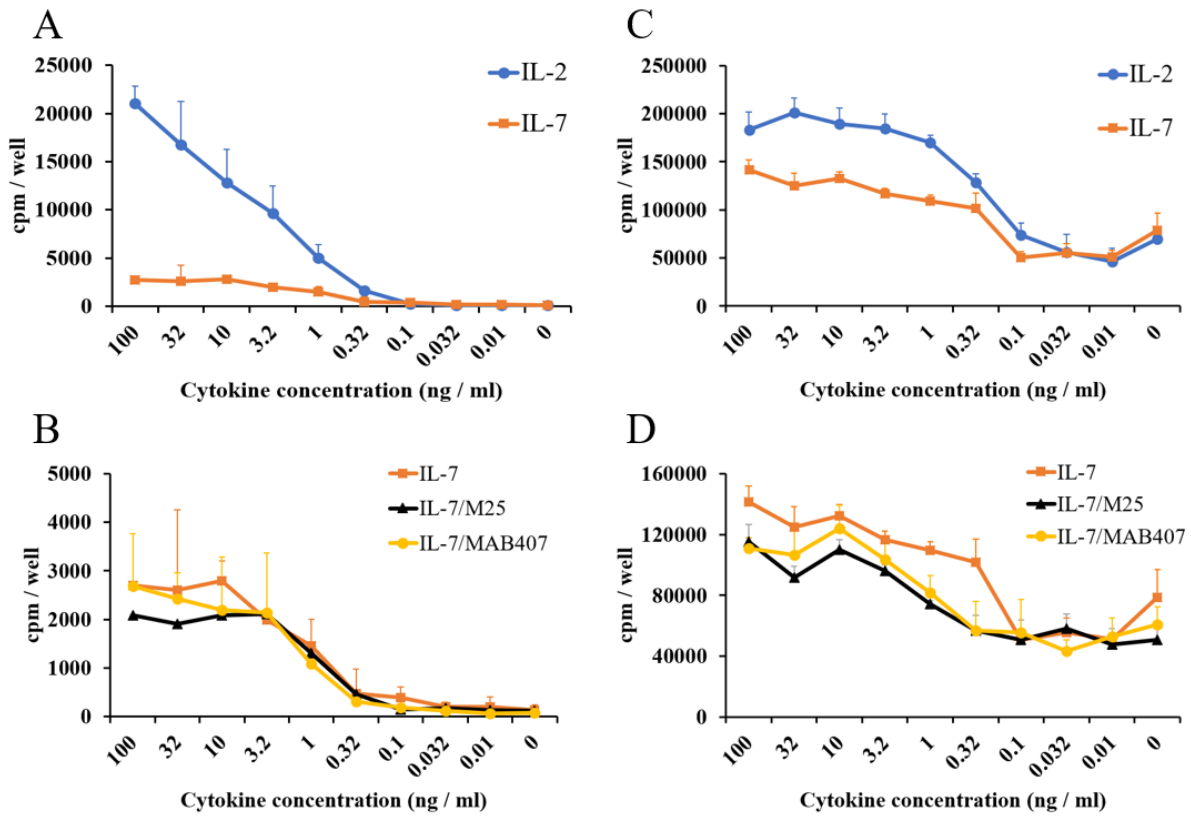

Figure 17. IL-7ic don't possess increased biological activity in comparison to free IL-7 in terms of induction of proliferation of activated CD4$^+$ and CD8$^+$ T cells *in vitro*. CD8$^+$ and CD4$^+$ T cells were sorted by negative selection from spleen and lymph nodes of naïve C57BL/6 mice. Cells were seeded into 96-well flat-bottom plates at 1x10^5/well in 200 µl media with αCD3 mAb (10 µg/ml). IL-2, IL-7, IL-7/M25 or IL-7/MAB407 were added at concentrations ranging from 0.01 to 100 ng/ml. Plates were cultivated in 5% CO_2 at 37°C. Cells were harvested 72 h later. [^{3}H] thymidine was added for the last 8 h and its incorporation to the cell DNA was measured. Proliferation of activated CD4$^+$ T cells incubated with IL-2 and IL-7 (**A**) or IL-7, IL-7/M25 and IL-7/MAB407 (**B**). Proliferation of activated CD8$^+$ T cells incubated with IL-2 and IL-7 (**C**) or IL-7, IL-7/M25 and IL-7/MAB407. Data are presented as means of 4 measurements +/- SD.

5.2.1.3. Viability of naïve CD4$^+$ and CD8$^+$ T cells in vitro

IL-7 didn't induce proliferation of naïve resting CD4$^+$ and CD8$^+$ T cells while high concentrations of IL-2 provided potent mitogenic stimuli to these cells (Fig. 16A, 16C). We conducted an *in vitro* experiment examining both survival and proliferation of naïve CD4$^+$ and CD8$^+$ T cells to confirm this finding.

Purified CD4$^+$ and CD8$^+$ T cells from spleen and lymph nodes of naïve OT-II and OT-I mice, respectively, were labeled with CFSE. Cells were seeded into 96-well flat-bottom plates at 1x10^5/well and were incubated with IL-2, IL-7, IL-7/M25 or IL-7/MAB407 at titrated concentrations. Plates were then cultured in 5% CO_2 at 37°C. Cells were washed and stained

with FVD after 120 h in culture. The cell viability, size and CFSE dilution were analyzed by flow cytometry.

IL-7 provided survival signals to naïve OT-II $CD4^+$ T cells at relatively low concentrations (0.1 ng/ml) whereas IL-2 was able to do so only at high concentrations (Fig. 18A, 18B). Even concentration as low as 0.01 ng/ml of IL-7 increased naïve $CD4^+$ T cell viability in comparison to control or equivalent dose of IL-2 (Fig. 18A). Both IL-7/M25 and IL-7/MAB407 had comparable effects on naïve $CD4^+$ T cell survival (Fig. 18A, 18B).

Cell size was measured in order to prove the presence of blasts. Cells from media supplemented with 100 ng/ml of IL-2 were slightly bigger on average than cells incubated with equivalent amounts of IL-7 or both IL-7ic (Fig. 18C) showing that proliferation of naïve $CD4^+$ T cells might occur in this case.

To confirm this, we examined CFSE profiles of naïve $CD4^+$ T cells. High concentrations of IL-2 provoked about noticeably higher proliferation of naïve $CD4^+$ T cells than comparable concentrations of IL-7 (Fig. 19), which is in accordance with our previous finding (Fig. 16A). Proliferation of naïve $CD4^+$ T cells induced by IL-7/M25 and IL-7/MAB407 was very mild and comparable to IL-7 or weaker (Fig. 19).

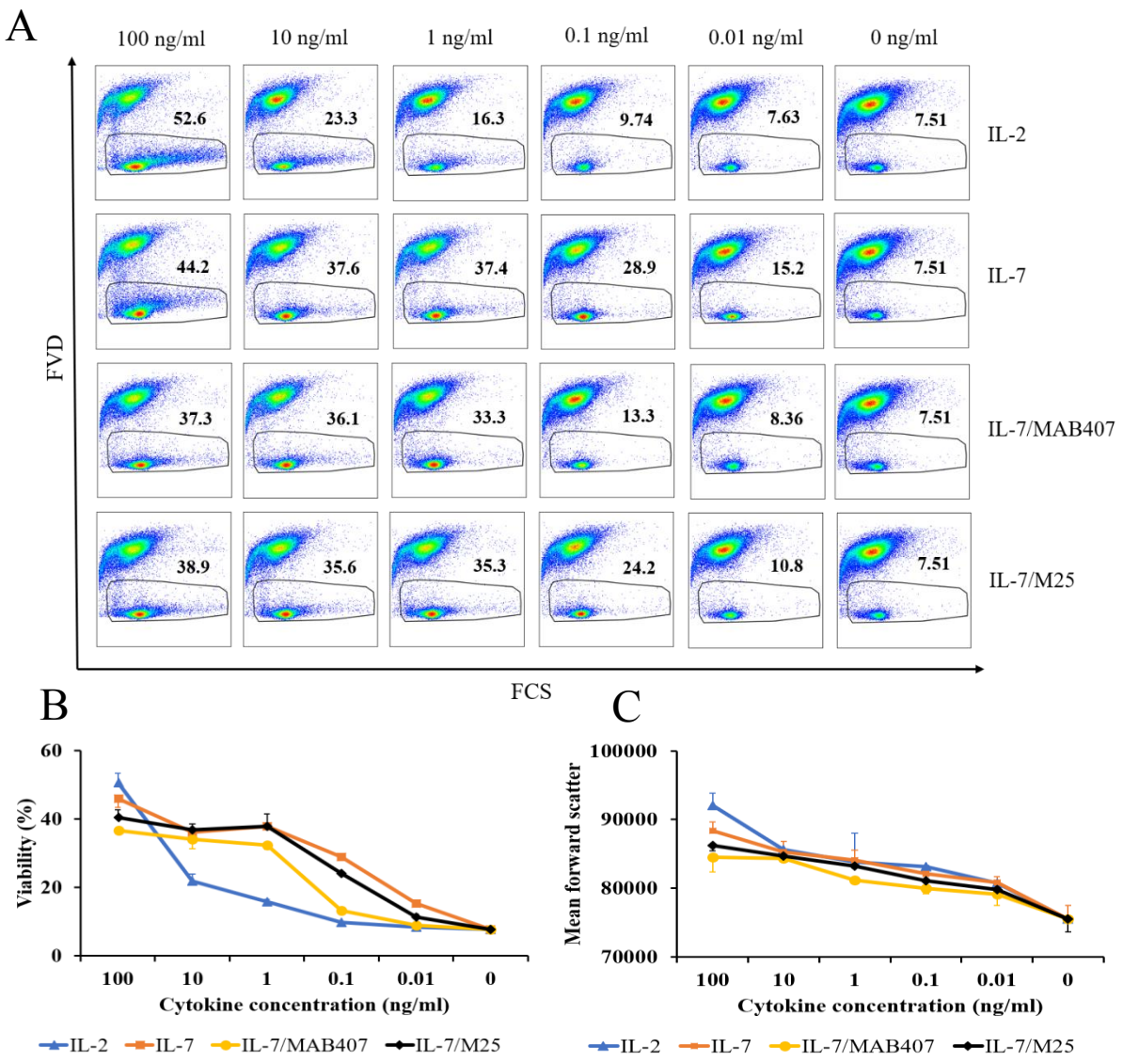

Figure 18. IL-7 efficiently prevents naïve CD4⁺ T cell death *in vitro* while IL-2 is effective only at high concentrations. Naïve OT-II $CD4^+$ T cells were labeled with CFSE and incubated with IL-2, IL-7, IL-7/MAB407 or IL-7/M25 at concentrations ranging from 0.01 to 100 ng/ml. Cells were then cultivated in 5% CO_2 at 37°C. Cells were harvested and stained with Fixable Viability Dye (FVD) after 120 h in culture. (**A**) Relative number of viable cells within $CD3^+CD4^+$ cells at various cytokine concentrations. One representative sample out of 2-3/group is shown. (**B**) Quantification of relative numbers of viable $CD3^+CD4^+$ T cells. (**C**) Size of viable $CD3^+CD4^+$ T cells determined by mean forward scatter at titrated cytokine concentrations. Data are presented as means +/- SD.

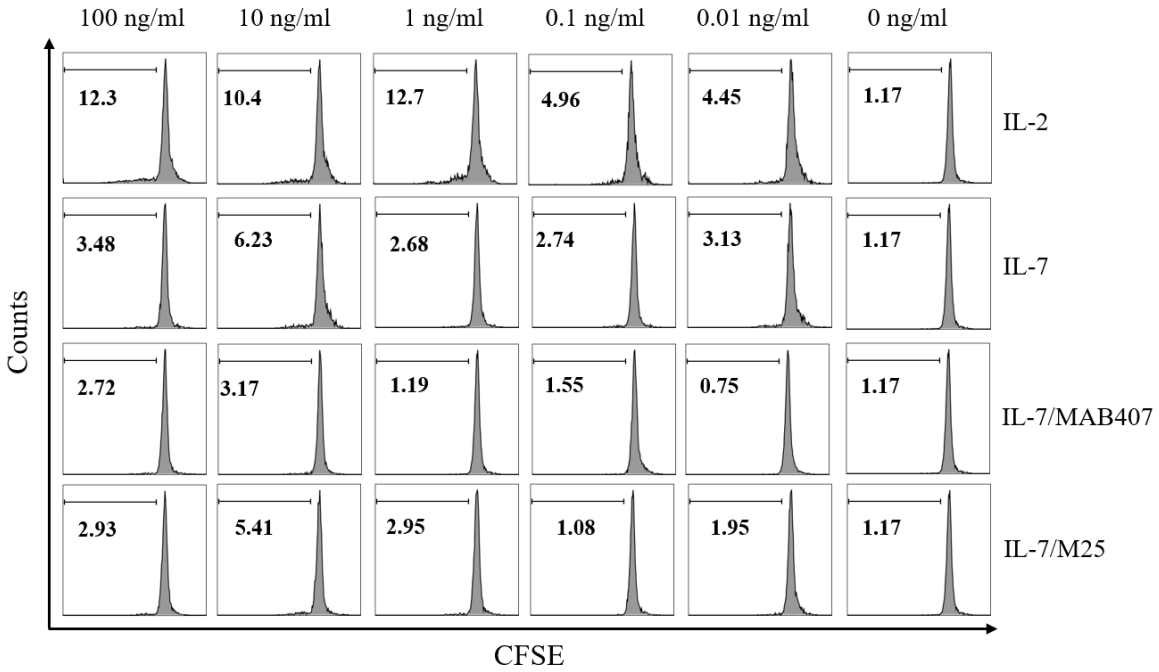

Figure 19. IL-2, but not IL-7 and IL-7ic, induces naïve CD4$^+$ T cell proliferation *in vitro*. Flow cytometry analysis of CFSE dilution of naïve CD4$^+$ T cells incubated with titrated concentrations of IL-2, IL-7, IL-7/MAB407 or IL-7/M25. The data are from the same experiment as described in Fig. 18. One representative sample out of 2-3/group is shown.

IL-7 prevented cell death of naïve OT-I CD8$^+$ T cells *in vitro* even at low concentrations (Fig. 20A, 20B). IL-2 provided the cells with comparable survival signals only at 100 ng/ml. The viability of OT-I CD8$^+$ T cells incubated with 1 ng/ml of IL-2 was comparable to control, whereas equivalent dose of IL-7 increased the cell viability by 13-fold (Fig 20A, 20B). Both IL-7/M25 and IL-7/MAB407 had similar effects on naïve CD8$^+$ T cell viability as IL-7 (Fig. 20A, 20B).

CD8$^+$ T cell size was markedly enlarged in case of incubation with IL-2 at concentrations 100 – 1 ng/ml (Fig. 20C). Equivalent amount of IL-7, IL-7/MAB407 or IL-7/M25 didn't induce such effect. Lower concentration of any cytokine failed to have any effect on the formation of blasts (Fig. 20C).

IL-2 was much more potent than IL-7 in terms of induction of naïve CD8$^+$ T cell proliferation *in vitro* (Fig. 21), which further confirmed our previous data (Fig. 16C). 1 ng/ml of IL-2 in media induced robust proliferation of naïve CD8$^+$ T cell, whereas only small fraction of cells proliferated in media supplemented with equivalent amount of IL-7. IL-2 acted as a mitogenic factor even at 0.01 ng/ml whereas IL-7 had a negligible effect at this concentration. IL-7/M25 and IL-7/MAB407 showed similar activity as IL-7 (Fig. 21).

Our data indicate that IL-7 doesn't induce naïve T cell proliferation *in vitro*. Unlike IL-2, it acts rather as prosurvival factor for naïve T cells at both high and low concentrations. IL-7ic possess comparable activity to IL-7 *in vitro*.

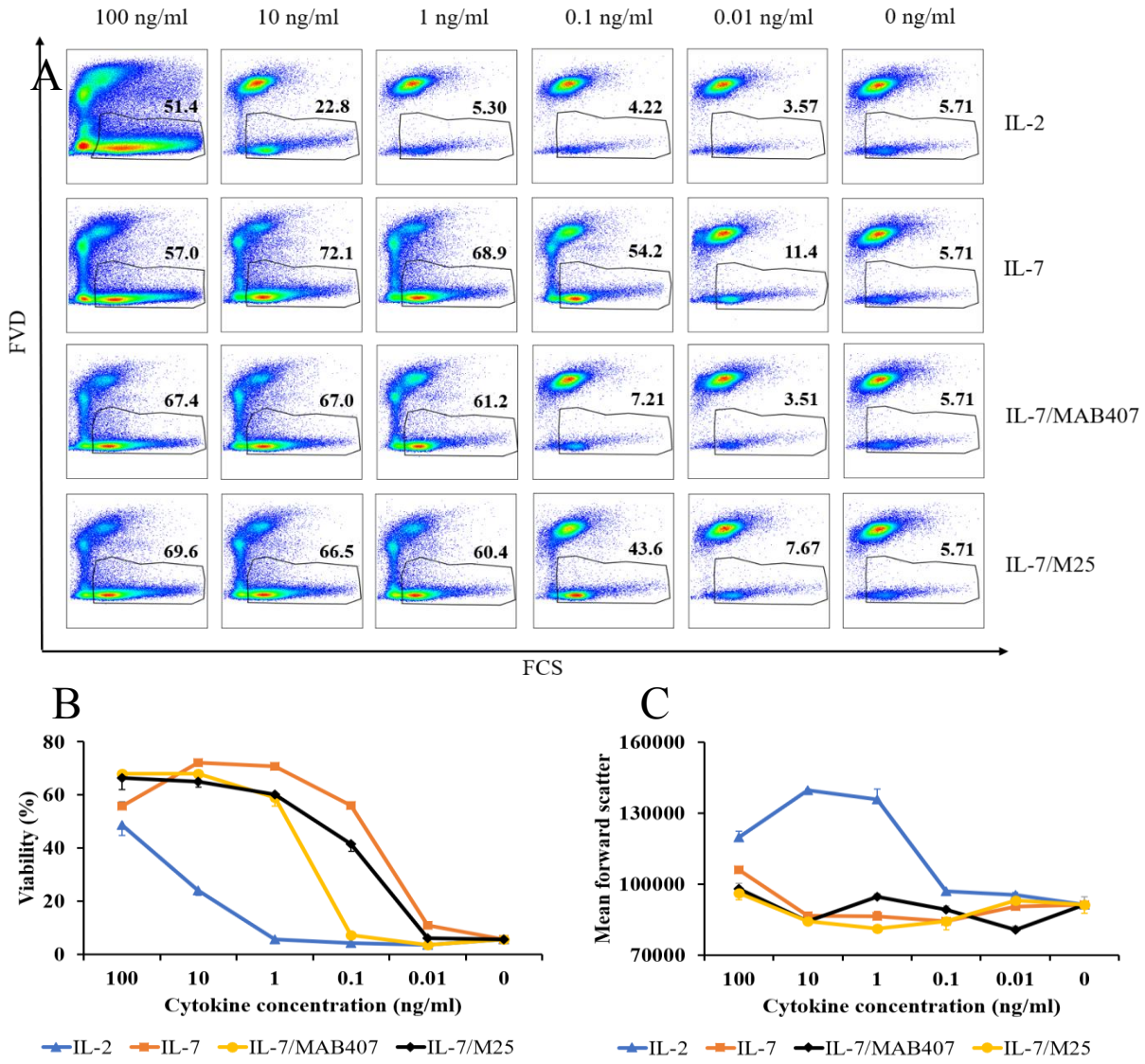

Figure 20. IL-7 efficiently prevents naïve CD8⁺ T cell death *in vitro* while IL-2 is effective only at high concentration. Naïve OT-I CD8⁺ T cells were labeled with CFSE and incubated with IL-2, IL-7, IL-7/MAB407 or IL-7/M25 at concentrations ranging from 0.01 to 100 ng/ml. Cells were then cultivated in 5% CO_2 at 37°C. Cells were harvested and stained with Fixable Viability Dye (FVD) after 120 h in culture. (**A**) Relative number of viable cells within $CD3^+CD8^+$ cells at various cytokine concentrations. One representative sample out of 2-3/group is shown. (**B**) Quantification of relative numbers of viable $CD3^+CD8^+$ T cells. (**C**) Size of viable $CD3^+CD8^+$ T cells determined by mean forward scatter at titrated cytokine concentrations. Data are presented as means +/- SD.

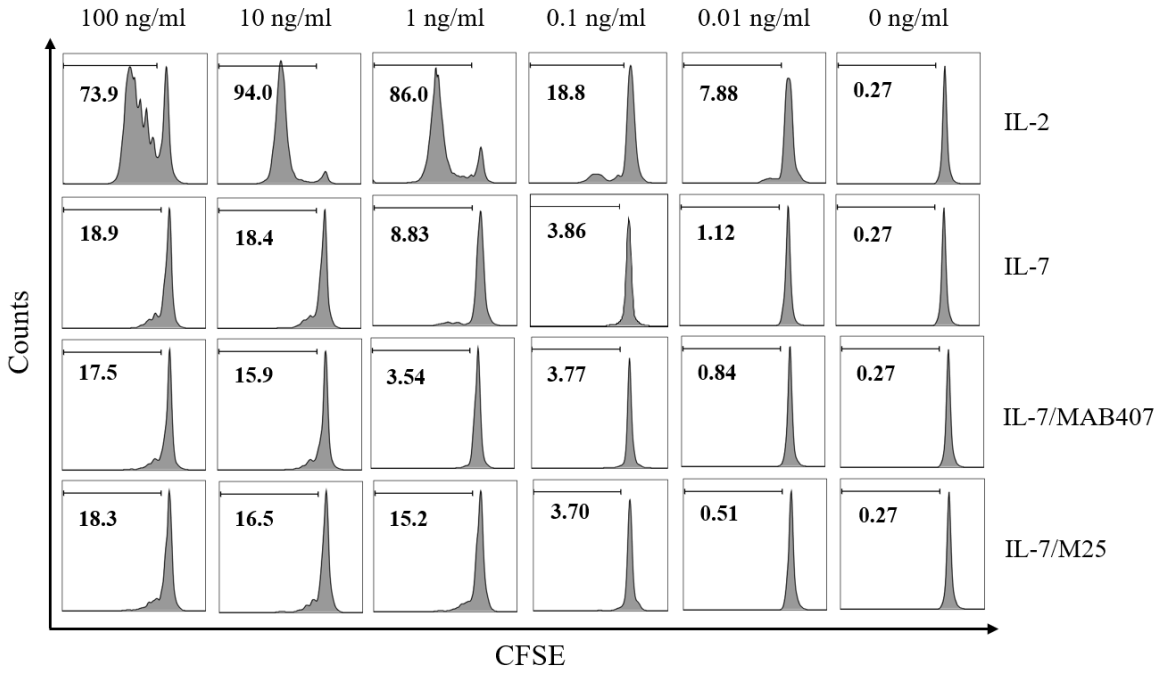

Figure 21. IL-2 is far more potent than IL-7 or IL-7ic in terms of induction of naïve CD8$^+$ T cell proliferation *in vitro*. Flow cytometry analysis of CFSE dilution of naïve CD8$^+$ T cells incubated with titrated concentrations of IL-2, IL-7, IL-7/MAB407 or IL-7/M25. The data are from the same experiment as described in Fig. 20. One representative sample out of 2-3/group is shown.

5.2.2. Biological activity of IL-7ic *in vivo*

5.2.2.1. Effects of IL-7ic on B and T cells

Our next goal was to determine the biological activity of IL-7ic on various immunocompetent cell populations *in vivo* and compare it to free IL-7. BALB/c mice (n=2-3) were i.p. injected with 4 daily doses of PBS (control), IL-7 (1 µg), M25 mAb (5 µg), or IL-7ic (1 µg of IL-7 eq.). Mice were sacrificed 48 h after the final dose and their spleens were harvested and analyzed by flow cytometry (Fig. 22A).

Spleens of mice treated with IL-7/M25 were visibly enlarged in comparison to mice injected with free IL-7, although the differences in absolute numbers of splenocytes weren't significant due to high variation among the mice in IL-7/M25-treated group (Fig. 22B). The cellularity of IL-7/MAB407 and IL-7-treated mice were comparable (Fig. 22B).

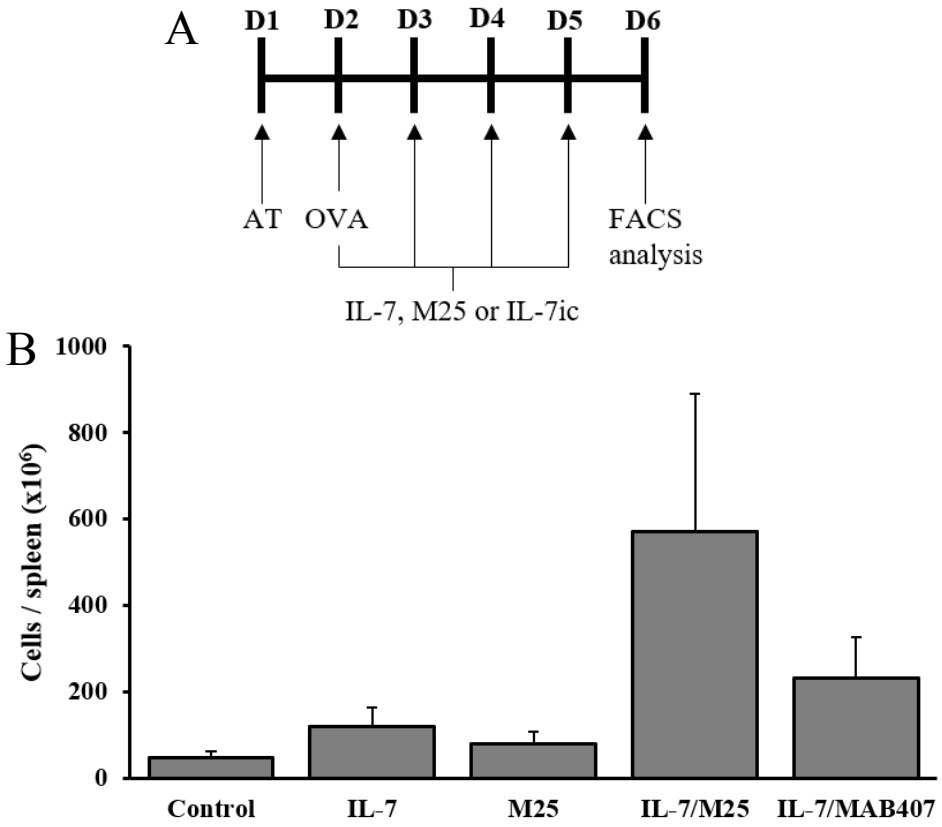

Figure 22. Spleen cellularity in mice treated with IL-7 or IL-7ic. (**A**) Schema of the experimental setup. BALB/c mice (n=2-3) received i.p. injection of PBS (control), IL-7 (1 µg), M25 mAb (5 µg), IL-7/M25 (1 µg IL-7 + 5 µg M25 mAb) or IL-7/MAB407 (1 µg IL-7 + 5 µg MAB407 mAb) every day for 4 following days. Mice were sacrificed 48 h after the last dose, their spleens were harvested and numbers of splenocytes were counted. (**B**) Absolute number of splenocytes. Data are presented as means +/- SD. Statistical significance was determined by two-tailed unpaired Student t test.

The analysis of B cells revealed that there was a decrease in the relative number of $CD3^-$ $B220^+$ cells in spleens of IL-7/M25-treated mice in comparison to mice injected with free IL-7 (Fig. 23A, 23C). IL-7/MAB407 had no such effect (Fig. 23A, 23C). The relative number of B cells slightly, but not significantly, declined also in M25 mAb-treated mice (Fig. 23A, 23C).

Next, we analyzed changes in the splenic T cell compartment. Interestingly, there was a shift in the $CD4^+$:$CD8^+$ T cell ratio in favor of relative counts of $CD8^+$ T cells in mice treated with IL-7/M25 (Fig. 23B, 23D, 23E). Such phenomenon wasn't observed in IL-7/MAB407-treated mice (Fig. 23B, 23D, 23E).

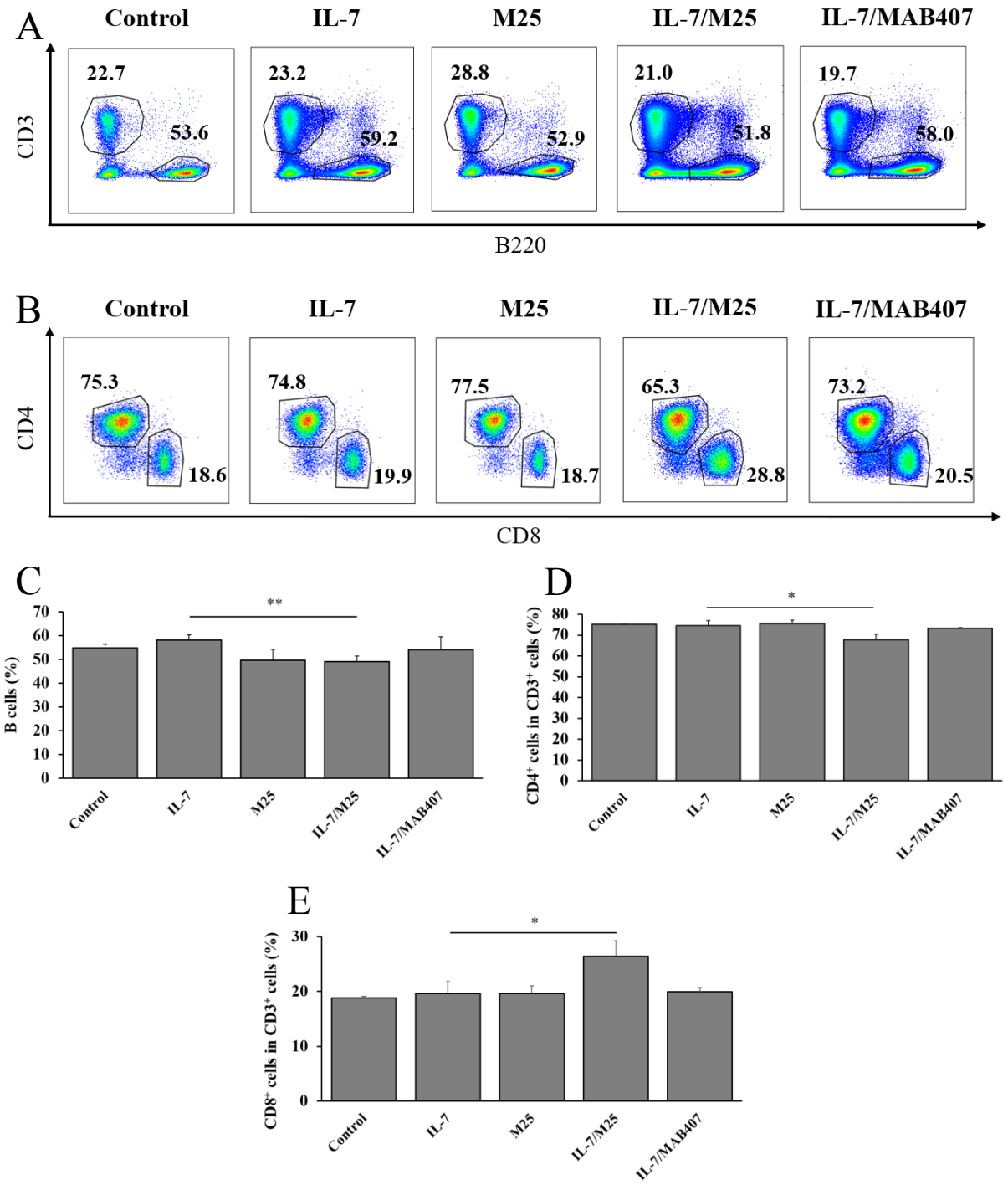

Figure 23. IL-7/M25 shift the CD4$^+$:CD8$^+$ T cell ratio in favor of CD8$^+$ T cells and decrease relative B cell counts in spleen in comparison to free IL-7 *in vivo*. Flow cytometry analysis of B and T cells of mice from the experiment described in Fig. 22. (**A**) Relative numbers of CD3$^+$B220$^-$ T (upper gate) and CD3$^-$B220$^+$ B (lower gate) cells within viable lymphocytes. One representative mouse is shown. (**B**) Relative numbers of CD4$^+$ (upper gate) CD8$^+$ (lower gate) T cells within viable CD3$^+$ lymphocytes. One representative mouse is shown. (**C**) Percentage of CD3$^-$B220$^+$ B cells within viable lymphocytes. Percentage of CD8$^+$ (**D**) and CD4$^+$ (**E**) T cells within viable CD3$^+$ T cells. **C**–**E** are presented as means of 2-3 mice +/- SD. Statistical significance was determined by two-tailed unpaired Student t test, *p < 0.05, **p < 0.01.

We also determined stimulatory activity of IL-7, IL-7/M25 and IL-7/MAB407 to induce proliferation of B and T cells. Our analysis was based on intracellular staining of Ki67

proliferation marker. Free IL-7 induced a mild proliferation of B cells (2-fold increase in comparison to control) whereas equivalent dose of IL-7/M25 drove more vigorous B cell division (4-fold increase in comparison to control) (Fig. 24A, 24D). Percentage of proliferating B cells in IL-7/MAB407-treated mice was increased about 2-fold and thus comparable to free IL-7 (Fig. 24A, 24D).

IL-7/M25 induced proliferation of $CD4^+$ T cells *in vivo*. We observed 2.7-fold increase in $Ki67^+$ $CD4^+$ T cells in IL-7/M25-treated mice in comparison to IL-7-treated mice (Fig. 24B, 24E). Again, IL-7/MAB407 showed activity comparable to free IL-7 (Fig. 24B, 24E).

IL-7/M25 induced 5.4-fold increase in proliferating $CD8^+$ T cells in comparison to free IL-7, while IL-7/MAB407 treatment didn't cause a significant increase in the relative number of dividing $CD8^+$ T cells (Fig. 24C, 24F).

Finally, we examined the capacity of IL-7/M25 to change the activation status of B and T cells in terms of CD25 expression *in vivo*. There was significantly increased percentage of $CD25^+$ cells within B cells in spleen of mice treated with IL-7/M25. When compared to B cells of mice treated with free IL-7, the increase was about 50-fold (Fig. 25A). IL-7/MAB407 treatment had no effect (Fig. 25A).

However, higher relative $CD25^+$ cell counts after IL-7/M25 treatment was a phenomenon unique solely to B cells. Neither $CD4^+$ (Fig. 25B) nor $CD8^+$ (Fig. 25C) T cells showed increased CD25 expression after IL-7/M25 administration in comparison to free IL-7.

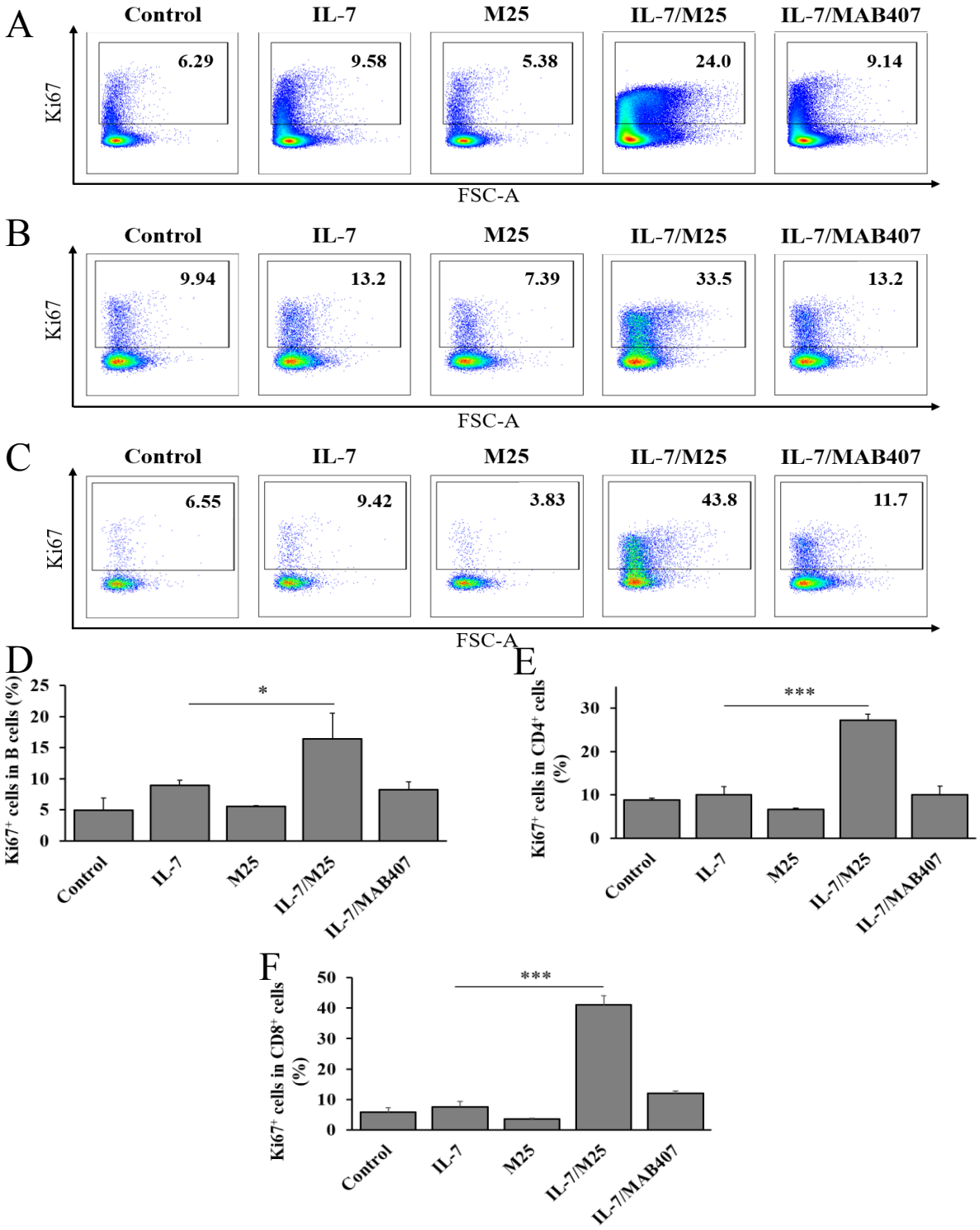

Figure 24. IL-7/M25 but neither free IL-7 nor IL-7/MAB407 induce B, CD8$^+$ and CD4$^+$ T cell proliferation *in vivo*. Intracellular flow cytometry analysis of Ki67 expression in B and T cells of mice from the experiment described in Fig. 22. (**A**) Relative numbers of Ki67$^+$ cells within viable CD3$^-$B220$^+$ B cells (**A**), CD3$^+$CD4$^+$ (**B**) and CD3$^+$CD8$^+$ (**C**) T cells. One representative mouse is shown. Percentage of Ki67$^+$ cells within viable CD3$^-$ B220$^+$ B (**D**), CD3$^+$CD4$^+$ (**E**) and CD3$^+$CD8$^+$ T (**F**) cells. **D**–**F** are presented as means of 2-3 mice +/- SD. Statistical significance was determined by two-tailed unpaired Student t test, *$p < 0.05$, ***$p < 0.001$.

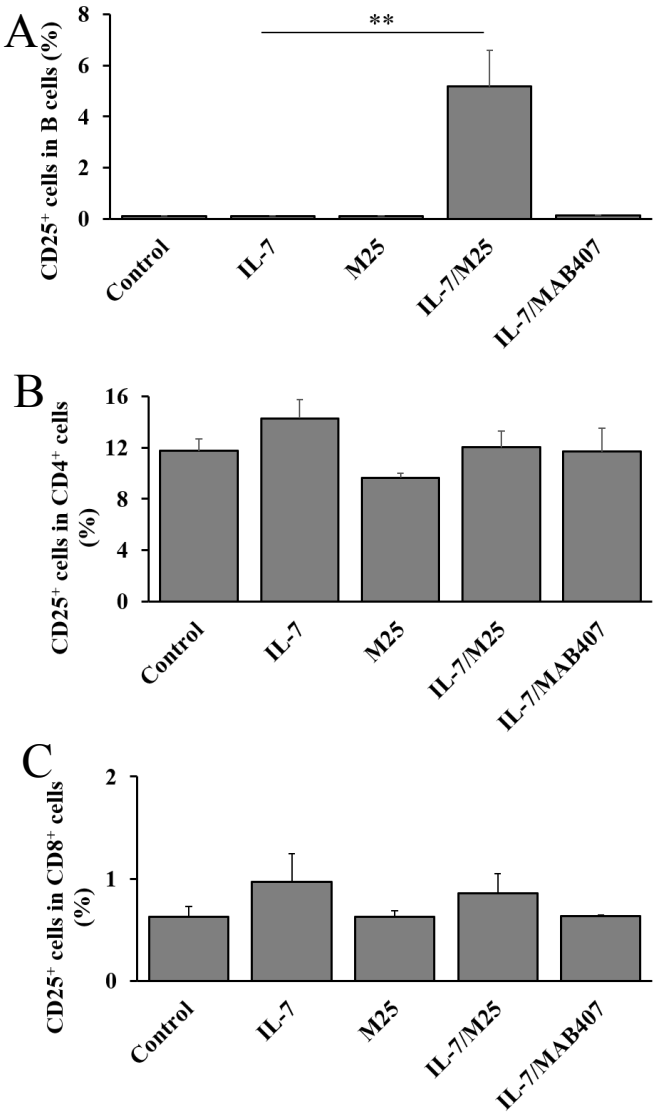

Figure 25. IL-7/M25 increase the activation status of B cells *in vivo*. Flow cytometry analysis of CD25 expression on B and T cells of mice from the experiment described in Fig. 22. Percentage of $CD25^+$ cells within viable $CD3^-B220^+$ B (**A**), $CD3^+CD4^+$ (**B**) and $CD3^+CD8^+$ (**C**) T cells. Data are presented as means of 2-3 mice +/- SD. Statistical significance was determined by two-tailed unpaired Student t test, **$p < 0.01$.

5.2.2.2. Comparison of biological activities of IL-7ic and IL-2ic

5.2.2.2.1 Stimulatory activity of IL-7ic and IL-2 ic for B and T cells

Our previous data revealed that IL-7/M25, but not IL-7/MAB407, had enhanced *in vivo* biological activity in comparison to free IL-7. Increased biological activity manifested as improved capacity of IL-7/M25 to induce proliferation of B cells (Fig. 24A, 24D), $CD4^+$ (Fig. 24B, 24E) and $CD8^+$ (Fig. 24C, 24F) T cells and to increase CD25 expression in B cells in spleen (Fig. 25A). We further showed that only IL-7/M25 treatment decreased the relative number of B cells (Fig. 23A, 23C) and $CD4^+$ T cells (Fig. 23B, 23E) in spleen, while relative counts of $CD8^+$ T cells (Fig. 23B, 23D) were increased in comparison to free IL-7.

The goal of our next experiment was to confirm this data and compare it to *in vivo* effects of IL-2ic. Thus, C57BL/6 mice (n=3) were i.p. injected with 4 daily doses of PBS, IL-2 (1 μg), IL-7 (1 μg), IL-2ic (1 μg of IL-2 eq.) or IL-7ic (1 μg of IL-7 eq.). Mice were sacrificed 24 h after the final dose and their spleens were harvested and analyzed by flow cytometry (Fig. 26A).

There was a mild decrease in relative numbers of B cells in IL-7/M25-treated group in comparison to free IL-7, although just above the limit of statistical significance (Fig. 26B). Relative counts of B cells didn't differ between IL-7/MAB407 and IL-7-treated mice (Fig. 26B). Neither IL-2/S4B6 nor IL-2/JES6-1 changed the relative numbers of splenic B cells in comparison to IL-2 (Fig. 26B).

IL-2/S4B6 treatment led to relative decrease of $CD4^+$ T cells in spleen compared to free IL-2 (Fig. 26C). The relative counts of $CD4^+$ T cells remained unchanged in mice treated with IL-2/JES6-1 (Fig. 26C). No significant differences among IL-7, IL-7/M25 and IL-7/MAB407 groups were found (Fig. 26C).

Mice treated with IL-7/M25 showed increased relative numbers of $CD8^+$ T cells in spleen compared to mice treated with IL-7 (Fig. 26D). There was a prominent rise in relative $CD8^+$ T cell counts in mice treated with IL-2/S4B6 in comparison to mice injected with free IL-2 (Fig. 26D), presumably because of the massive expansion of MP $CD8^+$ T cells [49]. Neither IL-7/MAB407 nor IL-2/JES6-1 treatment induced changes in relative $CD8^+$ T cell numbers in spleen in comparison to treatment with their respective free cytokines (Fig. 26D).

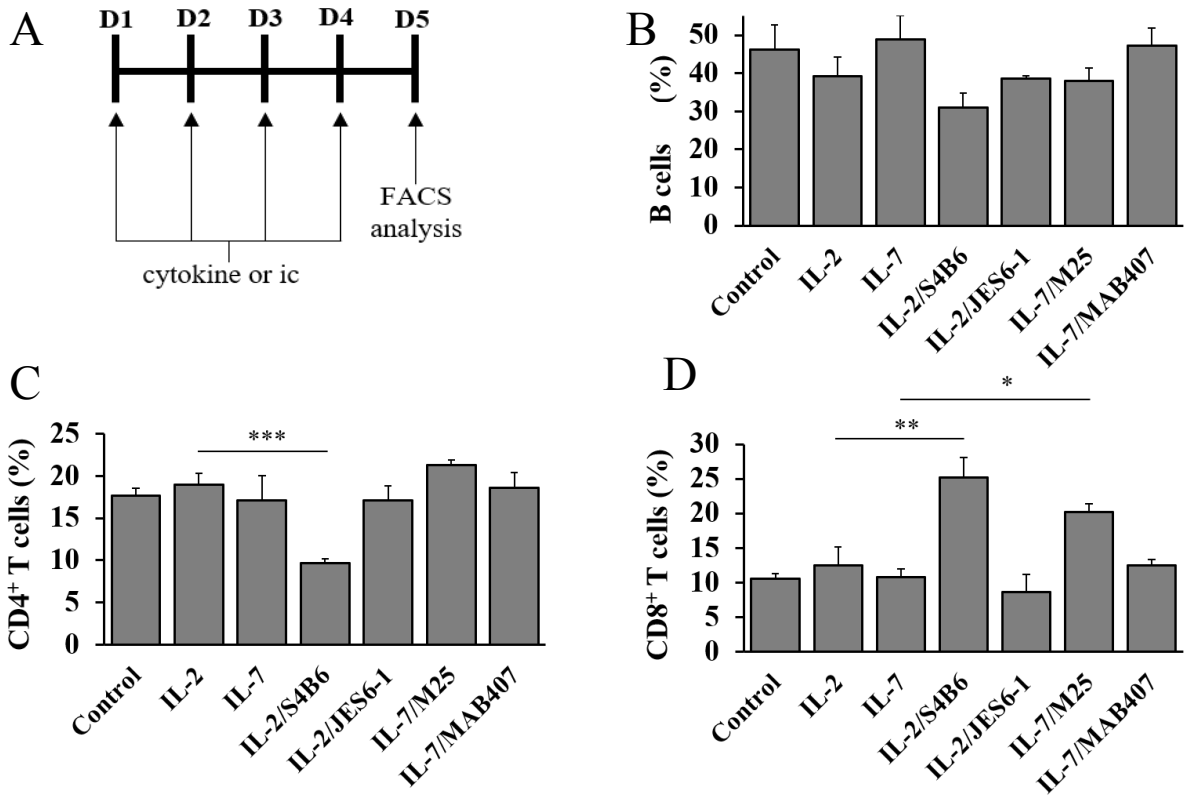

Figure 26. Both IL-2/S4B6 and IL-7/M25 act predominantly on CD8$^+$ T cells. (**A**) Schema of the experimental setup. C57BL/6 mice (n=3) received i.p. injection of PBS (control), IL-2 (1 µg), IL-7 (1 µg), IL-2/S4B6 (1 µg IL-2 + 5 µg S4B6 mAb) or IL-2/JES6-1 (1 µg IL-2 + 5 µg JES6-1 mAb), IL-7/M25 (1 µg IL-7 + 5 µg M25 mAb), or IL-7/MAB407 (1 µg IL-7 + 5 µg MAB407 mAb) every day for 4 following days. Mice were sacrificed 24 h after the final dose and their spleens were analyzed by flow cytometry. Percentage of CD3$^-$B220$^+$ B (**B**), CD4$^+$ (**C**) and CD8$^+$ (**D**) T cells within viable lymphocytes. Data are presented as means of 3 mice +/- SD. Statistical significance was determined by two-tailed unpaired Student t test, *$p < 0.05$, **$p < 0.01$, ***$p < 0.001$.

Next, we analyzed Ki67 expression in B and T cells. The only group with increased number of proliferating B cells in comparison to either control or free cytokine was the one treated with IL-7/M25 (Fig. 27A). IL-2ic didn't affect B cell proliferation in spleen (Fig. 27A).

CD4$^+$ T cell proliferation was induced by both IL-2/S4B6 and IL-2/JES6-1 in comparison to free IL-2 (Fig. 27B). There was also an increase in relative numbers of Ki67$^+$CD4$^+$ T cells in mice treated with IL-7/M25 compared to mice injected with IL-7 alone (Fig. 27B). IL-7/MAB407 didn't induce CD4$^+$ T cell proliferation.

Enhanced proliferation of CD8$^+$ T cells was induced by IL-2/JES6-1 (16.3%) compared to the cytokine alone (7.1%) (Fig. 27C). However, much greater expansion of Ki67$^+$CD8$^+$ T was driven by IL-2/S4B6 (48.9%) (Fig. 27C). About the same effect on splenic CD8$^+$ T cell

division were shown to have IL-7/M25 (48.8%) (Fig. 27C). IL-7 (17.6%) and IL-7/MAB407 (14%) displayed about the same potency to drive $CD8^+$ T cell proliferation (Fig. 27C).

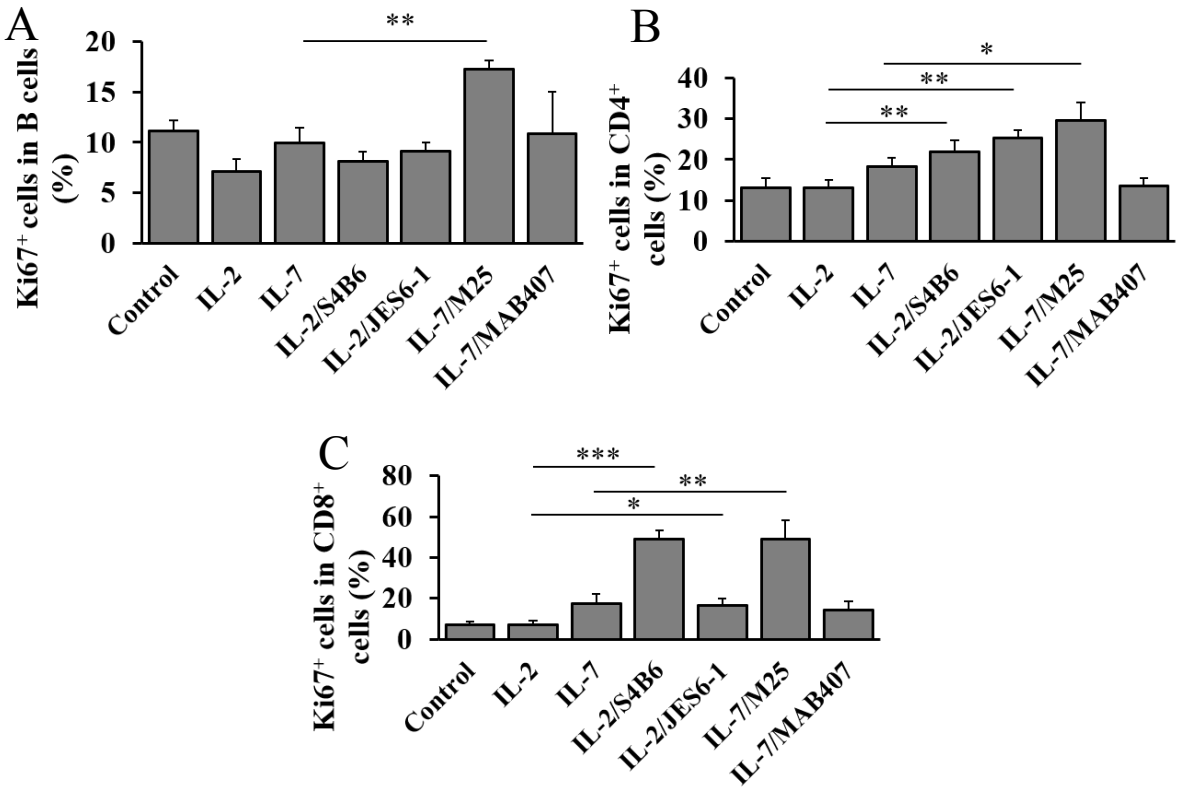

Figure 27. IL-7/M25, IL-2/S4B6 and IL-2/JES6-1 enhance $CD8^+$ and $CD4^+$ T cell proliferation *in vivo*. Flow cytometry analysis of Ki67 in B and T cells of mice from the experiment described in Fig. 26. Percentage of $Ki67^+$ cells within viable $CD3^-B220^+$ B (**A**), $CD3^+CD4^+$ (**B**) and $CD3^+CD8^+$ (**C**) T cells. Data are presented as means of 3 mice +/- SD. Statistical significance was determined by two-tailed unpaired Student t test, *$p < 0.05$, **$p < 0.01$, ***$p < 0.001$.

5.2.2.2.2. Effects of IL-7ic and IL-2ic on Tregs, NK cells and memory $CD4^+$ and $CD8^+$ T cells

We also studied effects of IL-2ic and IL-7ic on other populations of immunocompetent cells *in vivo*. We decided to figure out whether there were changes in Treg counts after IL-2ic and IL-7ic administration. We thus analyzed relative counts of $CD3^+CD4^+CD25^+FoxP3^+$ Treg cells within the $CD3^+CD4^+$ T cell compartment. We observed 4.2-fold increase in expansion of Tregs in spleen of mice treated with IL-2/JES6-1 in comparison to IL-2-induced expansion (Fig. 28A, 28B). Injections of IL-2/S4B6 also stimulated an increase in relative Treg counts (2.8-fold in comparison to free IL-2) (Fig. 28A, 28B). Significant decrease in relative numbers of Tregs was seen in mice treated with IL-7/M25 or IL-7/MAB407 (1.6-fold or 2-fold, respectively, in

comparison to free IL-7) (Fig. 28A, 28B). This is most probably due to an increase in relative counts of non-Treg $CD3^+CD4^+$ T cells.

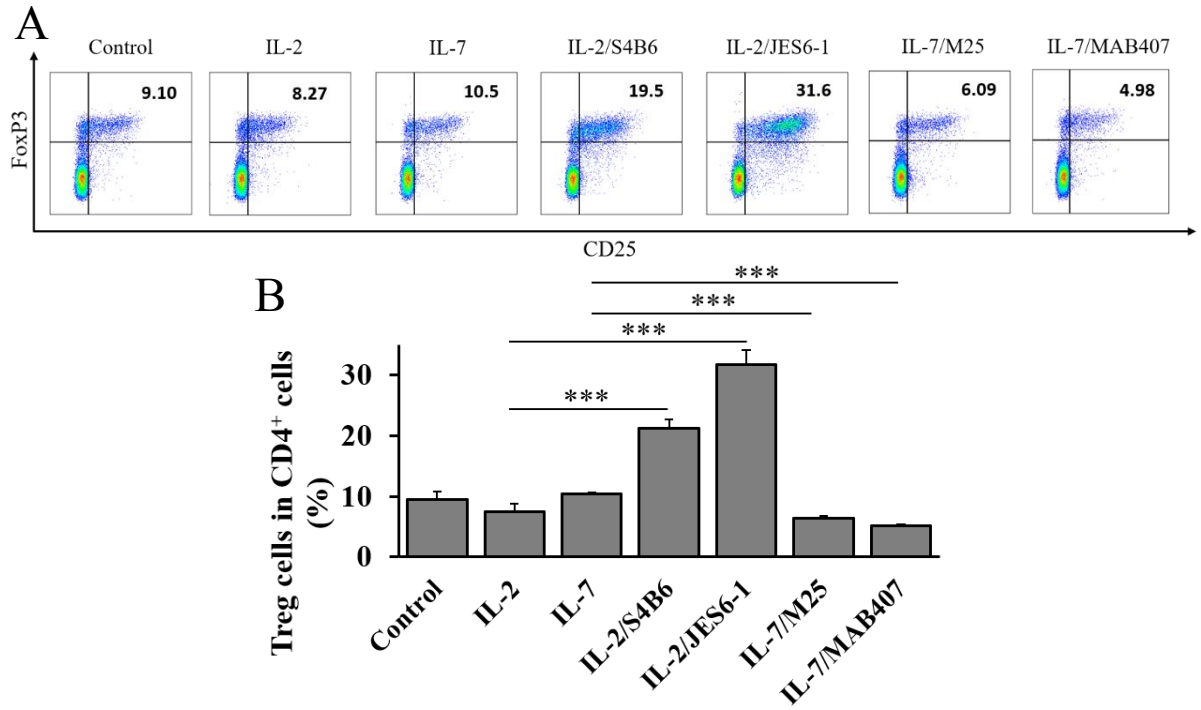

Figure 28. IL-7/M25 and IL-7/MAB407 decrease the relative counts of Tregs in comparison to free IL-7 *in vivo*. Flow cytometry analysis of spleen of mice from the experiment described in Fig. 26. (**A**) Relative numbers of $CD25^+FoxP3^+$ cells within viable $CD3^+CD4^+$ T cells. One representative mouse is shown. (**B**) Percentage of $CD25^+FoxP3^+$ cells within viable $CD3^+CD4^+$ T cells. Data are presented as means of 3 mice +/- SD. Statistical significance was determined by two-tailed unpaired Student t test, ***$p < 0.001$.

Only IL-2/S4B6 drove prominent expansion of $CD3^-NK1.1^+$ NK cell population in spleen (6.2-fold increase in comparison to free IL-2) (Fig. 29A, 29B). Furthermore, we noticed moderate but significant decrease in relative counts of NK cells in IL-7/M25-treated group (1.5-fold increase in comparison to free IL-7) (Fig. 29A, 29B).

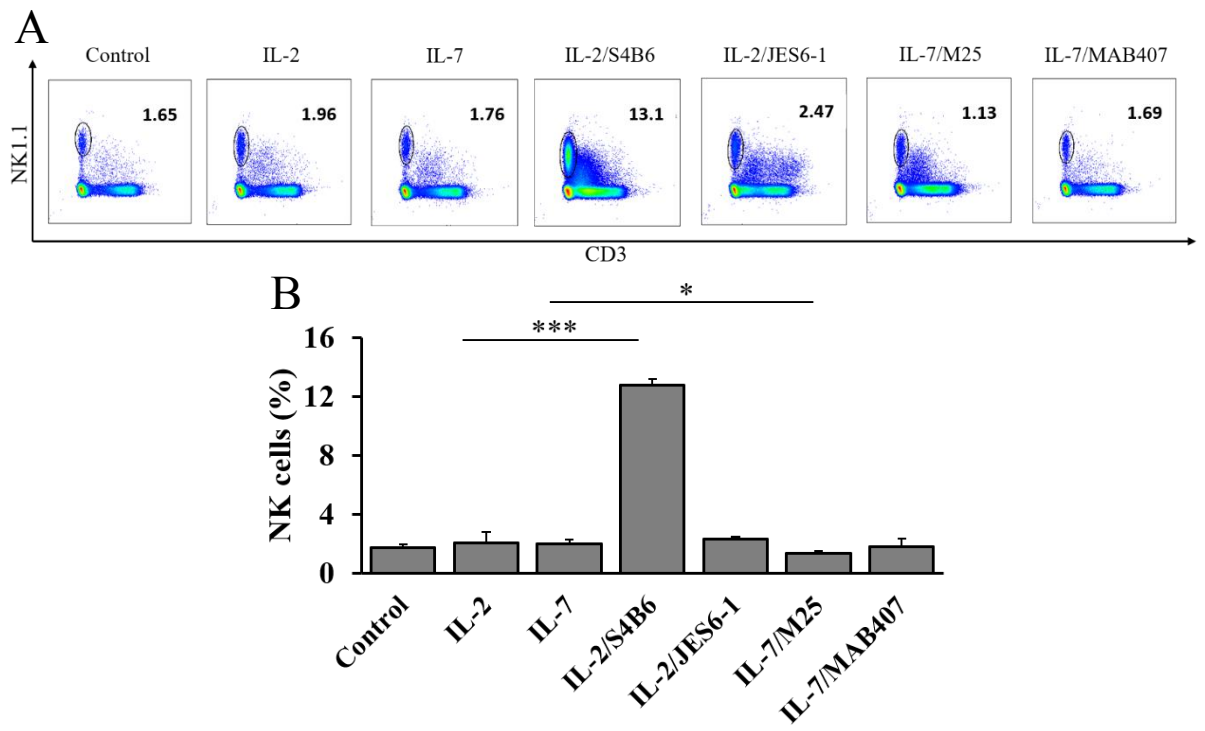

Figure 29. IL-2/S4B6 induce NK cell expansion *in vivo*. Flow cytometry analysis of spleen of mice from the experiment described in Fig. 26. (**A**) Relative numbers of $CD3^-NK1.1^+$ cells within viable lymphocytes. One representative mouse is shown. (**B**) Percentage of $CD3^-NK1.1^+$ cells within viable lymphocytes. Data are presented as means of 3 mice +/- SD. Statistical significance was determined by two-tailed unpaired Student t test, *$p < 0.05$, ***$p < 0.001$.

We have already described distinct effects of IL-7 and IL-7/M25 on relative counts (Fig. 23B, 23E, 26C) and Ki67 expression (Fig. 24B, 24E, 27B) of splenic $CD4^+$ T cells *in vivo*. As IL-7 is, together with IL-15, a non-redundant cytokine for memory T cell homeostasis [72], we examined whether IL-7 and IL-7/M25 had a different effect on this cell subset. However, no significant difference between IL-7 and either IL-7ic was observed (Fig. 30A, 30B). IL-2ic had no effect on expansion of memory $CD4^+$ T cells (Fig. 30A, 30B).

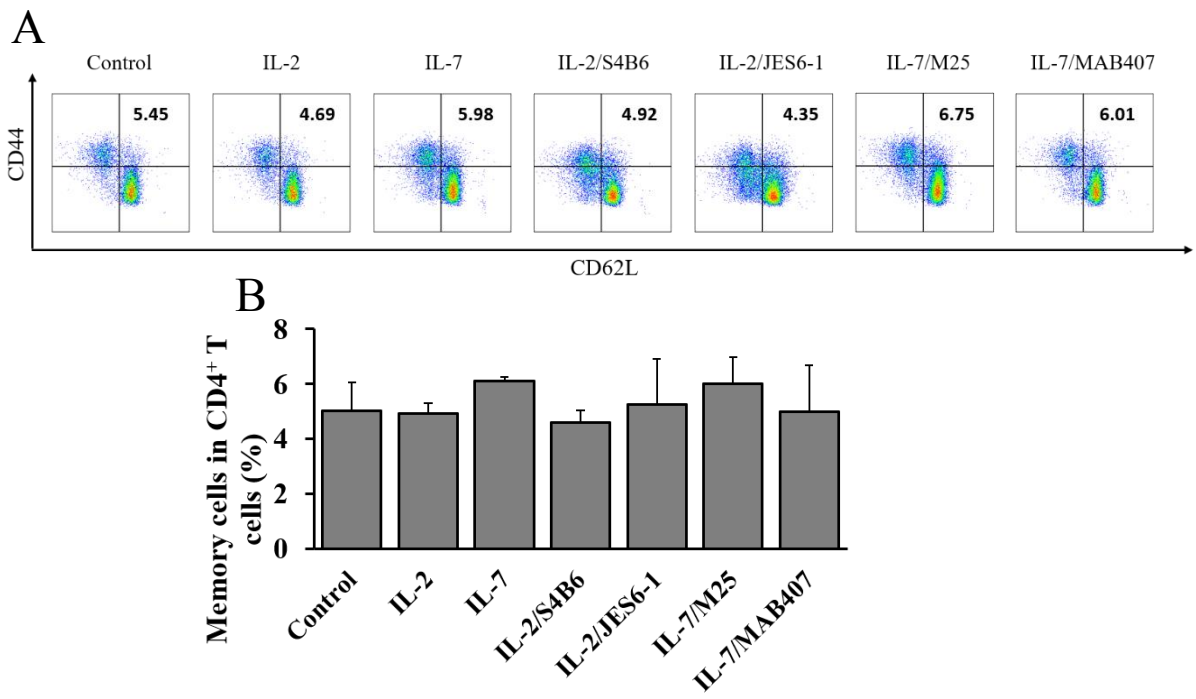

Figure 30. Neither IL-2ic nor IL-7ic affect memory CD4$^+$ T cells. Flow cytometry analysis of spleen of mice from the experiment described in Fig. 26. (**A**) Relative numbers of CD44^{high}CD62L^{high} cells within viable CD3$^+$CD4$^+$ T cells. One representative mouse is shown. (**B**) Percentage of CD44^{high}CD62L^{high} cells within viable CD3$^+$CD4$^+$ T cells. Data are presented as means of 3 mice +/- SD. Statistical significance was determined by two-tailed unpaired Student t test.

Although IL-2 and IL-7 treatment had little effect on CD3$^+$CD8$^+$CD44^{high}CD122^{high} MP T cells, IL-2/S4B6 and IL-7/M25 stimulated their 4.9-fold and 1.9-fold expansion, respectively, in comparison to the free cytokine (Fig. 31A, 31B). Neither IL-2/JES6-1 nor IL-7/MAB407 showed activities superior to the respective free cytokines (Fig. 31A, 31B).

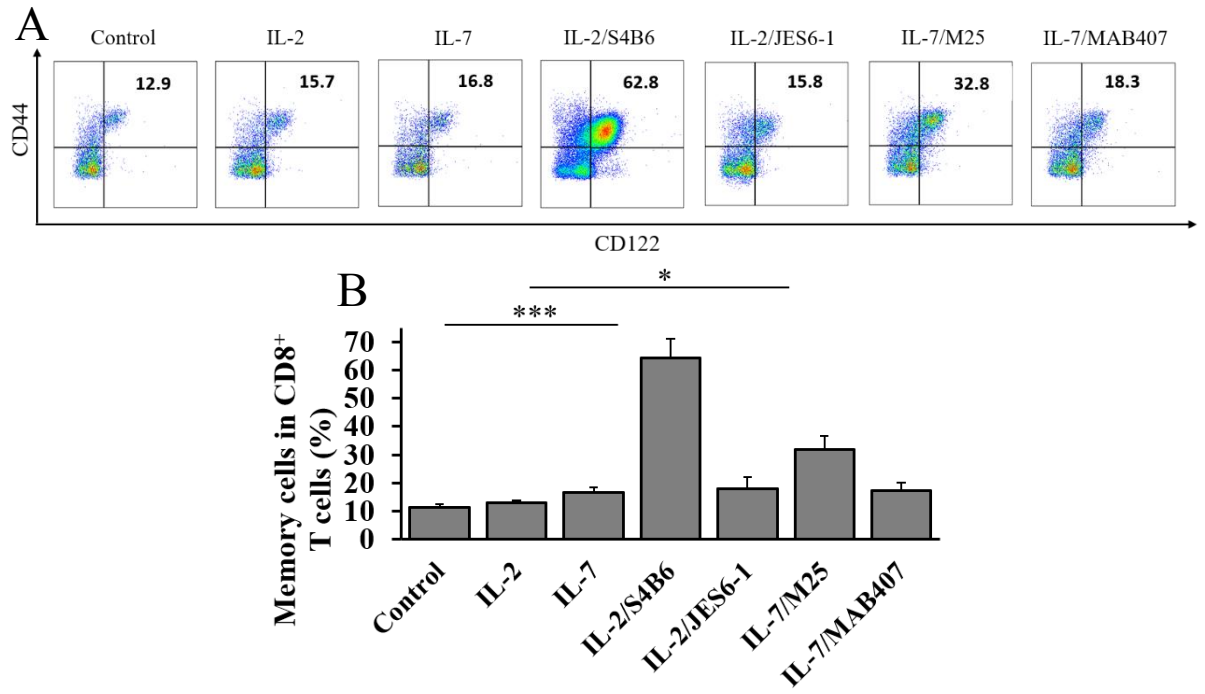

Figure 31. Memory CD8$^+$ T cells are expanded by IL-2/S4B6 and IL-7/M25 in comparison to free cytokines *in vivo*. Flow cytometry analysis of spleen of mice from the experiment described in Fig. 26. (**A**) Relative numbers of CD44^{high}CD122^{high} cells within viable CD3$^+$CD8$^+$ T cells. One representative mouse is shown. (**B**) Percentage of CD44^{high}CD122^{high} cells within viable CD3$^+$CD8$^+$ T cells. Data are presented as means of 3 mice +/- SD. Statistical significance was determined by two-tailed unpaired Student t test, *p < 0.05, ***p < 0.001.

5.2.2.3. Effects of IL-7ic on recently activated CD4$^+$ and CD8$^+$ T cells

We wanted to examine the effect of IL-7/M25 and IL-7/MAB407 on activated CD8$^+$ and CD4$^+$ T cell as these are the key players in cancer cell eradication by the immune system. We thus conducted an adoptive transfer experiment where purified OT-I/CD45.1 CD8$^+$ and OT-II/CD45.1 CD4$^+$ T cells were i.v. injected into C57BL/6 (CD45.2) congenic recipient mice (n=3) at 7.5x10^5 and 1.5x10^6 cells per mouse, respectively. One group of mice was left untreated and served as a negative control. Other groups received i.p. injection of OVA 24 h after the cell transfer. Mice were further treated with 4 daily doses of IL-7 (1 µg), IL-7ic (1 µg of IL-7 eq.) (Fig. 32A). The spleens of the recipient mice were harvested 24 h after the final dose and donor T cells was analyzed by flow cytometry.

Neither IL-7/M25 nor IL-7/MAB407 were more potent in inducing expansion of activated CD4$^+$ (Fig. 32B, 32C) and CD8$^+$ (Fig. 32B, 32D) T cells in comparison to free IL-7. Free IL-7 induced 5.8-fold expansion of recently activated donor CD4$^+$ T cells relative to the negative control while IL-7/M25 and IL-7/MAB407 mediated 10.1-fold and 6.7-fold expansion, respectively, which was not a significant difference (Fig. 32B, 32C). Effect of IL-7,

IL-7/M25 and IL-7/MAB407 on expansion of recently activated CD8$^+$ T cells was comparable (Fig. 32B, 32D).

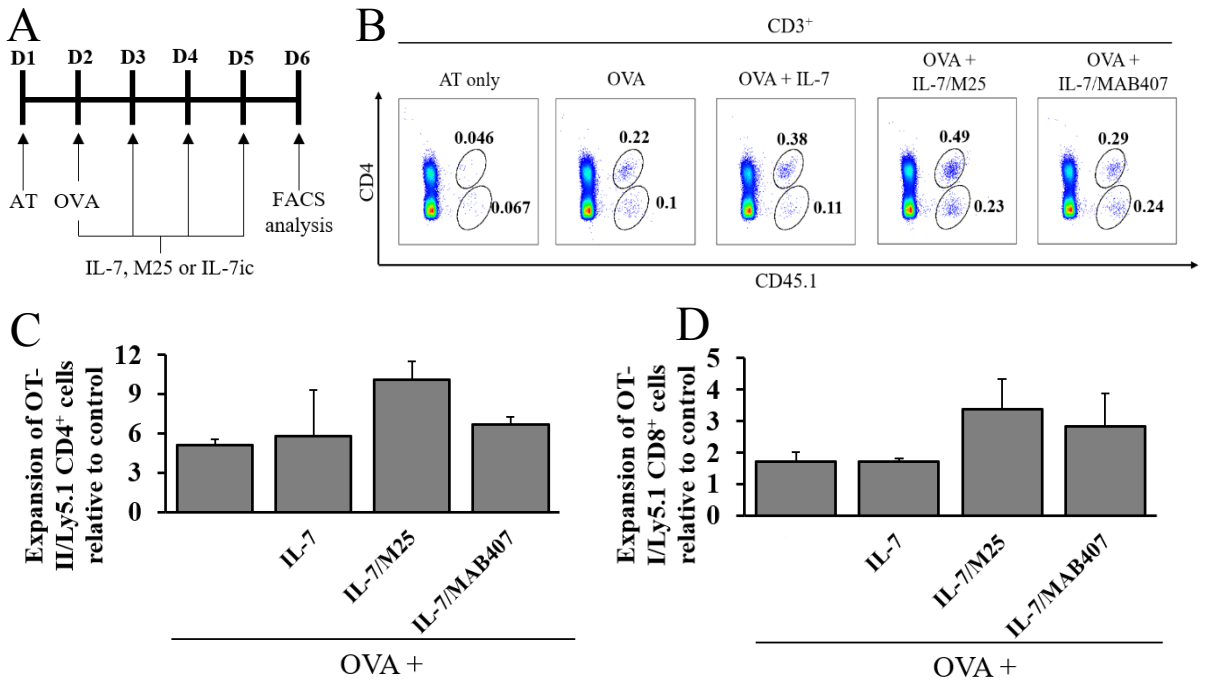

Figure 32. IL-7ic don't induce expansion of recently activated CD4$^+$ and CD8$^+$ T cells *in vivo*. (**A**) Schema of the adoptive transfer experiment. 7.5x10^5 OT-I/CD45.1 CD8$^+$ and 1.5x10^6 OT-II/CD45.1 CD4$^+$ T cells were adoptively transferred (AT) into C57BL/6 (CD45.2) recipient mice (n=3) and stimulated with i.p. administrated OVA (75 µg). Mice were then either left with no further treatment or injected with IL-7 (1 µg), IL-7/M25 (1 µg of IL-7 eq.) or IL-7/MAB407 (1 µg of IL-7 eq.) for 4 consecutive days. Negative control group (AT only) was left untreated after the cell transfer. Mice were sacrificed 24 h after the final dose and their spleens were analyzed by flow cytometry. (**B**) Relative expansion of activated donor CD3$^+$CD$^+$ T cells (CD3$^+$CD45.1$^+$ CD4$^-$, lower gate) and CD3$^+$CD4$^+$ T cells (CD3$^+$CD45.1$^+$ CD4$^+$, upper gate). One representative mouse is shown. Quantification of relative numbers of donor OT-II/CD45.1 CD4$^+$ (**C**) and OT-I/CD45.1 CD8$^+$ T cells (**D**) relative to negative control. Data are presented as means +/- SD. Statistical significance was determined by two-tailed unpaired Student t test.

5.2.3. Antitumor activity of IL-7ic in combination with αCTLA-4 plus αPD-1 mAbs

We demonstrated that IL-7/M25 expanded CD8$^+$ T cells *in vivo* (Fig. 23B, 24C, 24F, 27C), although proliferation of B cells (Fig. 24A, 24D, 27A) and CD4$^+$ T cells (Fig. 24B, 24E, 27B) was also induced. Population of MP CD8$^+$ T cells was remarkably boosted in IL-7/M25-treated mice (Fig. 31A, 31B), while relative Treg counts were significantly decreased (Fig. 28 A, 28B). Taken together, we presumed that IL-7/M25 might possess antitumor properties.

We decided to examine antitumor activities of IL-7/M25 in combination with αCTLA-4 plus αPD-1 mAbs since this approach might benefit from IL-7/M25-mediated CD8$^+$ T cell expansion.

5.2.3.1. IL-7/M25 and αCTLA-4 plus αPD-1 mAbs combination therapy in CT26 tumor model

BALB/c mice (n=8) were s.c. inoculated with $2x10^5$ CT26 tumor cells on day 0. Mice received injection of PBS or IL-7/M25 (1 µg of IL-7 eq.), on days 4, 5, 6 and/or αCTLA-4 (100 µg) plus αPD-1 (100 µg) mAbs on days 7, 10 and 13 (Fig. 33A). Tumor size was measured, and survival of mice was recorded.

Surprisingly, we observed a significant abrogation of αCTLA-4 plus αPD-1 mAbs-mediated antitumor effect in group of mice treated with IL-7/M25 and mAbs combination therapy (Fig. 33B, 33C). IL-7/M25 administration negatively affected both tumor growth (Fig. 33B) and mice survival (Fig. 33C) in checkpoint inhibitors-treated mice. αCTLA-4 plus αPD-1 mAbs therapy led to a complete cure of 5 out of 8 mice, while only 1 out of 8 mice was a long-term survivor in IL-7/M25 and mAbs combination-treated group (Fig. 33C). IL-7/M25 treatment alone showed no effect in comparison to control mice.

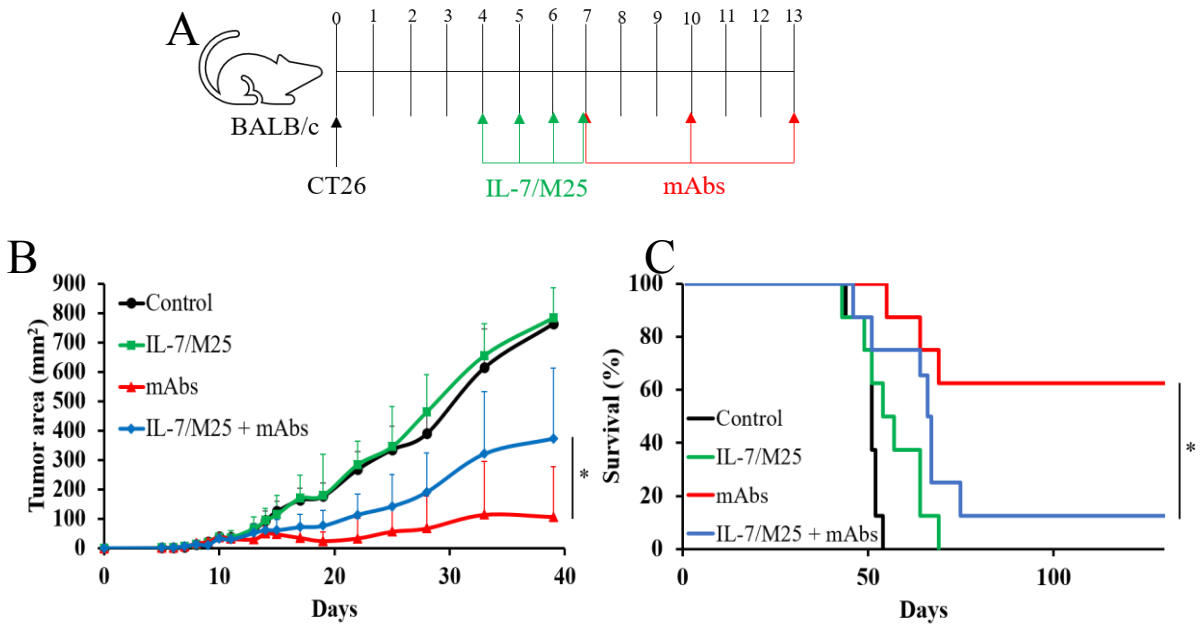

Figure 33. IL-7/M25 abrogate the antitumor effect of αCTLA-4 plus αPD-1 mAbs in mouse CT26 colon carcinoma tumor model. (A) Schema of the tumor therapy experiment. BALB/c mice (n=8) were s.c. inoculated with $2x10^5$ CT26 cells in 100 µl PBS on day 0. Mice were i.p. injected with PBS (control) or IL-7/M25 (1 µg of IL-7 eq.) on days 4, 5, 6, 7 and/or αCTLA-4 (100 µg) plus αPD-1 (100 µg) mAbs (mAbs) on days 7, 10 and 13. (**B**) Growth of CT26 tumors (mean +/-SD). (**C**) Experimental mice survival. Statistical significance was determined by two-tailed unpaired Student t test for tumor growth assessment and log-rang Mantel-Cox test for survival analysis, *$p < 0.05$.

5.2.3.2. IL-7/M25 and αCTLA-4 plus αPD-1 mAbs combination therapy in MC38 tumor model

We found out that IL-7/M25 dampened the antitumor effect mediated by αCTLA-4 plus αPD-1 mAbs in CT26 tumor model (Fig. 33B, 33C). We wanted to determine whether it was

an effect unique to CT26 carcinoma or rather a general phenomenon that applies to other tumor models. We thus decided to test IL-7/M25 and mAbs combination in MC-38 tumor model.

C57BL/6 mice (n=6) were s.c. inoculated with $5x10^5$ MC38 tumor cells on day 0. Mice received i.p. injection of PBS or IL-7/M25 (1 µg of IL-7 eq.) on days 4, 5, 6, and/or αCTLA-4 (100 µg) plus αPD-1 (100 µg) mAbs on days 7, 10 and 13 (Fig. 34A).

The therapeutic effect of αCTLA-4 plus αPD-1 mAbs was again abrogated when IL-7/M25 were administrated (Fig. 34B, 34C). Checkpoint inhibitor therapy resulted in striking reduction of the tumor burden. However, tumor growth in mice treated with IL-7/M25 and mAbs combination was comparable to untreated mice (Fig. 34B). 83% of mice treated with αCTLA-4 plus αPD-1 mAbs alone were completely cured, while in the combination group only 33% of mice were long-term survivors (Fig. 34C). IL-7/M25 treatment alone had no effect on MC38 tumor growth and mice survival.

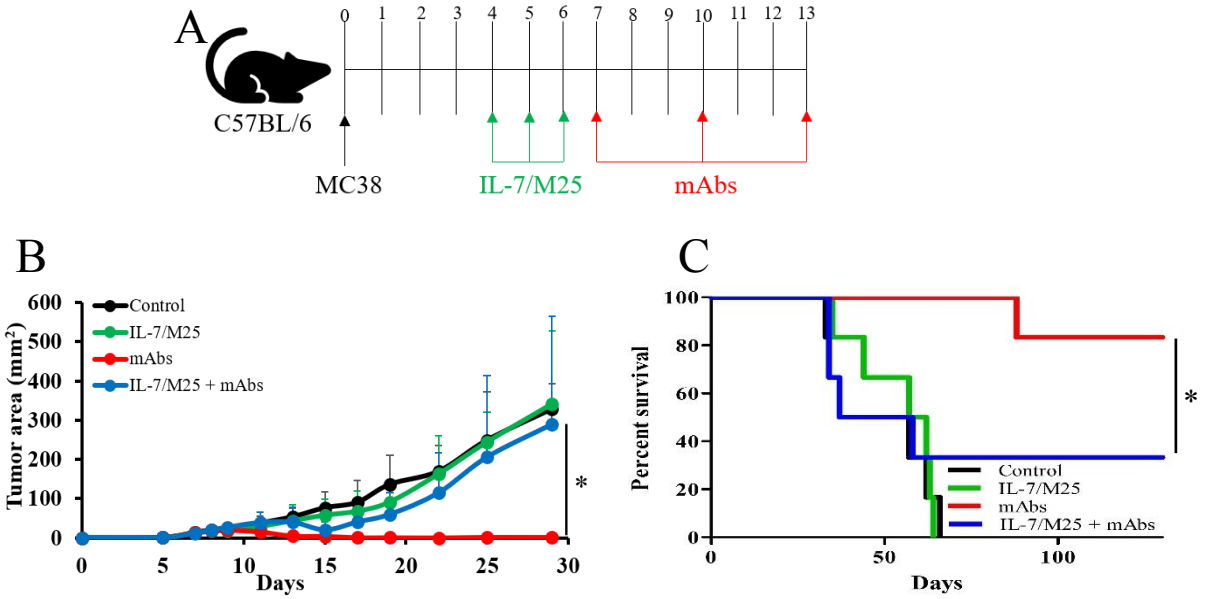

Figure 34. IL-7/M25 abrogate the antitumor effect of αCTLA-4 plus αPD-1 mAbs in mouse MC38 colon carcinoma tumor model. (A) Schema of the tumor therapy experiment. C57BL/6 mice (n=6) were s.c. inoculated with $5x10^5$ MC38 cells in 100 µl PBS on day 0. Mice were i.p. injected with PBS (control) or IL-7/M25 (1 µg of IL-7 eq.) on days 4, 5, 6 and/or αCTLA-4 (100 µg) plus αPD-1 (100 µg) mAbs (mAbs) on days 7, 10 and 13. (**B**) Growth of MC38 tumors (mean +/-SD). (**C**) Experimental mice survival. Statistical significance was determined by two-tailed unpaired Student t test for tumor growth assessment and log-rang Mantel-Cox test for survival analysis, *$p < 0.05$.

5.2.3.3. IL-7/M25 and αCTLA-4 plus αPD-1 mAbs combination therapy in B16F10 tumor model

We wanted to finally confirm our unexpected finding that IL-7/M25 dampen the antitumor activity of αCTLA-4 plus αPD-1 mAbs treatment and that it might be a general phenomenon as the same effect was observed in 2 different tumor models. We chose to finally test our hypothesis in B16F10 melanoma.

C57BL/6 mice (n=7) were s.c. inoculated with $5x10^5$ B16F10 tumor cells on day 0. Mice received i.p. injection of PBS or IL-7/M25 (1 µg of IL-7 eq.) on days 4, 5, 6, 7 and/or αCTLA-4 (100 µg) plus αPD-1 (100 µg) mAbs on days 7, 10 and 13 (Fig. 35A).

IL-7/M25 and αCTLA-4 plus αPD-1 mAbs combination therapy was significantly less potent in reducing B16F10 tumor growth than treatment with mAbs only (Fig. 35B). No significant difference between these two groups was noticed in terms of prolongation of mice survival (Fig. 35C). Nevertheless, we confirmed that IL-7/M25 tended to dampen the antitumor activity of checkpoint inhibitors in another mouse tumor model.

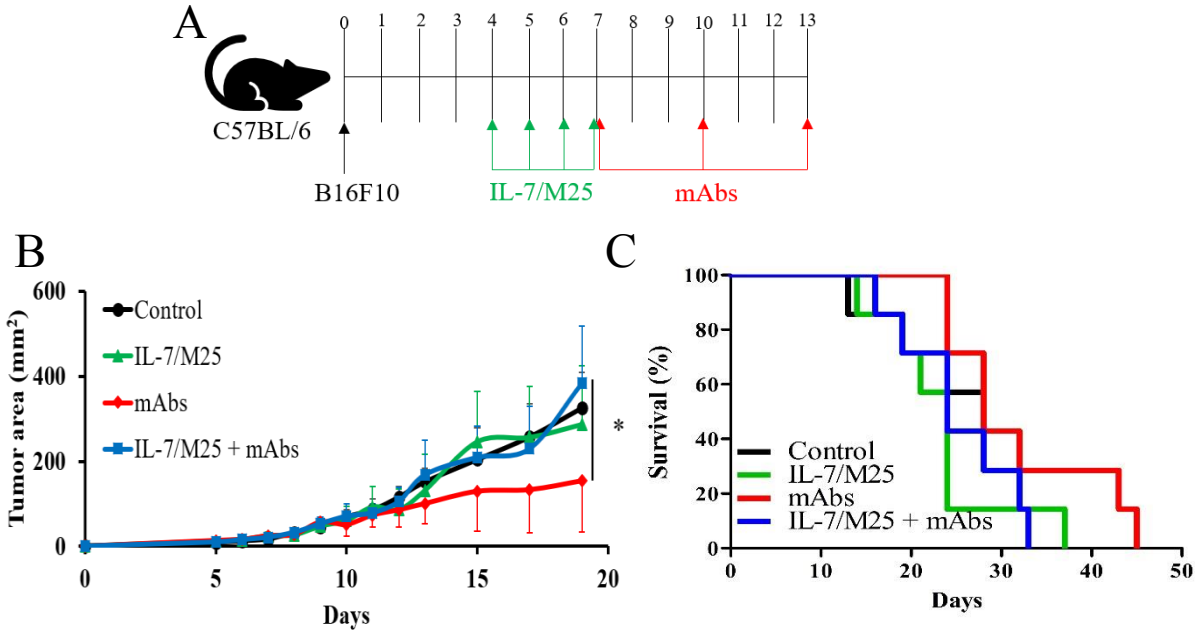

Figure 35. IL-7/M25 abrogate the antitumor effect of αCTLA-4 plus αPD-1 mAbs in mouse B16F10 melanoma tumor model. (A) Schema of the tumor therapy experiment. C57BL/6 mice (n=7) were s.c. inoculated with $5x10^5$ B10F10 cells in 100 µl PBS on day 0. Mice were i.p. injected with PBS (control) or IL-7/M25 (1 µg of IL-7 eq.) on days 4, 5, 6, 7 and/or αCTLA-4 (100 µg) plus αPD-1 (100 µg) mAbs (mAbs) on days 7, 10 and 13. (**B**) Growth of B16F10 tumors (mean +/-SD). (**C**) Experimental mice survival. Statistical significance was determined by two-tailed unpaired Student t test for tumor growth assessment and log-rang Mantel-Cox test for survival analysis, *$p < 0.05$.

5.2.3.4. IL-7 and αCTLA-4 plus αPD-1 mAbs combination therapy in CT26 tumor model

We conducted a control experiment in order to confirm that only IL-7/M25 but not free IL-7 or IL-7/MAB407 dampened the antitumor activity of αCTLA-4 plus αPD-1 mAbs. BALB/c mice (n=8-9) were s.c. inoculated with $2x10^5$ CT26 tumor cells on day 0. Mice received i.p. injection of PBS, IL-7 (1 µg) or IL-7/MAB407 (1 µg of IL-7 eq.) on days 4, 5, 6 and/or αCTLA-4 (75 µg) plus αPD-1 (75 µg) mAbs on days 7, 10 and 13 (Fig. 36A).

Neither IL-7 nor IL-7/MAB407 had a significant effect on potent antitumor activity of αCTLA-4 plus αPD-1 mAbs (Fig. 36B, 36C). Checkpoints inhibitors alone and in combination with either IL-7 or IL-7/MAB407 efficiently suppressed CT26 tumor growth (Fig. 36B). As for mice lifespan prolongation, slightly, but not significantly improved effects were observed in both combination groups compared to mAbs group (Fig. 36C). 62% of mAbs-treated mice were long-term survivors, while the combination of mAb and IL-7 or IL-7/MAB407 cured 89% or 75% of mice, respectively.

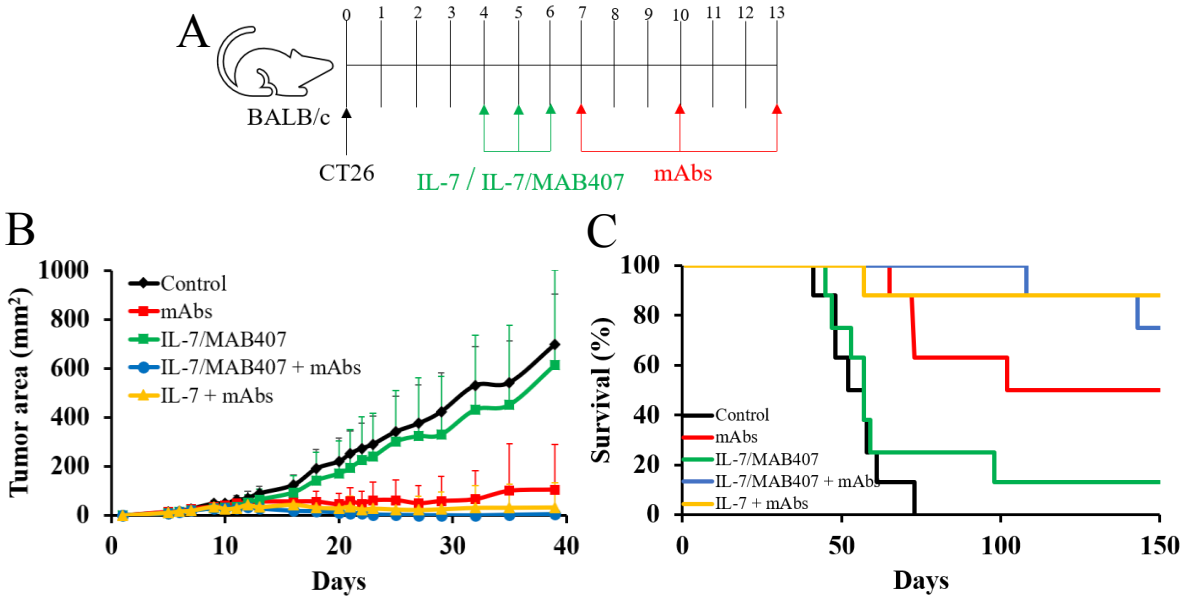

Figure 36. IL-7 and IL-7/MAB407 don't interfere with the antitumor effect of αCTLA-4 plus αPD-1 mAbs in mouse CT26 colon carcinoma tumor model. (A) Schema of the tumor therapy experiment. BALB/c mice (n=8-9) were s.c. inoculated with $2x10^5$ CT26 cells in 100 µl PBS on day 0. Mice were i.p. injected with PBS (control), IL-7 (1 µg) or IL-7/MAB407 (1 µg of IL-7 eq.) on days 4, 5, 6 and/or αCTLA-4 (75 µg) plus αPD-1 (75 µg) mAbs (mAbs) on days 7, 10 and 13. (**B**) Growth of CT26 tumors (mean +/-SD). (**C**) Experimental mice survival. Statistical significance was determined by two-tailed unpaired Student t test for tumor growth assessment and log-rang Mantel-Cox test for survival analysis.

5.2.4. IL-7/M25 do not dampen antitumor activity of αCTLA-4 plus αPD-1 mAbs through production of IL-10 and TGF-β

We demonstrated that IL-7/M25 abrogated antitumor effect of αCTLA-4 plus αPD-1 mAbs in several experimental tumor models (Fig. 33-35) while equivalent dose of IL-7 had no such effect (Fig. 36). We thus wanted to elucidate the mechanism of this surprising and unexpected phenomenon.

Our idea was that IL-7/M25 administration might expand a cell population with immunosuppressive properties which would dampen the effect of immune checkpoint inhibitors. Immunosuppressive IL-10-producing B regulatory cells seemed to be potential

candidates as these cells were shown to promote tumor growth [120] and our flow cytometry analysis revealed that B cell proliferation (Fig. 24A, 24D, 27A) and CD25 expression in B cells (Fig. 25A) were induced by IL-7/M25.

In order to shed light on this issue, we decided to determine levels of immunosuppressive cytokines IL-10 and TGF-β after IL-7 and IL-7/M25 administration. We also examined production of other cytokines such as IL-4, IL-6 and IFN-γ to see whether there was a difference between their production in IL-7 and IL-7/M25-treated mice.

BALB/c mice (n=3) were i.p. injected with 4 daily doses of PBS, IL-7 (1 μg), M25 mAb (5 μg) or IL-7/M25 (1 μg of IL-7 eq.). Mice were sacrificed 48 h after the final dose and their sera were collected. Cytokine levels in sera were determined by ELISA.

We only succeeded in measuring the level of TGF-β (Fig. 37B), as the levels of IL-4 (Fig. 37D), IL-6 (Fig. 37C), IL-10 (Fig. 37A) and IFN-γ (Fig. 37E) were undetectable. No increase in TGF- β secretion was observed in IL-7/M25-treated mice in comparison to control (Fig. 37B).

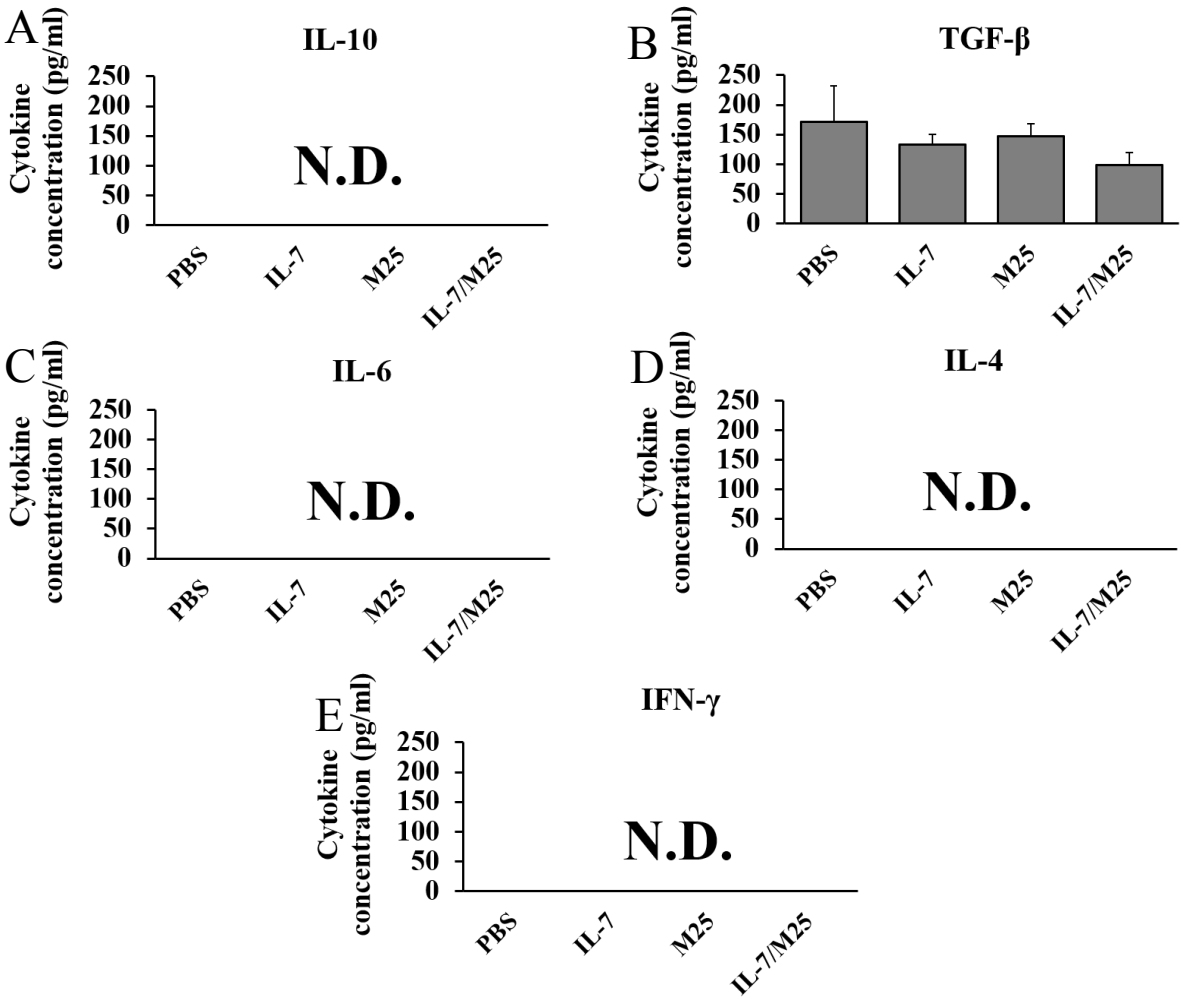

Figure 37. IL-7/M25 don't induce production of IL-10, TGF-β, IL-6, IL-4 and IFN-γ *in vivo*. BALB/c mice (n=2-3) received i.p. injection of PBS (control), IL-7 (1 µg), M25 mAb (5 µg) or IL-7/M25 complex (1 µg IL-7 + 5 µg M25 mAb), every day for 4 following days. Mice were sacrificed 48 h after the final dose and their sera were collected. IL-10 (**A**), TGF-β (**B**), IL-6 (**C**), IL-4 (**D**) and IFN-γ (**E**) concentration was determined by ELISA, N.D. = not determined. Statistical significance was determined by two-tailed unpaired Student t test.

We thus excluded our original idea that IL-7/M25 might expand IL-10-producing B regulatory cells. Because of the fact that IL-10 level wasn't detectable in sera of any mouse (Fig. 37A), we conducted a final flow cytometry experiment to confirm that there were no IL-10-producing B cells after administration of IL-7/M25.

C57BL/6 mice (n=3) were i.p. injected with 4 daily doses PBS, IL-7 (1 µg), M25 mAb (5 µg) or IL-7/M25 (1 µg of IL-7 eq.). Mice were sacrificed 24 h after the final dose. Their spleens were harvested and stained for surface markers and for IL-10 intracellularly. Cells were subsequently analyzed by flow cytometry (Fig. 38A).

There was a comparable level of IL-10 producing B cells among all 4 experimental groups of mice (Fig. 38B, 38C). We then examined IL-10 production in $CD4^+$ and $CD8^+$ T cells. However, we detected no increased population of IL-10-producing cells in either $CD4^+$ (Fig. 38D, 38E) or $CD8^+$ (Fig. 38F, 38G) T cells isolated from mice treated with IL-7/M25.

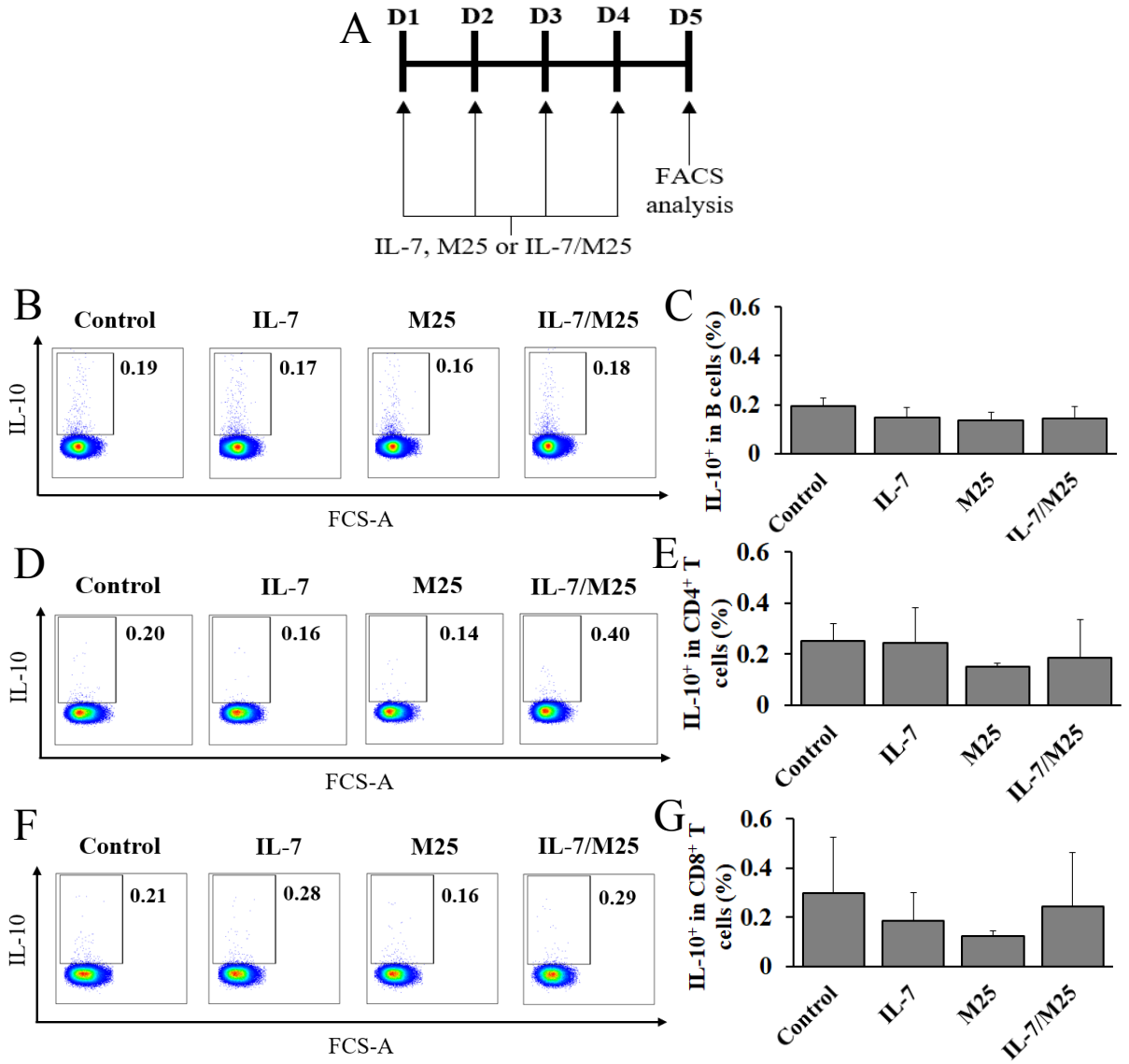

Figure 38. IL-7/M25 don't induce IL-10 production in B and T cells *in vivo*. (**A**) Schema of the experimental setup. C57BL/6 mice (n=3) received i.p. injection of PBS (control), IL-7 (1 µg), M25 mAb (5 µg) or IL-7/M25 (1 µg IL-7 + 5 µg M25 mAb) every day for 4 following days. Mice were sacrificed 24 h after the last dose and their spleens were analyzed by flow cytometry. Relative numbers (**B**) and percentage (**C**) of $IL\text{-}10^+$ cells within viable $CD3^-B220^+$ B cells. Relative numbers (**D**) and percentages (**E**) of $IL\text{-}10^+$ cells within viable $CD3^+CD4^+$ T cells. Relative numbers (**F**) and percentage (**G**) of $IL\text{-}10^+$ cells within viable $CD3^+CD8^+$ T cells. **C**, **E** and **G** are presented as means of 3 mice +/- SD. Statistical significance was determined by two-tailed unpaired Student t test.

6. DISCUSSION

The goal of tumor immunotherapy is to stimulate the immune system to recognize and eliminate cancer cells. Immunotherapy through checkpoint inhibition has gained particular attention as it showed potent antitumor activity in a vast number of cancers. However, its efficacy is limited to immunogenic tumors. Thus, combination therapy is likely to be necessary to increase the response rate in cancer patients. Immunotherapy using high dose of IL-2 is another immunotherapeutic approach used for treatment of metastatic melanoma and renal carcinoma. However, IL-2 immunotherapy has not been widely adopted since it has serious drawbacks such as short *in vivo* half-life of IL-2, unwanted Treg stimulation and serious toxicities like VLS. Modified IL-2 formulations are thus being investigated to overcome the shortcomings of IL-2 immunotherapy.

The use of IL-2ic composed of rIL-2 and anti-IL-2 mAb is a promising strategy as IL-2ic were shown to have much longer half-life in circulation and lower toxicity in comparison to free IL-2. One of our major aims was to investigate potential synergism between checkpoint inhibitor therapy and IL-2/S4B6. We hypothesized that dampening of inhibitory signals in recently expanded T cells could provide potent antitumor effect.

Surprisingly, our results show that both IL-2/S4B6 and IL-2/JES6-1 failed to drive expansion of activated $CD4^+$ T cells *in vivo*. IL-2 stimulates both $CD4^+$ and $CD8^+$ T cells to proliferate but the kinetics of the response is probably different. It has been proposed that $CD4^+$ T cells acquire IL-2 responsiveness later than $CD8^+$ T cells as massive phosphorylation of STAT5 was observed only in $CD8^+$ T cells after 24 h of IL-2 stimulation [121]. The distinct features of IL-2 responsiveness might originate in different CD122 abundance on $CD4^+$ and $CD8^+$ T cells. Unlike naive $CD8^+$ T cells, naïve $CD4^+$ express undetectable levels of CD122 so their response to activation stimuli is delayed [122]. Unexpectedly, both IL-2/S4B6 and IL-2/JES6-1 administration induced relative decrease of activated $CD4^+$ T cells in comparison with IL-2. However, we don't draw any conclusions from this finding as the expansion of activated $CD4^+$ T cell was negligible in all experimental groups relative to negative control. Statistically significant difference is thus probably accidental.

Investigation of possible synergism of antitumor activities of IL-2/S4B6 and αCTLA-4 plus αPD-1 mAbs was one of our major goals. Tumor-specific effector $CD8^+$ T cells are believed to be the key players in the eradication of cancer cells. We thus analyzed the potential of αCTLA-4 plus αPD-1 mAbs to augment the expansion of recently activated $CD8^+$ T cells driven by IL-2/S4B6 or IL-2/JES6-1. We show that the expansion of recently activated OT-I

$CD8^+$ T cells driven by IL-2/S4B6 was further augmented by αCTLA-4 plus αPD-1 mAbs administration only in case that OVA was used to activate OT-I $CD8^+$ T cells. We observed no potentiation when OT-I $CD8^+$ T cells were primed with SIINFEKL peptide. Since SIINFEKL is a low molecular peptide, it is probable that it binds directly to MHC-I grove on various cells and activates OT-I $CD8^+$ T cells rapidly throughout the body upon administration. Contrary to that, OVA needs to be fragmented, proteolytically cleaved and trans-presented to $CD8^+$ T cells by APC in secondary lymphoid organs which reflects the physiologic process much more and allows the effect of checkpoint blockade to come out. The expansion of OVA-activated OT-I $CD8^+$ T cells mediated by IL-2/JES6-1 wasn't increased by αCTLA-4 plus αPD-1 mAbs administration. A possible explanation could be that IL-2/JES6-1-mediated expansion of activated $CD8^+$ T cells reached a maximal possible level and further potentiation is thus impossible.

IL-2/S4B6 showed no anticancer activity in CT26 tumor model in stated dosing regimen. There is no report on antitumor efficacy of IL-2/S4B6 in CT26 tumor model in the literature. It is thus probable that IL-2/S4B6 therapy isn't capable of inducing antitumor response in CT26 colon carcinoma in spite of the fact that it is a highly immunogenic tumor cell line [123]. There are other experimental tumor models where IL-2/S4B6 were shown to be ineffective in inhibiting tumor growth such as RENCA renal carcinoma [56] and LM8 osteosarcoma [58].

No synergistic antitumor effect between IL-2/S4B6 and αCTLA-4 plus αPD-1 mAbs was observed in 2 other tumor models tested. αCTLA-4 plus αPD-1 mAbs showed anticancer activity in both MC38 colon carcinoma and EL4 T cell lymphoma, however, no improvement in antitumor activity was achieved when IL-2/S4B6 were added into treatment protocol.

It is difficult to speculate why IL-2/S4B6 don't enhance the antitumor activity of αCTLA-4 plus αPD-1 mAbs since such combination should in theory provide a more efficient treatment. It is possible that synergism of antitumor activities of checkpoint inhibitors and IL-2/S4B6 exists but only in some dosing/timing regimen and/or tumor models. This is a probable explanation as another group who has recently had the very same idea to test efficacy of IL-2ic and checkpoint inhibitor combination therapy reported that there was a synergy between IL-2/MAB602 and αCTLA-4 or αPD-1 mAb [124]. However, highly immunogenic B16F10-OVA tumor model combined with intensive IL-2/MAB602 treatment for 5 consecutive days were used in their study. Using of non-physiological tumor model and high IL-2ic dosing regimen thus might be the reason why they saw synergism of antitumor activities of IL-2ic and checkpoint inhibitors.

IL-2/S4B6 monotherapy exerted no or little anticancer effect in any tumor model tested which was a surprising finding. It has already been reported by others that IL-2/S4B6 was capable to inhibit tumor growth but only when administrated before the tumors became palpable [19, 125]. It is clear that dosage of IL-2/S4B6 must be carefully chosen in order to achieve anticancer efficacy. It has also been proposed that a complete abrogation of IL-2/S4B6 stimulatory activity on T and NK cells could occur when excessive dose of IL-2/S4B6 is administrated [60]. This might be the reason why IL-2/S4B6 tended to worsen αCTLA-4 plus αPD-1 mAbs therapy in some experiments. IL-2/S4B6 combined with CTLA-4 plus PD-1 blockade might have rendered T cells overstimulated and thus unfunctional.

Combination of IL-2 based therapy and immune checkpoint inhibitors is currently extensively studied. Even though our results suggest no potentiation of αCTLA-4 plus αPD-1 mAbs-mediated antitumor response by IL-2/S4B6 administration, other groups achieved more success with IL-2 or its variants. Both high dose IL-2 and αCTLA-4 mAb are treatment modalities approved for treating metastatic melanoma. Combination of these approaches showed better antitumor response in comparison to either agent alone in mice bearing B10F16 melanoma [126]. However, both αCTLA-4 mAb and IL-2 treatment were administered before tumors became visible which does not reflect the real situation in clinical practice. Combination of IL-2 and checkpoint inhibitor therapy have also been tested in clinical trials. The first one investigated antitumor effect of combined IL-2 and αCTLA-4 mAb therapy in patients with metastatic melanoma. No synergistic effect of the combined therapy was observed [127]. However, there are several clinical trials in progress addressing this promising combination therapy as promising. NKTR-214 is IL-2 with conjugated polyethylene glycol (PEG) chains which are released in a way resulting in preferential CD122 binding and thereby mimicking IL-2/S4B6 to some extent [128]. Antitumor activity of NKTR-214 is being tested either alone or in combination with nivolumab, ipilimumab and other checkpoint blockers in 11 clinical trials based on favorable outcomes in preclinical mouse tumor models [129]. However, potential synergism of anticancer activity of NKTR-214 and checkpoint inhibitors in cancer patients remains to be proven.

We spent more time characterizing IL-7ic contrary to our original expectations as there was no synergism of antitumor activities of IL-2/S4B6 and αCTLA-4 plus αPD-1 mAb. The knowledge of biological activities of IL-7ic is limited in comparison to IL-2ic, so we aimed to describe the effect of IL-7ic on immune cell populations in more detail.

We found out that IL-2 and IL-7 had different impacts on naïve $CD4^+$ and $CD8^+$ T *in vitro*. IL-7 provided naïve $CD4^+$ and $CD8^+$ T cells with prosurvival signals, while IL-2 acted as

a potent mitogenic factor. The thus confirmed the observation which has already been done by others [130].

Next, we characterized biological activities of IL-7ic *in vivo*. We showed that only IL-7/M25 but not IL-7/MAB407 displayed higher biological activity in comparison to free IL-7 *in vivo*, which is consistent with a previous report [109]. IL-7/MAB407 thus served as a control henceforth. We observed a vigorous proliferation of B cells in spleens of IL-7/M25-treated mice which was in accord with what had previously been reported [51]. There was a marked difference between the effects of IL-7ic and IL-2ic on Treg cells. It was an expected finding as Tregs are $CD127^{low}$ [98] and require IL-2 to expand [33]. We showed that both IL-2/S4B6 and IL-2/JES6-1 stimulated Treg cells *in vivo* with IL-2/JES6-1 being more potent in this regard which is in concordance with the finding of Boyman *et. al*. [49]. IL-2/S4B6 were the only agent capable to drive expansion of NK cells. IL-7/M25 administration, on the other hand, caused mild but significant decrease of the relative number of NK cells in spleen which is consistent with the fact that IL-7 is dispensable cytokine for homeostasis of NK cells [102]. Neither IL-7 nor IL-7/M25 stimulated the expansion of recently activated T cells. This finding met our expectations as T cells are known to downregulate CD127 expression upon activation [80].

IL-7/M25 dampened the anticancer activity of αCTLA-4 plus αPD-1 mAbs in all tested tumor models. We were of course interested in elucidating this phenomenon. It seemed possible that IL-7/M25 administration might expand cell population(s) with immunosuppressive properties. Our previous flow cytometry analysis showed increased counts of proliferating and $CD25^{+}$ B cells. We thus assumed that IL-7/M25 administration might provoked expansion of B regulatory cells. These have been reported to secret high levels of IL-10 and thus support the immunosuppressive feature of tumor microenvironment [120]. However, neither TGF-β nor IL-10 levels were elevated in sera of IL-7/M25-treated mice. Subsequent flow cytometry analysis confirmed no induction of IL-10 producing in B or T cells after IL-7/M25 administration.

It is interesting to describe immunostimulatory agent which inhibits antitumor activity of checkpoint blockade-based treatment, especially in today's era of checkpoint inhibitor immunotherapy. The potency of IL-7/M25 to abrogate antitumor efficacy of αCTLA-4 plus αPD-1 mAbs is thus a phenomenon which requires attention.

However, it is difficult to explain the phenomenon. We believe that IL-7/M25 administration can stimulate a population of immunocompetent cell with immunosuppressive activity. Our flow cytometry analysis indicates that IL-7/M25 rather possess immunostimulatory properties, although it is important to realize that the analysis was done

only in spleen of healthy mice. It might would have been worthwile to examine the immune infiltration in tumors of mice treated with combined IL-7/M25 and αCTLA-4 plus αPD-1 mAbs therapy. It is possible that IL-7/M25 treatment induced some changes in the tumor environment that were not present in spleen of healthy mice. Moreover, our *in vivo* analysis was rather superficial as we only determined the effects of IL-7/M25 on major immune cell populations, but we don't know much about their detailed phenotype and functional capacities.

There are hints in the literature that may help us explain the phenomenon of IL-7/M25-mediated neutralization of antitumor activity of αCTLA-4 plus αPD-1 mAbs, but it is not sure whether these are applicable to our case. It has been reported that IL-7/M25 administration increased numbers of IL-10-producing B regulatory cells, Tregs and myeloid-derived suppressor cells (MDSC) [131]. However, it is important to point out that the study was conducted in septic mice, which is quite a different setting from the tumor-bearing mice. Authors claimed that an early IL-7 treatment which started in the acute phase of sepsis had different outcomes compared to that which started in the immunosuppressive phase. Only the latter was associated with expansion of cells with immunoregulatory functions. The question arises whether IL-7/M25 administration might bring about similar immunosuppressive features in the immunosuppressive milieu of the tumor surroundings.

There is an increasing number of reports reflecting the importance of IL-7 pathway in αCTLA-4 plus αPD-1 mAbs-mediated tumor eradication. It has been recently reported that antitumor activity of αPD-1 mAb was potentiated by IL-7 administration in mice [132]. There are actually more reports which are inconsistent with our finding. Shi *et al.* showed that CTLA-4 and PD-1 blockade upregulated CD127 on $CD4^+$ and $CD8^+$ tumor infiltrating lymphocytes. Strikingly, potent antitumor activity of αCTLA-4 plus αPD-1 mAbs was completely abolished in $CD127^{-/-}$ mice. Authors also showed that IL-7 blockade with M25 mAb significantly abrogated anticancer activity of αCTLA-4 plus αPD-1 mAbs [133]. These results indicate that blockade of IL-7 but not its administration dampen the therapeutic effect of checkpoint inhibitors. There thus might be an alternative explanation of IL-7/M25-mediated abrogation of antitumor activity of αCTLA-4 plus αPD-1 mAbs in context of these findings. It is possible that M25 mAb actually mediates the effect that we observed. We don't know much about the fate of IL-7/M25 in mice. It is possible that IL-7/M25 dissociate after some time and IL-7 is rapidly cleared from the circulation due to its small molecular weight whereas M25 mAb persists in the organism, binds to endogenous IL-7 and neutralizes it. Indeed, M25 mAb is not capable to boost activity of endogenous IL-7 [109] and is routinely used to neutralize IL-7 *in vivo*. Unfortunately,

we didn’t include the appropriate control group in our tumor therapy experiments, so it is just a hypothesis which remains to proven.

7. CONCLUSIONS

We found out that antitumor activity of IL-2/S4B6 did not synergize with that of αCTLA-4 plus αPD-1 mAbs in either tumor model tested. Surprisingly, IL-7/M25 significantly abrogated antitumor activity of αCTLA-4 plus αPD-1 mAbs in all tumor models employed.
The conclusions of the thesis are:

- IL-2/S4B6 and IL-2/JES6-1 drive robust expansion of recently activated $CD8^+$ T cells *in vivo* while expansion driven by the same dose of free IL-2 is negligible. IL-2/JES6-1 is more potent than IL-2/S4B6 in this regard.
- IL-2/S4B6 and IL-2/JES6-1 are not capable to drive expansion of recently activated $CD4^+$ T cell *in vivo*.

- Expansion of SIINFEKL-activated $CD8^+$ T cells driven by IL-2/S4B6 or IL-2/JES6-1 *in vivo* is not potentiated by αCTLA-4 plus αPD-1 mAbs.
- Expansion of OVA-activated $CD8^+$ T cells driven by IL-2/S4B6 *in vivo* is further potentiated by αCTLA-4 plus αPD-1 mAbs, however, this does not apply for IL-2/JES6-1.

- There is no synergism between antitumor activity of IL-2/S4B6 and αCTLA-4 plus αPD-1 mAbs in CT26, MC38 and EL4 experimental tumor models.

- Biological activity of IL-7/M25 in T cells is comparable to free IL-7 *in vitro*.
- IL-7/M25 shift the $CD4^+$:$CD8^+$ T cell ratio in favor of $CD8^+$ T cells in spleen and stimulate proliferation of B and T cells *in vivo*. Free IL-7 has no effect at the same dose.
- IL-7/M25 decrease the relative counts of Tregs *in vivo.* Free IL-7 has no effect at the same dose.
- IL-7/M25 expand memory $CD8^+$ but not memory $CD4^+$ T cells *in vivo*. Free IL-7 has no effect at the same dose.
- Both free IL-7 and IL-7/M25 has no stimulatory activity for recently activated $CD4^+$ and $CD8^+$ T cells *in vivo*.

- IL-7/M25 administration dampens the antitumor effect of αCTLA-4 plus αPD-1 mAbs in CT26, MC-38 and B16F10 tumor models. Free IL-7 has no effect at the same dose.
- Neither IL-7/M25 nor IL-7 induce IL-10 and TGF-β production *in vivo*.

8. REFERENCES

1. Liao, W., J.X. Lin, and W.J. Leonard, *Interleukin-2 at the crossroads of effector responses, tolerance, and immunotherapy.* Immunity, 2013. **38**(1): p. 13-25.
2. Taniguchi, T., et al., *Structure and expression of a cloned cDNA for human interleukin-2.* Nature, 1983. **302**(5906): p. 305-10.
3. Kashima, N., et al., *Unique structure of murine interleukin-2 as deduced from cloned cDNAs.* Nature, 1985. **313**(6001): p. 402-4.
4. Jain, J., C. Loh, and A. Rao, *Transcriptional regulation of the IL-2 gene.* Curr Opin Immunol, 1995. **7**(3): p. 333-42.
5. Martins, G.A., et al., *Blimp-1 directly represses Il2 and the Il2 activator Fos, attenuating T cell proliferation and survival.* J Exp Med, 2008. **205**(9): p. 1959-65.
6. Granucci, F., et al., *Inducible IL-2 production by dendritic cells revealed by global gene expression analysis.* Nat Immunol, 2001. **2**(9): p. 882-8.
7. Jiang, S., et al., *Activated CD1d-restricted natural killer T cells secrete IL-2: innate help for CD4+CD25+ regulatory T cells?* Eur J Immunol, 2005. **35**(4): p. 1193-200.
8. Gaffen, S.L., S. Wang, and M.E. Koshland, *Expression of the immunoglobulin J chain in a murine B lymphoma is driven by autocrine production of interleukin 2.* Cytokine, 1996. **8**(7): p. 513-24.
9. Boomer, J.S. and J.M. Green, *An enigmatic tail of CD28 signaling.* Cold Spring Harb Perspect Biol, 2010. **2**(8): p. a002436.
10. Papiernik, M., et al., *Regulatory CD4 T cells: expression of IL-2R alpha chain, resistance to clonal deletion and IL-2 dependency.* Int Immunol, 1998. **10**(4): p. 371-8.
11. Niu, P., et al., *Transcriptional profiling of interleukin-2-primed human adipose derived mesenchymal stem cells revealed dramatic changes in stem cells response imposed by replicative senescence.* Oncotarget, 2015. **6**(20): p. 17938-57.
12. Nelson, B.H. and D.M. Willerford, *Biology of the interleukin-2 receptor.* Adv Immunol, 1998. **70**: p. 1-81.
13. Leonard, W.J., et al., *Molecular cloning and expression of cDNAs for the human interleukin-2 receptor.* Nature, 1984. **311**(5987): p. 626-31.
14. Hemar, A., et al., *Endocytosis of interleukin 2 receptors in human T lymphocytes: distinct intracellular localization and fate of the receptor alpha, beta, and gamma chains.* J Cell Biol, 1995. **129**(1): p. 55-64.
15. Boyman, O. and J. Sprent, *The role of interleukin-2 during homeostasis and activation of the immune system.* Nat Rev Immunol, 2012. **12**(3): p. 180-90.
16. Sakaguchi, S., et al., *Immunologic self-tolerance maintained by activated T cells expressing IL-2 receptor alpha-chains (CD25). Breakdown of a single mechanism of self-tolerance causes various autoimmune diseases.* J Immunol, 1995. **155**(3): p. 1151-64.
17. Roediger, B., et al., *Cutaneous immunosurveillance and regulation of inflammation by group 2 innate lymphoid cells.* Nat Immunol, 2013. **14**(6): p. 564-73.
18. Rolink, A., et al., *IL-2 receptor alpha chain (CD25, TAC) expression defines a crucial stage in pre-B cell development.* Int Immunol, 1994. **6**(8): p. 1257-64.
19. Krieg, C., et al., *Improved IL-2 immunotherapy by selective stimulation of IL-2 receptors on lymphocytes and endothelial cells.* Proc Natl Acad Sci U S A, 2010. **107**(26): p. 11906-11.
20. Robb, R.J., A. Munck, and K.A. Smith, *T cell growth factor receptors. Quantitation, specificity, and biological relevance.* J Exp Med, 1981. **154**(5): p. 1455-74.
21. Siegel, J.P., et al., *The IL-2 receptor beta chain (p70): role in mediating signals for LAK, NK, and proliferative activities.* Science, 1987. **238**(4823): p. 75-8.
22. Mingari, M.C., et al., *Human interleukin-2 promotes proliferation of activated B cells via surface receptors similar to those of activated T cells.* Nature, 1984. **312**(5995): p. 641-3.
23. Miyazaki, T., et al., *Functional activation of Jak1 and Jak3 by selective association with IL-2 receptor subunits.* Science, 1994. **266**(5187): p. 1045-7.

24. Ross, S.H., et al., *Phosphoproteomic Analyses of Interleukin 2 Signaling Reveal Integrated JAK Kinase-Dependent and -Independent Networks in CD8(+) T Cells.* Immunity, 2016. **45**(3): p. 685-700.
25. Bensinger, S.J., et al., *Distinct IL-2 receptor signaling pattern in CD4+CD25+ regulatory T cells.* J Immunol, 2004. **172**(9): p. 5287-96.
26. Huynh, A., et al., *Control of PI(3) kinase in Treg cells maintains homeostasis and lineage stability.* Nat Immunol, 2015. **16**(2): p. 188-96.
27. Morgan, D.A., F.W. Ruscetti, and R. Gallo, *Selective in vitro growth of T lymphocytes from normal human bone marrows.* Science, 1976. **193**(4257): p. 1007-8.
28. Wilson, E.B. and A.M. Livingstone, *Cutting edge: CD4+ T cell-derived IL-2 is essential for help-dependent primary CD8+ T cell responses.* J Immunol, 2008. **181**(11): p. 7445-8.
29. Miyazaki, T., et al., *Three distinct IL-2 signaling pathways mediated by bcl-2, c-myc, and lck cooperate in hematopoietic cell proliferation.* Cell, 1995. **81**(2): p. 223-31.
30. Ku, C.C., et al., *Control of homeostasis of CD8+ memory T cells by opposing cytokines.* Science, 2000. **288**(5466): p. 675-8.
31. Laurence, A., et al., *Interleukin-2 signaling via STAT5 constrains T helper 17 cell generation.* Immunity, 2007. **26**(3): p. 371-81.
32. Yu, A., et al., *A low interleukin-2 receptor signaling threshold supports the development and homeostasis of T regulatory cells.* Immunity, 2009. **30**(2): p. 204-17.
33. Malek, T.R., et al., *CD4 regulatory T cells prevent lethal autoimmunity in IL-2Rbeta-deficient mice. Implications for the nonredundant function of IL-2.* Immunity, 2002. **17**(2): p. 167-78.
34. Barron, L., et al., *Cutting edge: mechanisms of IL-2-dependent maintenance of functional regulatory T cells.* J Immunol, 2010. **185**(11): p. 6426-30.
35. Refaeli, Y., et al., *Biochemical mechanisms of IL-2-regulated Fas-mediated T cell apoptosis.* Immunity, 1998. **8**(5): p. 615-23.
36. Khatri, V.P., et al., *Ultra low dose interleukin-2 therapy promotes a type 1 cytokine profile in vivo in patients with AIDS and AIDS-associated malignancies.* J Clin Invest, 1998. **101**(6): p. 1373-8.
37. Van Gool, F., et al., *Interleukin-5-producing group 2 innate lymphoid cells control eosinophilia induced by interleukin-2 therapy.* Blood, 2014. **124**(24): p. 3572-6.
38. Suzuki, H., et al., *Abnormal development of intestinal intraepithelial lymphocytes and peripheral natural killer cells in mice lacking the IL-2 receptor beta chain.* J Exp Med, 1997. **185**(3): p. 499-505.
39. DiSanto, J.P., et al., *Lymphoid development in mice with a targeted deletion of the interleukin 2 receptor gamma chain.* Proc Natl Acad Sci U S A, 1995. **92**(2): p. 377-81.
40. Abbas, A.K., et al., *Revisiting IL-2: Biology and therapeutic prospects.* Sci Immunol, 2018. **3**(25).
41. Mule, J.J., S. Shu, and S.A. Rosenberg, *The anti-tumor efficacy of lymphokine-activated killer cells and recombinant interleukin 2 in vivo.* J Immunol, 1985. **135**(1): p. 646-52.
42. Rosenberg, S.A., et al., *Observations on the systemic administration of autologous lymphokine-activated killer cells and recombinant interleukin-2 to patients with metastatic cancer.* N Engl J Med, 1985. **313**(23): p. 1485-92.
43. Rosenberg, S.A., et al., *Treatment of 283 consecutive patients with metastatic melanoma or renal cell cancer using high-dose bolus interleukin 2.* JAMA, 1994. **271**(12): p. 907-13.
44. Rosenberg, S.A., *IL-2: the first effective immunotherapy for human cancer.* J Immunol, 2014. **192**(12): p. 5451-8.
45. Sereti, I., et al., *In vivo expansion of CD4CD45RO-CD25 T cells expressing foxP3 in IL-2-treated HIV-infected patients.* J Clin Invest, 2005. **115**(7): p. 1839-47.
46. Ahmadzadeh, M. and S.A. Rosenberg, *IL-2 administration increases CD4+ CD25(hi) Foxp3+ regulatory T cells in cancer patients.* Blood, 2006. **107**(6): p. 2409-14.
47. Klatzmann, D. and A.K. Abbas, *The promise of low-dose interleukin-2 therapy for autoimmune and inflammatory diseases.* Nat Rev Immunol, 2015. **15**(5): p. 283-94.
48. Rosenzwajg, M., et al., *Immunological and clinical effects of low-dose interleukin-2 across 11 autoimmune diseases in a single, open clinical trial.* Ann Rheum Dis, 2019. **78**(2): p. 209-217.

49. Boyman, O., et al., *Selective stimulation of T cell subsets with antibody-cytokine immune complexes.* Science, 2006. **311**(5769): p. 1924-7.
50. Levin, A.M., et al., *Exploiting a natural conformational switch to engineer an interleukin-2 'superkine'.* Nature, 2012. **484**(7395): p. 529-33.
51. Finkelman, F.D., et al., *Anti-cytokine antibodies as carrier proteins. Prolongation of in vivo effects of exogenous cytokines by injection of cytokine-anti-cytokine antibody complexes.* J Immunol, 1993. **151**(3): p. 1235-44.
52. Tomala, J., et al., *In vivo expansion of activated naive CD8+ T cells and NK cells driven by complexes of IL-2 and anti-IL-2 monoclonal antibody as novel approach of cancer immunotherapy.* J Immunol, 2009. **183**(8): p. 4904-12.
53. Lin, G.H., et al., *In vivo accumulation of T cells in response to IL-2/anti-IL-2 mAb complexes is dependent in part on the TNF family ligand 4-1BBL.* Immunol Cell Biol, 2012. **90**(7): p. 743-7.
54. Letourneau, S., et al., *IL-2/anti-IL-2 antibody complexes show strong biological activity by avoiding interaction with IL-2 receptor alpha subunit CD25.* Proc Natl Acad Sci U S A, 2010. **107**(5): p. 2171-6.
55. Verdeil, G., et al., *Adjuvants targeting innate and adaptive immunity synergize to enhance tumor immunotherapy.* Proc Natl Acad Sci U S A, 2008. **105**(43): p. 16683-8.
56. Han, K.H., et al., *Effects of stimulating interleukin -2/anti- interleukin -2 antibody complexes on renal cell carcinoma.* BMC Urol, 2016. **16**: p. 2.
57. Klevorn, L.E., et al., *Rescue of Tolerant CD8+ T Cells during Cancer Immunotherapy with IL2:Antibody Complexes.* Cancer Immunol Res, 2016. **4**(12): p. 1016-1026.
58. Takahashi, Y., et al., *Radiation Enhances the Efficacy of Antitumor Immunotherapy with an Immunocomplex of Interleukin-2 and Its Monoclonal Antibody.* Anticancer Res, 2017. **37**(12): p. 6799-6806.
59. Zingg, D., et al., *The Histone Methyltransferase Ezh2 Controls Mechanisms of Adaptive Resistance to Tumor Immunotherapy.* Cell Rep, 2017. **20**(4): p. 854-867.
60. Hamilton, S.E., et al., *IL-2 complex treatment can protect naive mice from bacterial and viral infection.* J Immunol, 2010. **185**(11): p. 6584-90.
61. Rajasagi, N.K. and B.T. Rouse, *IL-2 complex treatment amplifies CD8(+) T cell mediated immunity following herpes simplex virus-1 infection.* Microbes Infect, 2016. **18**(12): p. 735-746.
62. Webster, K.E., et al., *In vivo expansion of T reg cells with IL-2-mAb complexes: induction of resistance to EAE and long-term acceptance of islet allografts without immunosuppression.* J Exp Med, 2009. **206**(4): p. 751-60.
63. Liu, R., et al., *Expansion of regulatory T cells via IL-2/anti-IL-2 mAb complexes suppresses experimental myasthenia.* Eur J Immunol, 2010. **40**(6): p. 1577-89.
64. Polhill, T., et al., *IL-2/IL-2Ab complexes induce regulatory T cell expansion and protect against proteinuric CKD.* J Am Soc Nephrol, 2012. **23**(8): p. 1303-8.
65. Spangler, J.B., et al., *Antibodies to Interleukin-2 Elicit Selective T Cell Subset Potentiation through Distinct Conformational Mechanisms.* Immunity, 2015. **42**(5): p. 815-25.
66. Mahr, B., et al., *IL-2/alpha-IL-2 Complex Treatment Cannot Be Substituted for the Adoptive Transfer of Regulatory T cells to Promote Bone Marrow Engraftment.* PLoS One, 2016. **11**(1): p. e0146245.
67. Lee, W.W., et al., *Virus infection drives IL-2 antibody complexes into pro-inflammatory agonists in mice.* Sci Rep, 2016. **6**: p. 37603.
68. Phelan, J.D., T. Orekov, and F.D. Finkelman, *Cutting edge: mechanism of enhancement of in vivo cytokine effects by anti-cytokine monoclonal antibodies.* J Immunol, 2008. **180**(1): p. 44-8.
69. Arenas-Ramirez, N., J. Woytschak, and O. Boyman, *Interleukin-2: Biology, Design and Application.* Trends Immunol, 2015. **36**(12): p. 763-777.
70. Margolin, K., et al., *Phase I trial of BAY 50-4798, an interleukin-2-specific agonist in advanced melanoma and renal cancer.* Clin Cancer Res, 2007. **13**(11): p. 3312-9.
71. Lupton, S.D., et al., *Characterization of the human and murine IL-7 genes.* J Immunol, 1990. **144**(9): p. 3592-601.
72. Fry, T.J. and C.L. Mackall, *Interleukin-7: from bench to clinic.* Blood, 2002. **99**(11): p. 3892-904.

73. Gao, J., et al., *Mechanism of Action of IL-7 and Its Potential Applications and Limitations in Cancer Immunotherapy.* Int J Mol Sci, 2015. **16**(5): p. 10267-80.
74. Watanabe, M., et al., *Interleukin 7 is produced by human intestinal epithelial cells and regulates the proliferation of intestinal mucosal lymphocytes.* J Clin Invest, 1995. **95**(6): p. 2945-53.
75. Heufler, C., et al., *Interleukin 7 is produced by murine and human keratinocytes.* J Exp Med, 1993. **178**(3): p. 1109-14.
76. Soslau, G., et al., *Cytokine mRNA expression in human platelets and a megakaryocytic cell line and cytokine modulation of platelet function.* Cytokine, 1997. **9**(6): p. 405-11.
77. Kroncke, R., et al., *Human follicular dendritic cells and vascular cells produce interleukin-7: a potential role for interleukin-7 in the germinal center reaction.* Eur J Immunol, 1996. **26**(10): p. 2541-4.
78. Sorg, R.V., et al., *Human dendritic cells express functional interleukin-7.* Immunobiology, 1998. **198**(5): p. 514-26.
79. Benjamin, D., et al., *B cell IL-7. Human B cell lines constitutively secrete IL-7 and express IL-7 receptors.* J Immunol, 1994. **152**(10): p. 4749-57.
80. Kaech, S.M., et al., *Selective expression of the interleukin 7 receptor identifies effector CD8 T cells that give rise to long-lived memory cells.* Nat Immunol, 2003. **4**(12): p. 1191-8.
81. Cortez, V.S., M.L. Robinette, and M. Colonna, *Innate lymphoid cells: new insights into function and development.* Curr Opin Immunol, 2015. **32**: p. 71-7.
82. Reche, P.A., et al., *Human thymic stromal lymphopoietin preferentially stimulates myeloid cells.* J Immunol, 2001. **167**(1): p. 336-43.
83. Goodwin, R.G., et al., *Cloning of the human and murine interleukin-7 receptors: demonstration of a soluble form and homology to a new receptor superfamily.* Cell, 1990. **60**(6): p. 941-51.
84. Park, J.H., et al., *Suppression of IL7Ralpha transcription by IL-7 and other prosurvival cytokines: a novel mechanism for maximizing IL-7-dependent T cell survival.* Immunity, 2004. **21**(2): p. 289-302.
85. Ouyang, W., et al., *An essential role of the Forkhead-box transcription factor Foxo1 in control of T cell homeostasis and tolerance.* Immunity, 2009. **30**(3): p. 358-71.
86. Xue, H.H., et al., *GA binding protein regulates interleukin 7 receptor alpha-chain gene expression in T cells.* Nat Immunol, 2004. **5**(10): p. 1036-44.
87. ElKassar, N. and R.E. Gress, *An overview of IL-7 biology and its use in immunotherapy.* J Immunotoxicol, 2010. **7**(1): p. 1-7.
88. von Freeden-Jeffry, U., et al., *Lymphopenia in interleukin (IL)-7 gene-deleted mice identifies IL-7 as a nonredundant cytokine.* J Exp Med, 1995. **181**(4): p. 1519-26.
89. Sportes, C., et al., *Phase I study of recombinant human interleukin-7 administration in subjects with refractory malignancy.* Clin Cancer Res, 2010. **16**(2): p. 727-35.
90. Komschlies, K.L., et al., *Administration of recombinant human IL-7 to mice alters the composition of B-lineage cells and T cell subsets, enhances T cell function, and induces regression of established metastases.* J Immunol, 1994. **152**(12): p. 5776-84.
91. Candeias, S., et al., *Defective T-cell receptor gamma gene rearrangement in interleukin-7 receptor knockout mice.* Immunol Lett, 1997. **57**(1-3): p. 9-14.
92. Hassan, J. and D.J. Reen, *Human recent thymic emigrants--identification, expansion, and survival characteristics.* J Immunol, 2001. **167**(4): p. 1970-6.
93. von Freeden-Jeffry, U., et al., *The earliest T lineage-committed cells depend on IL-7 for Bcl-2 expression and normal cell cycle progression.* Immunity, 1997. **7**(1): p. 147-54.
94. Jiang, Q., et al., *Distinct regions of the interleukin-7 receptor regulate different Bcl2 family members.* Mol Cell Biol, 2004. **24**(14): p. 6501-13.
95. Takada, K. and S.C. Jameson, *Self-class I MHC molecules support survival of naive CD8 T cells, but depress their functional sensitivity through regulation of CD8 expression levels.* J Exp Med, 2009. **206**(10): p. 2253-69.
96. Jacobs, S.R., R.D. Michalek, and J.C. Rathmell, *IL-7 is essential for homeostatic control of T cell metabolism in vivo.* J Immunol, 2010. **184**(7): p. 3461-9.
97. Schluns, K.S., et al., *Interleukin-7 mediates the homeostasis of naive and memory CD8 T cells in vivo.* Nat Immunol, 2000. **1**(5): p. 426-32.

98. Bayer, A.L., et al., *A function for IL-7R for CD4+CD25+Foxp3+ T regulatory cells.* J Immunol, 2008. **181**(1): p. 225-34.
99. Surh, C.D. and J. Sprent, *Homeostatic T cell proliferation: how far can T cells be activated to self-ligands?* J Exp Med, 2000. **192**(4): p. F9-F14.
100. Martin, C.E., et al., *Interleukin-7 Availability Is Maintained by a Hematopoietic Cytokine Sink Comprising Innate Lymphoid Cells and T Cells.* Immunity, 2017. **47**(1): p. 171-182 e4.
101. Pellegrini, M., et al., *IL-7 engages multiple mechanisms to overcome chronic viral infection and limit organ pathology.* Cell, 2011. **144**(4): p. 601-13.
102. Moore, T.A., et al., *Inhibition of gamma delta T cell development and early thymocyte maturation in IL-7 -/- mice.* J Immunol, 1996. **157**(6): p. 2366-73.
103. Sportes, C., et al., *Administration of rhIL-7 in humans increases in vivo TCR repertoire diversity by preferential expansion of naive T cell subsets.* J Exp Med, 2008. **205**(7): p. 1701-14.
104. Andersson, A., et al., *IL-7 promotes CXCR3 ligand-dependent T cell antitumor reactivity in lung cancer.* J Immunol, 2009. **182**(11): p. 6951-8.
105. Tang, J.C., et al., *IL-7 inhibits tumor growth by promoting T cell-mediated antitumor immunity in Meth A model.* Immunol Lett, 2014. **158**(1-2): p. 159-66.
106. Rosenberg, S.A., et al., *IL-7 administration to humans leads to expansion of CD8+ and CD4+ cells but a relative decrease of CD4+ T-regulatory cells.* J Immunother, 2006. **29**(3): p. 313-9.
107. Levy, Y., et al., *Effects of recombinant human interleukin 7 on T-cell recovery and thymic output in HIV-infected patients receiving antiretroviral therapy: results of a phase I/IIa randomized, placebo-controlled, multicenter study.* Clin Infect Dis, 2012. **55**(2): p. 291-300.
108. Thiebaut, R., et al., *Repeated Cycles of Recombinant Human Interleukin 7 in HIV-Infected Patients With Low CD4 T-Cell Reconstitution on Antiretroviral Therapy: Results of 2 Phase II Multicenter Studies.* Clin Infect Dis, 2016. **62**(9): p. 1178-1185.
109. Boyman, O., et al., *IL-7/anti-IL-7 mAb complexes restore T cell development and induce homeostatic T Cell expansion without lymphopenia.* J Immunol, 2008. **180**(11): p. 7265-75.
110. Martin, C.E., et al., *IL-7/anti-IL-7 mAb complexes augment cytokine potency in mice through association with IgG-Fc and by competition with IL-7R.* Blood, 2013. **121**(22): p. 4484-92.
111. Becklund, B.R., et al., *The aged lymphoid tissue environment fails to support naive T cell homeostasis.* Sci Rep, 2016. **6**: p. 30842.
112. Buchbinder, E.I. and A. Desai, *CTLA-4 and PD-1 Pathways: Similarities, Differences, and Implications of Their Inhibition.* Am J Clin Oncol, 2016. **39**(1): p. 98-106.
113. Krummel, M.F. and J.P. Allison, *CTLA-4 engagement inhibits IL-2 accumulation and cell cycle progression upon activation of resting T cells.* J Exp Med, 1996. **183**(6): p. 2533-40.
114. Phan, G.Q., et al., *Cancer regression and autoimmunity induced by cytotoxic T lymphocyte-associated antigen 4 blockade in patients with metastatic melanoma.* Proc Natl Acad Sci U S A, 2003. **100**(14): p. 8372-7.
115. Larkin, J., F.S. Hodi, and J.D. Wolchok, *Combined Nivolumab and Ipilimumab or Monotherapy in Untreated Melanoma.* N Engl J Med, 2015. **373**(13): p. 1270-1.
116. Ishida, Y., et al., *Induced expression of PD-1, a novel member of the immunoglobulin gene superfamily, upon programmed cell death.* EMBO J, 1992. **11**(11): p. 3887-95.
117. Latchman, Y., et al., *PD-L2 is a second ligand for PD-1 and inhibits T cell activation.* Nat Immunol, 2001. **2**(3): p. 261-8.
118. Ribas, A. and J.D. Wolchok, *Cancer immunotherapy using checkpoint blockade.* Science, 2018. **359**(6382): p. 1350-1355.
119. Chae, Y.K., et al., *Current landscape and future of dual anti-CTLA4 and PD-1/PD-L1 blockade immunotherapy in cancer; lessons learned from clinical trials with melanoma and non-small cell lung cancer (NSCLC).* J Immunother Cancer, 2018. **6**(1): p. 39.
120. Sarvaria, A., J.A. Madrigal, and A. Saudemont, *B cell regulation in cancer and anti-tumor immunity.* Cell Mol Immunol, 2017. **14**(8): p. 662-674.
121. Au-Yeung, B.B., et al., *IL-2 Modulates the TCR Signaling Threshold for CD8 but Not CD4 T Cell Proliferation on a Single-Cell Level.* J Immunol, 2017. **198**(6): p. 2445-2456.
122. Smith, G.A., J. Taunton, and A. Weiss, *IL-2Rbeta abundance differentially tunes IL-2 signaling dynamics in CD4(+) and CD8(+) T cells.* Sci Signal, 2017. **10**(510).

123. Lechner, M.G., et al., *Immunogenicity of murine solid tumor models as a defining feature of in vivo behavior and response to immunotherapy.* J Immunother, 2013. **36**(9): p. 477-89.
124. Caudana, P., et al., *IL2/Anti-IL2 Complex Combined with CTLA-4, But Not PD-1, Blockade Rescues Antitumor NK Cell Function by Regulatory T-cell Modulation.* Cancer Immunol Res, 2019. **7**(3): p. 443-457.
125. Tomala, J., et al., *Antitumor activity of IL-2/anti-IL-2 mAb immunocomplexes exerts synergism with that of N-(2-hydroxypropyl)methacrylamide copolymer-bound doxorubicin conjugate due to its low immunosuppressive activity.* Int J Cancer, 2011. **129**(8): p. 2002-12.
126. Kohlhapp, F.J., et al., *NK cells and CD8+ T cells cooperate to improve therapeutic responses in melanoma treated with interleukin-2 (IL-2) and CTLA-4 blockade.* J Immunother Cancer, 2015. **3**: p. 18.
127. Maker, A.V., et al., *Tumor regression and autoimmunity in patients treated with cytotoxic T lymphocyte-associated antigen 4 blockade and interleukin 2: a phase I/II study.* Ann Surg Oncol, 2005. **12**(12): p. 1005-16.
128. Bentebibel, S.E., et al., *A First-in-Human Study and Biomarker Analysis of NKTR-214, a Novel IL2Rbetagamma-Biased Cytokine, in Patients with Advanced or Metastatic Solid Tumors.* Cancer Discov, 2019. **9**(6): p. 711-721.
129. ClinicalTrials.gov. 2019 August1, 2019]; Available from: https://clinicaltrials.gov/ct2/results?cond=&term=NKTR-214&cntry=&state=&city=&dist=.
130. Rathmell, J.C., et al., *IL-7 enhances the survival and maintains the size of naive T cells.* J Immunol, 2001. **167**(12): p. 6869-76.
131. Kulkarni, U., et al., *IL-7 treatment augments and prolongs sepsis-induced expansion of IL-10-producing B lymphocytes and myeloid-derived suppressor cells.* PLoS One, 2018. **13**(2): p. e0192304.
132. Pfannenstiel, L.W., et al., *Immune-Checkpoint Blockade Opposes CD8(+) T-cell Suppression in Human and Murine Cancer.* Cancer Immunol Res, 2019. **7**(3): p. 510-525.
133. Shi, L.Z., et al., *Interdependent IL-7 and IFN-gamma signalling in T-cell controls tumour eradication by combined alpha-CTLA-4+alpha-PD-1 therapy.* Nat Commun, 2016. **7**: p. 12335.